THESIS

LIFE CYCLE COST ANALYSIS FOR JOINT ELIMINATION RETROFITS AND THERMAL LOADING ON COLORADO BRIDGES

Submitted by

Aura Lee Harper-Smith Kelly

Department of Civil and Environmental Engineering

In partial fulfillment of the requirements

For the degree of Master of Science

Colorado State University

Fort Collins, Colorado

Spring 2017

Master's Committee:

Advisor: Hussam Mahmoud
Co-Advisor: Rebecca Atadero

Kelly Strong

ABSTRACT

LIFE CYCLE COST ANALYSIS FOR JOINT ELIMINATION RETROFITS AND THERMAL LOADING ON COLORADO BRIDGES

Bridge expansion joints are a particularly troublesome component of bridges and many Departments of Transportation (DOTs) are looking for a solution to deteriorating expansion joints on highway bridges. Bridge expansion joints create a break in the structural continuity of a bridge allowing clogging gravels and corroding chlorides to enter. They are designed to absorb thermal movements of the bridge between two bridge elements. There are three main issues regarding expansion joint: maintenance, knowledge about thermal movements, and costs.

In order to prevent deterioration due to expansion joints the joints must be cleaned regularly and replaced promptly after failure. However, most DOTs do not have the personnel, time or resources to maintain expansion joints in their districts which leads to bridge deterioration. Other similar maintenance and component issues have been addressed using a Life Cycle Cost Analysis. For this to be used on expansion joints the three main issues of thermal knowledge, maintenance, and costs must first be addressed.

The main goal of this project is to help transportation agencies make better decisions about bridge expansion joints. The specific objectives of this study are to 1) expand understanding of thermal loading effects on bridge expansion joints and 2) conduct a LCCA for joint elimination and retrofits for bridges in Colorado. These objectives were accomplished utilizing data from in field instrumentation and finite element models. The study has been

developed jointly between the Colorado Department of Transportation (CDOT) and researchers at Colorado State University

Three main tasks were conducted to achieve the objectives: 1) collect and analyze long-term thermal loading data from existing bridges to assess thermal loading impacts on joints; 2) perform a parametric study using a calibrated finite element model to further understanding of joint behavior and retrofit options under thermal loads; 3) perform a LCCA for bridge expansion joint retrofitting including impacts on bridge superstructure.

The significance of this work includes the results of the data collection and analysis, the parametric study, and the LCCA findings. The preliminary data on the concrete bridge C-17-AT presented in this thesis only accounts for mid-winter temperatures. However, these limited observations do imply that if CDOT is interested in removing an expansion joint, the bridge superstructure and retrofit option would need to support the movement of the bridge. The parametric study and data analysis of thermal gradients indicate a stark need for further research into thermal gradients experienced by bridges. Finally, the LCCA concluded that a retrofit continuous bridge design would provide the most cost effective design by decreasing joint replacement costs and pier cap corrosion.

ACKNOWLEDGMENTS

I want to thank the CDOT Research Board for their funding and support. Jessica Martinez for her help gathering cost data, bridge information, field instrumentation, and support. Hussam Mahmoud and Rebecca Atadero for their work and support as my advisors throughout this research. Kelly Strong for his support and participation on my committee. Karly Rager for her help in field instrumentation and her development of the finite element model. Mehrdad Memari for his help in field instrumentation. Bashir Ahmadi for his help in field instrument maintenance. Nathan Kelly for his support, help on data collection trips, and help with coding. Stephanie Pilkington for her support and help on data collection trips.

TABLE OF CONTENTS

LIST OF TABLES

LIST OF FIGURES

CHAPTER 1

INTRODUCTION

1.1 Statement of the Problem

Bridges are old, deteriorating, and causing problems for many Departments of Transportation (DOTs). Bridge expansion joints are a particularly troublesome component of bridges and many DOTs are looking for a solution to deteriorating expansion joints on highway bridges. In fact, the present state of most highway bridges is drawing the attention of not only DOTs but also researchers and users. The need for a different maintenance strategy or a new solution to bridge expansion joints is apparent.

Bridge expansion joints create a break in the structural continuity of a bridge. They are designed to absorb thermal movements of the bridge between two bridge elements. Notably, expansion joints, and bearings, require regular maintenance throughout their life-span in order to function properly and thus inhibit damage to the bridge superstructure (Hawk 2003). A clogged joint can induce un-designed for stresses into the girders and abutments. A leaking joint can introduce corrosion into the superstructure below, primarily the pier caps (Lam et al. 2008). Deicing salts and chemicals used in colder regions increase the likelihood of corrosion beginning in the superstructure if a leaking joint is present. Additionally, for bridges located in the mountains, where chains are used on vehicles, can experience deterioration that is more extensive. These issues are what caused expansion joints to be named by the American Association of State Highway and Transportation Officials (AASHTO) as the second most common bridge maintenance issue behind concrete bridge decks (AASHTO, 2012).

There are three many issues regarding expansion joint: maintenance, knowledge about thermal movements, and costs. Expansion joints are very susceptible to a lack of maintenance due to DOTs lacking the people and resources to maintain their numerous bridge expansion joints regularly. A bridge expansion joint needs to be cleaned regularly, once very few months and repair to protect it from clogging and leakage due to a damaged or worn out seal. However, this type of maintenance is beyond the scope of DOTs, and consequently removing the expansion joints from existing bridges altogether might solve this maintenance issue. The second issue is a lack of current research on thermal effects on bridge joints, how much movement is induced by thermal loads, how much stress. Without knowing how important expansion joints are to bridge behavior, bridge movement and stress, it is hard to know how removing the expansion joints would affect the overall structure. Finally, costs are an issue that needs addressing. Costs are important in any long-term decision such as this one, DOTs need to know what makes the most economic sense regarding expansion joints. The economic issue could be addressed utilizing a life cycle cost analysis (LCCA) in conjunction with data analyzing the effects of temperature on joint behavior. Consequently, a more cost effective solution is could be obtained for the issue of deteriorating expansion joints in existing bridges that does not require frequent extensive maintenance and uses knowledge of thermal effects.

The use of life-cycle cost analysis (LCCA) in infrastructure design, maintenance, and repair is becoming more prevalent around the US as well as around the world. The public is becoming more interested in how officials use tax dollars, and thus encouraging agencies to look into and utilize better methods of infrastructure analysis for higher cost efficiency (Al-Wazeer, Harris, and Nutakor 2005; Ozbay et al. 2004). Stanford University defines LCCA concisely when they say it is the "process of evaluating the economic performance of a building [or other

piece of infrastructure] over its entire life" (University 2005). A LCCA of expansion joints on existing bridges in this manner could build on results of data regarding thermal behavior of bridge joints.

1.2 Objectives and Scope of Research

The main goal of this project is to help transportation agencies make better decisions about bridge expansion joints. The specific objectives of this study are to 1) expand understanding of thermal loading effects on bridge expansion joints and 2) conduct a LCCA for joint elimination and retrofits for bridges in Colorado. These objectives were accomplished utilizing data from in field instrumentation and finite element models. The study has been developed jointly between the Colorado Department of Transportation (CDOT) and researchers at Colorado State University. The study is composed of two stages. The first stage was to select two bridges for analysis, once with a steel superstructure and one with a reinforced concrete super structure, develop finite element modes of each bridge, and instrument the steel bridge. The second stage of the study was to instrument the reinforced concrete bridge, analyze the data collected from both bridges and conduct a LCCA for expansion joint retrofit options. This thesis composes the second stage of this study; the first stage was conducted by Karly Rager.

Three main tasks were conducted to achieve the objectives: 1) collect and analyze long-term thermal loading data from existing bridges to assess thermal loading impacts on joints; 2) perform a parametric study using a calibrated finite element model to further understanding of joint behavior and retrofit options under thermal loads; 3) perform a LCCA for bridge expansion joint retrofitting including impacts on bridge superstructure. Instrumenting bridges and collecting long-term data for Task 1 will afford CDOT with knowledge of joint movement and responses to

temperature which can be compared to standard thermal loadings from AASHTO. The parametric study in Task 2 will provide information regarding joint response to different clogging stiffness, thermal gradients, and retrofit options. This information can then inform parts of the LCCA and retrofit options for CDOT. The LCCA for Task 3 will provide CDOT with recommendations and costs regarding joint retrofitting on existing bridges. This LCCA will help provide a more cost effective solution that will meet the needs of CDOT and its existing bridges.

Due to this thesis composing the second stage of the study the research focuses on the two objectives listed above, expanding thermal knowledge and conducting a LCCA. In to fulfill these objectives this thesis covers the following

- A literature review of current research in LCCA of existing bridges
- The instrumentation, data collection, and data analysis for the selected reinforced concrete bridge
- A controlled load test for the reinforced concrete bridge's finite element model validation
- A parametric study analyzing the joints response to different clogging stiffness, thermal gradients, and retrofit options
- A LCCA of bridge expansion joints and retrofitting.

CHAPTER 2

LITERATURE REIEW FOR LIFE-CYCLE COST ANALYSIS OF BRIDGES WITH EXPANSION JOINTS

2.1 Introduction

LCCA involves determining all costs associated with a piece of infrastructure over its design life. These costs range from design and construction to maintenance and user costs to environmental and vulnerability costs (Frangopol and Liu 2007; Marques Lima and de Brito 2010; Hawk 2003; Safi, Sundquist, and Karoumi 2015; Kim et al. 2010; Hatami and Morcous 2014; Reigle and Zaniewski 2002). Once all costs have been identified, they are referenced to a point in time and the total calculated. This total cost for an infrastructure's entire life-span is the life-cycle cost (LCC) which can then be compared to the life-cycle cost of other designs for the same piece of infrastructure. LCCA becomes an effective way to compare designs and support the choice of a particular design as the most economically effective choice overall even if its initial cost is high (Hatami and Morcous 2014). This can be particularly helpful when talking to the public or working in public design and construction (Al-Wazeer, Harris, and Nutakor 2005).

Like any analysis process LCCA is based on a couple of assumptions. Performing an LCCA assumes that there are multiple designs for the same desired piece of infrastructure, whether bridge, building, or roadway, and that each of these designs can meet the needs and required performance capabilities. Additionally, it is assumed that each of these designs has varying initial, operating, and maintenance costs and can have varying lengths of life-span (University 2005). Therefore, these assumptions must be true and taken into consideration when performing a LCCA. If the case of several designs having different life-spans is the case, they

must be manipulated to have a common life-cycle to compare them using a LCCA. For example, if design A has a life-span of 25 years and design B has a life-span of 50 years then an analysis could assume that at the end of design A's life span a second design A is built to have a life-span of 50 years' total. Then the combined consecutive construction of two design A's can be compared to design B using LCCA.

The LCCA process is laid out in Figure 2-1 below. Furthermore, designs with only one major component difference can be compared and the most cost effective design type chosen using LCCA. This creates a simpler analysis where only a few variables are different between the two designs. Kang, Lee, and Hong utilize this approach by analyzing two designs for the same bridge, where the two designs use different superstructure components, for example using prestressed concrete beams vs prestressed box girders (Kang et al. 2007). For their LCCA instead of analyzing the costs associated with every component of the bridge, they focus on only those associated with the superstructure leading to a slightly simplified analysis.

However, LCCA is not limited to newly designed infrastructure. This analysis approach can also be utilized when looking at deteriorating infrastructure in need of maintenance, repair, and/or replacement. When looking at existing infrastructure, costs of maintenance, repair, and replacement along with costs to users due to inconveniences are included in the life-cycle cost. These life-cycle costs can be compared for different methods of maintenance, repair, and replacement to determine the most economical long-term solution. After all "one of the main aspects to be considered in LCCA of infrastructure is the anticipated maintenance and/or rehabilitation to be performed throughout the structure's life span" (Osman 2005).

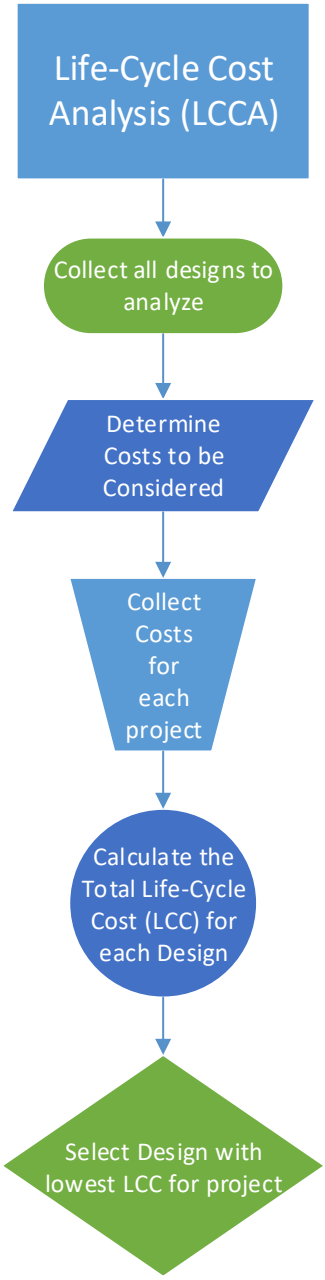

Figure 2-1 Life-Cycle Cost Analysis Process Flow Chart

Furthermore, according to Safi, Sundquist, and Karoumi in the European Union there is more extensive application of LCCA to existing structures in need management and relatively little application to new structures (Safi, Sundquist, and Karoumi 2015). This is despite the fact that LCCA applied to any structure will produce long term savings, and if applied to a new

structure it will produce the maximum savings because they were applied over the entire length of the structure's lifetime (Agency and Severn 2000). However, an existing structure can also benefit from LCCA due to the structural system being composed of many smaller parts and each of these has a different and likely shorter lifespan than the overall system. Furthermore, these components are not usually easy or simple to replace and therefore the costs associated with that replacement or repair can be critical (Riedel et al. 1998). This is not to say that designing a structure with these costs in mind at the beginning with an LCCA is not better in the long run, it is, however, using LCCA in the continued maintenance is also beneficial.

There are several aspects that hinder the application of LCCA to new structures. One that is proposed by Safi, et. al. that could be hindering the application of LCCA to new bridges in particular is the assumption that bridge management systems (BMSs) are completely separate from LCCA, when in reality much of the data used in BMS could help determine an accurate LCCA (Safi, Sundquist, and Karoumi 2015). Another problem could simply be an incomplete understanding of LCCA benefits among implementers (Goh and Yang 2014). Additionally, LCCA requires foresight, the funds to support a slightly more expensive design with long term savings in mind, and time to perform the analysis. These deterrents are slowly becoming overwhelmed by the benefits of LCCA as they become better known and supported by federal agencies.

As the benefits of using LCCA in infrastructure analysis become common knowledge, it is suspected that more and more states will implement it as a regular practice. Utilizing LCCA can enable government and state agencies to make the most economical design and repair decisions regarding public infrastructure over the infrastructure's entire life-span. This can lead

to minimized maintenance, repair, and replacement costs as well as minimize delays and costs to users over the structure's life-time.

All infrastructure is an investment; public infrastructure is an investment of the public's funds consequently, interest in the best use of funds for infrastructure maintenance is growing. According to Goh and Yang, before 1990 there was very little attention given to LCCA, however in 1990 the Federal Highway Administration began to encourage its use in projects and later made it mandatory for projects of $25 million or more (Goh and Yang 2014). Research and application have been increasing in all areas of infrastructure since this mandate. LCCA is becoming an integral part of design and maintenance of infrastructure and therefore should not be taken lightly.

2.2 Components of LCCA

Several components make up the costs analyzed in a LCCA. These components can mean slightly different things for different types of infrastructure, for example bridges versus buildings will have slightly different costs associated with them. Common cost components include: initial/construction, operation, maintenance, renewal/replacement, cost of capital, and user (Board 1998). Below, in Figure 2-2 is a flow chart showing the components of each cost, followed by a general description of each of the main components of cost that are related to LCCAs.

Initial Cost is perhaps the simplest component of LCCA cost components. The initial cost is what the project will cost up front. This includes the costs of the design, the contract, the project management, the construction, and the final inspection and certification, if necessary.

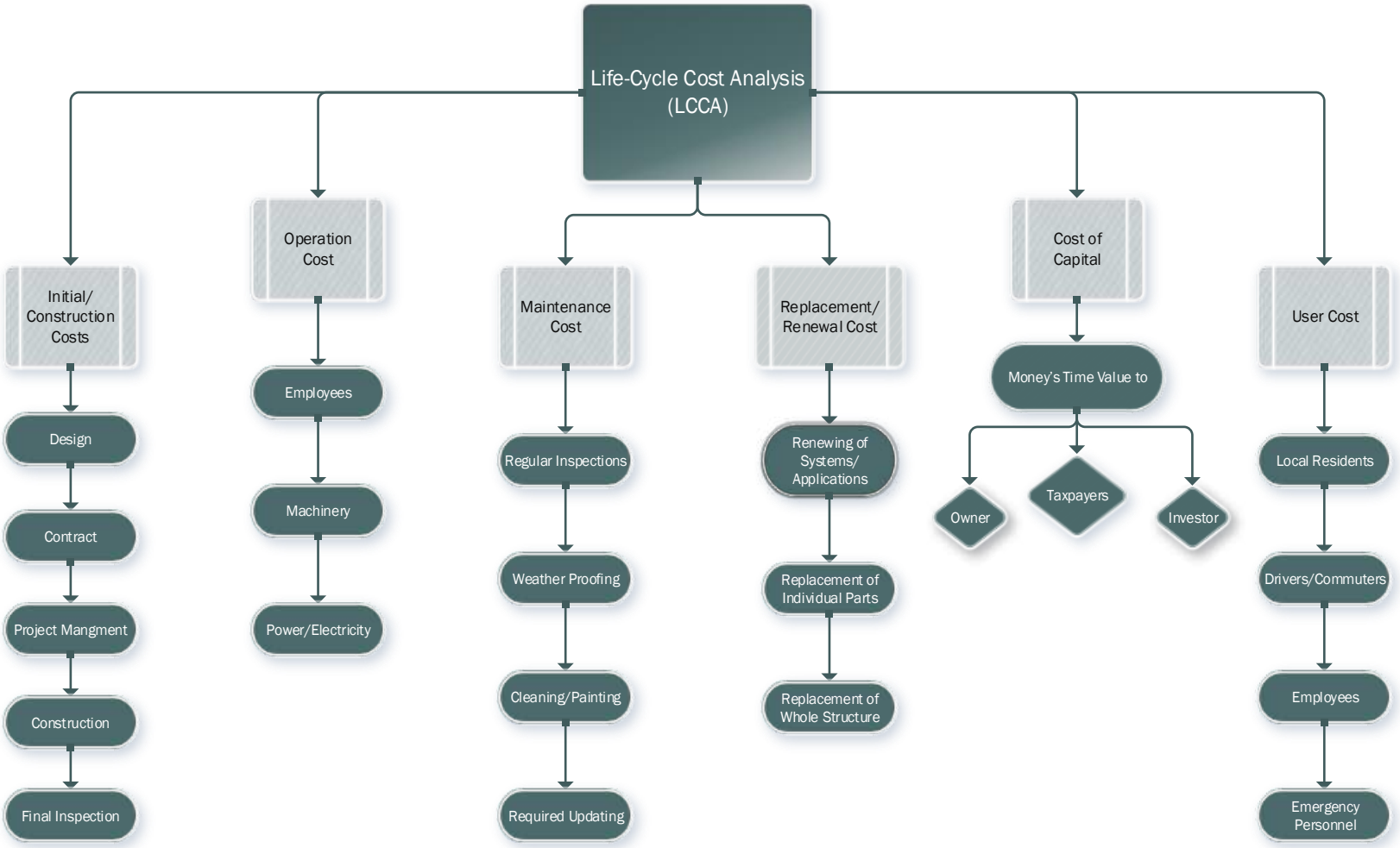

Figure 2-2 Life-Cycle Cost Analysis Costs Flow Chart

Initial cost is what has been traditionally used to choose which design to use for a project, independent of any of the other costs. The agency would traditionally receive several design bids and would choose the lowest bid (Safi et al., 2015). The lowest bid procurement process does not account for any of the other cost components occurring throughout the structure's life. Instead of choosing the project with the lowest initial bid, the design could be chosen based on lowest life cycle cost (LCC) bid, which is what is proposed to the European Union Directive by Safi, Sundquist, and Karoumi (2015).

Operation Cost is the cost needed to operate the infrastructure over its life-span. This cost varies greatly depending on the infrastructure being analyzed. Some structures will have little to no operational costs, such as a simple bridge. However, other structures, such as buildings, drawbridges, or toll roads will have various operation costs associated with employees and machinery. These costs could include employees to run the machinery or toll booths and electricity to power the structure.

Maintenance Cost is the cost of maintaining the infrastructure in a safe, usable, and functional condition. Maintenance costs can include regular inspections, weather proofing, cleaning, painting, and any type of required updating. Depending on the structure these maintenance costs could be as frequent as monthly or as infrequent as every few years. The importance of having funds to perform the maintenance is also going to depend on the structure. For example, the repainting of a steel bridge to prevent corrosion could have more importance then the repainting of a concrete building on schedule because the steel bridge is typically going to be more immediately susceptible to deterioration then the building.

Renewal/Replacement Costs depend on the object of analysis, whether the objective is renewal of the structure or replacement of the structure in part or entirety. Renewal costs would

be applicable to costs due to the renewing of software or electric systems. Whereas a replacement cost would apply to the replacement of anything connected to that piece of infrastructure or equipment. This could range from the replacement of a single element to the entire structure.

Cost of Capital is the money's time value to the owner, investor, or in the case of public works the taxpayers (Board 1998). This cost adjusts for the fact that choosing a design using LCCA often means a higher initial cost compared to designs that do not use LCCA and would have higher maintenance and repair costs later. Therefore, the money's time value is accounting for using that extra money to have a lower overall cost instead of using it to invest in something else.

User Cost includes any costs to users of the infrastructure or system. This can include costs to drivers and passengers due to construction or traffic blocks for repair or replacement ("Life Cycle Cost Optimisation in Highway Concrete Bridges Management," n.d.). Another example of user costs could be due to relocating of employees in the case of a building's repair or maintenance.

2.3 Components and Parameters Related to Bridge Maintenance

Bridge design, maintenance, repair, and replacement have specific costs within each general cost component of LCCA. Below Figure 2-3 shows a flow chart for the LCCA costs specific to bridges. In order to compose a thorough LCCA for a bridge, each component of the LCCA must include all aspects that affect the bridge. In other words, the parameters must be tailored to the infrastructure and its environment, in this case a bridge and the outdoors (Hawk 2003).

There are also parameters in addition to the cost components that need to be taken into consideration and are of particular interest to bridges. These include the service life of the bridge and the analysis period of the LCCA. The service life is the time period over which the components of the bridge and the bridge itself are in serviceable condition based on the industry standard for acceptable condition limits. The service life does not always equal the design life, a design life might account for repair or replacement of some bridge's substructure parts. However typical Best Management Practices (BMPs) assume a service life between 70 and 100 years. On the other hand, the analysis period is the period of time over which all costs in the LCCA are analyzed and brought to a total present value. This time period can be shorter or equal to the service life of the bridge, depending on the period the buyer wishes to analyze based on what years are of most importance. Nonetheless, typically the analysis period is made equal to the service life in order to simplify the LCCA (Hawk 2003). However, if the analysis period is less than the service life there is a value left due to the remaining serviceable life of the bridge.

Initial and construction costs are some of the simplest components of a LCCA for bridges. Both are constant values, with little uncertainty associated with them because they are onetime costs at the beginning of the bridge's life. The initial cost is composed of the design and contractor costs, while the construction cost is the cost of the construction materials, workers, and time, as well as any road closure costs due to the bridge's construction. This last aspect of construction cost affects user costs as a road or lane closure and/or detour will affect the drivers in the area.

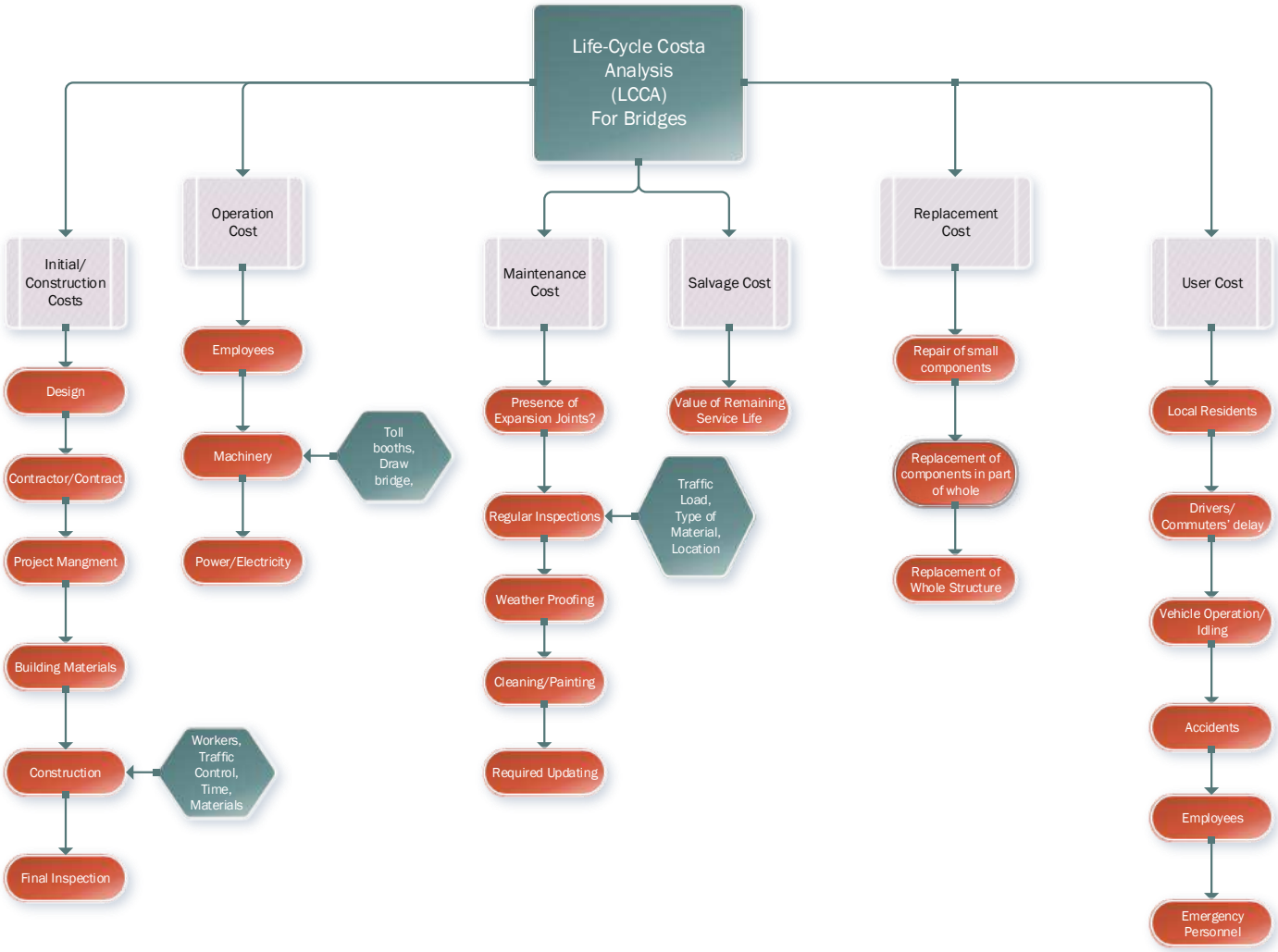

Figure 2-3 Life-Cycle Cost Analysis Costs Flow Chart for Bridges

The maintenance costs for bridges depend on several key factors. The planned life-span, the bridge structural material (i.e. steel or concrete), the anticipated traffic load, the environment, whether or not preventative maintenance is included (Reigle and Zaniewski 2002) all affect maintenance. Additionally, whether or not the bridge contains an expansion joint (and if it does, the type of expansion joint used) can also impact the maintenance costs. In fact, when considering the LCCA of a bridge with expansion joints, they "should be considered a critical factor" (Savioz, P. Spuler 2014). Expansion joints are very susceptible to clogging, corrosion, and deterioration due to dynamic load impacts on their various components, which are more delicate when compared to a steel or concrete girder. Consequently, the probability of maintenance needed on the bridge will increase with the presence of an expansion joint. Furthermore, because they are a weaker bridge component that spans the width of the bridge, they can have significant impacts on other costs such as user and replacement costs as well.

Repair and/or replacement costs for bridges are composed of the cost of repairing and/or replacing each component of the bridge with respect to that component's life-span in comparison to the overall bridge's desired life-span.

User Costs for a bridge are composed of costs to the drivers and residents who were affected by the closing of or limiting of traffic on the bridge due to maintenance, repair, or replacement. They are in some ways the most involved costs in an LCCA because they involve the public which increased variability. These costs are due to delays to drivers personally, costs of vehicles idling in traffic, and accident rate increases due to road work (Kim et al. 2010; Reigle and Zaniewski 2002). As such they should be minimized by minimizing the disruption caused by the repair or maintenance (Agency and Severn 2000). This could be done by limiting the closure to one lane at a time and performing maintenance, repair, or replacement in stages/portions.

These aspects can be categorized as three individual costs the sum of which equals the User costs included in a LCCA. Kim et al. (2010) define these costs and formulate the following equations to use in a LCCA. The driver delay cost, vehicle operating costs, and accident costs are defined in equation form below and all variables are listed in Table 2-1 (Kim et al. 2010).

$$\text{Driver Delay Cost} = \left(\frac{L}{S_a} - \frac{L}{S_n}\right) \times ADT \times N \times w \quad (2.1)$$

$$\text{Vehicle Operating Cost} = \left(\frac{L}{S_a} - \frac{L}{S_n}\right) \times ADT \times N \times r \quad (2.2)$$

$$\text{Accident Cost} = L \times ADT \times N \times (A_a \times A_n) \times c_a \quad (2.3)$$

Table 2-1 Parameters Assumed for User Cost Computation (Kim et al. 2010)

Parameters	Symbols
Length of Affected Roadway (km)	L
Average Daily Traffic (ADT)	ADT
Normal Driving Speed (kmph)	S_n
Roadwork Driving Speed (kmph)	S_a
Normal Accident Rate (per million vehicles)	A_n
Roadwork Accident Rate (per million vehicles)	A_a
Hourly Driver Cost (US$)	w
Hourly Vehicle Operating Cost (US$)	r
Cost per Accident (US$)	c_a
Required Days for Repair	N_{repair}
Required Days for Replacement	$N_{replace}$

Each of the parameters in Table 2-1are used in the three user cost equations (2.1), (2.2), and (2.3). Furthermore, each is specific to that bridge. Therefore, the parameters in Table 2-1 above are an example of parameters that might be used for a LCCA and would need to be adjusted for a different specific bridge based on its location, current rates, expect traffic, dimensions, and any other available information.

2.4 Maintenance of Bridges with Expansion Joints

The maintenance, repair, and replacement (MR&R) procedures and the costs associated with them for bridges are critical to a bridge's LCCA. The MR&R are a substantial portion of the total life cycle cost for a given bridge (Mao and Huang 2015). They can be divided up as MR&R costs for each component of the bridge, such as the beams, columns, deck, and expansion joints (Kang et al. 2007). In fact in 2002 a study showed that 20-50% of total infrastructure costs were due to MR&R in various countries (Mao and Huang 2015). Therefore, the cost of MR&R is directly related and important to the overall LCCA. The many factors that influence MR&R costs for bridges are summarized in Figure 2-4 below. Traditionally LCCA in general and MR&R costs specifically have been analyzed using statistical models and analysis, such as simple regression and overall trends to calculate costs based on collected data (Mao & Huang, 2015). Furthermore, many traditional LCCA methods also neglect user costs and preventative maintenance benefits and costs due to a lack of data or the complexity of the calculations which can affect all costs including MR&R costs (Reigle and Zaniewski 2002).

Various LCCA models are discussed further in Section 2.5, Current LCCA Models for Bridges. However, most models do not give a specific approach for the maintenance costs which can make it hard to determine that cost (Mao and Huang 2015; Hawk 2003). A more accurate and specific method would be to include probabilistic approaches, because "estimation depends on predicting how bridges deteriorate over time and what subsequent actions are taken" (Mao and Huang 2015). These costs should then be based on those predictions. Mao and Huang (2015) conducted a study to estimate the MR&R costs of a bridge using a Monte Carlo simulation applying probability distributions. They chose an expansion joint as their example bridge component, nonetheless the analysis could be applied to any bridge component and then

the sum of all MR&R costs for each component would equal the total MR&R costs for the bridge.

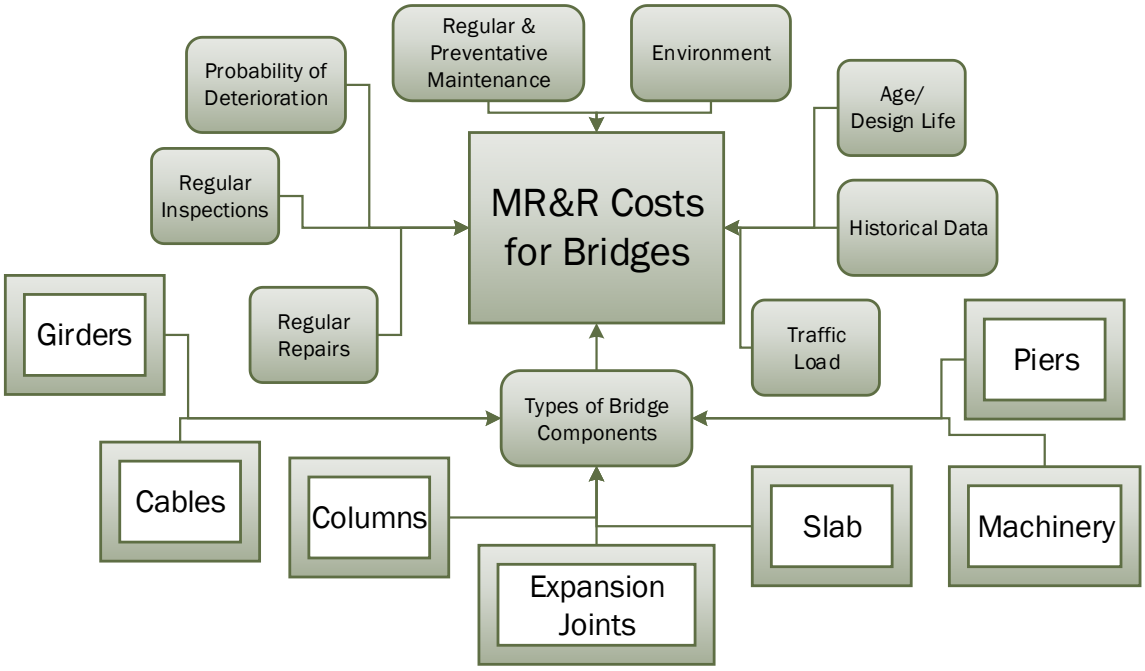

Figure 2-4 Factors affecting MR&R Costs for Bridges

However, using just a stochastic model utilizing probability of deterioration or defect and the probability that further deterioration will develop has limitations too. For example using a strict Markovian probability model might not account for unique factors affecting the current state of the bridge. The probability of transition from one form of deterioration to another requires sufficient observed data related to the specific bridge which may not be available, especially for newer bridges (Mao and Huang 2015). Furthermore, Huang and Mao argue that the future condition of the bridge is affected by the bridge's history, while Markov processes are in part defined by the fact that future conditions only depend on the current condition. While, probability should be a key part of predicting defects and deterioration and thus MR&R costs, it should not be the sole source of that information, other current and historical observations and the overarching deterioration processes should be used to enhance that prediction.

Typically, bridges are inspected visually for signs of deterioration and/or defects. While visual inspection can be subjective depending on the person, the bridge, and the governing guidelines or procedures, it still provides data for each aspect of a bridge. Furthermore, because bridges have been regularly visually inspected for the past forty years in the US and for many years in other countries as well, there is a wealth of data and knowledge that if made available could be used as a basis for a deterioration model prediction and the evaluation of MR&R costs (Mao and Huang 2015). These observations and archived data could be used to compliment a probability matrix in order to predict the future needs for MR&R of a bridge.

Furthermore, expansion joints are common in various forms in most bridges and are therefore a key, and at times critical, component for maintenance of a bridge, as well as a main component affecting costs in an LCCA. While most manufacturers will tout their expansion joints as having long service lives free of maintenance, in the field this is seldom true. In fact the joints are commonly the first bridge components to need maintenance or repair (Marques Lima and de Brito 2010). This is due to their experiencing millions of impact loads from vehicle wheels throughout their lifetime. These repeated impact loads can result in failure due to fatigue cracking (Savioz, P. Spuler 2014). Their deterioration can also be increased if water and/or debris is able to creep into the joint. Therefore, choosing the best type of expansion joint for the bridge and environment is critical to minimizing maintenance and replacement costs.

While joints are not an expensive part of the initial cost of a bridge, usually only about 1% of the total construction cost (Marques Lima and de Brito 2010), as discussed above they can have a disproportionate effect on the maintenance/replacement costs over the life span of the bridge. A study in Portugal showed that over “the previous 3 years, more than 20% of the bridge conservation costs were related [to] the repair and replacement of expansion joints” (Marques

Lima and de Brito 2010). However, some of the other cost parameters are indirect costs associated with expansion joints such as costs to users due to limited or detoured traffic when conducting maintenance or repair.

As relates to joint maintenance and repairs of defects, to minimize the damage and thus the cost, a preventative approach should be taken towards bridges and expansion joints rather than a corrective approach. A corrective approach only addresses the problem when it has become so bad as to threaten serviceability, whereas a preventative approach addresses the problem when it first begins to develop in order ensure that it does not grow worse.

The first step in a preventative approach to maintenance and repair costs is choosing the right expansion joint type. The Colorado Department of Transportation (CDOT) typically uses a Strip Seal expansion joint, otherwise known as an Elastomeric Seal expansion joint. This type of joint uses an elastomeric "v-shaped" neoprene gland strip inserted into two parallel steel rails to seal the joint (CDOT 2015). Below Figure 2-5 shows a drawing of a Strip Seal, per CDOT standards. There is another variation on the strip seal, called a "hump seal" which adds a second layer of neoprene that humps up as the joint closes and stretches out as the joint opens. This "humping" up when the joint seals can serve to push out any debris or dirt that might have fallen into joint (Savioz, P. Spuler 2014). The "hump seal" provides self-cleaning which can potentially slightly decrease the frequency of maintenance inspections needed for the joint.

Another way to implement a preventative approach is by locating any defects in the expansion joint early on in its development and fixing or correcting the issue to prevent degradation that might have otherwise been introduced by the defect (Marques Lima and de Brito 2010). What might start out as a small insignificant deterioration or defect, could become a much larger problem if it is left to be subject to continued loading and environmental effects.

This would exacerbate what started out as a small problem, cheap and simple to fix, turning it into a costlier operation that might require a more extensive road closure, affecting user costs.

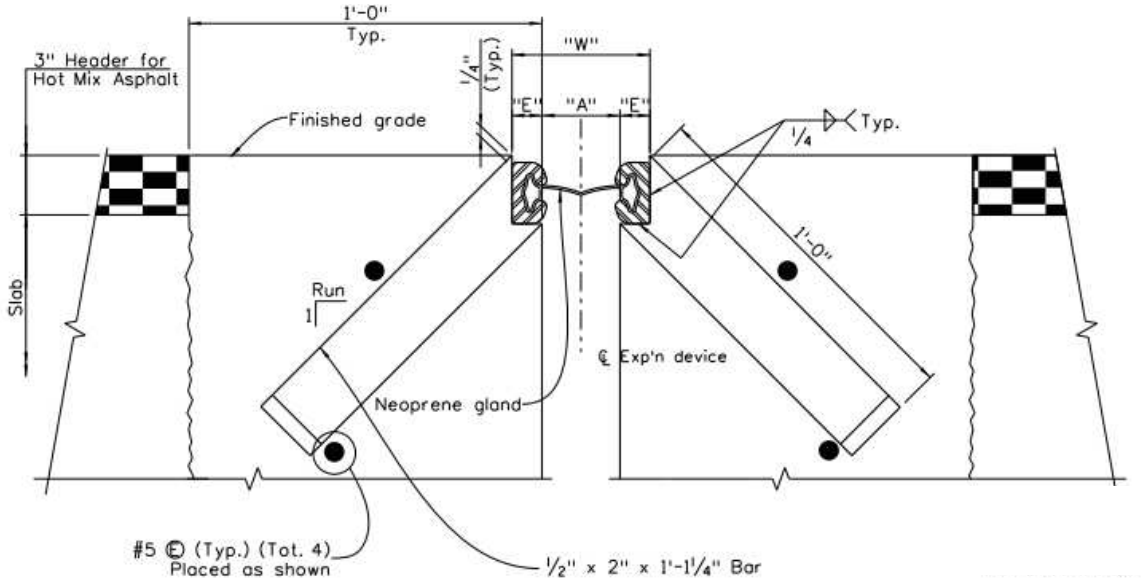

Figure 2-5 Section Thru Strip Seal Bridge Expansion Device (CDOT, 2015)

Regular bridge inspections for maintenance are part of the maintenance costs in a bridge's LCCA. While joint inspections are included in regular bridge inspections it is possible that they would need to be more frequent then the regular bridge inspection. This could be due to the degradation rate of a joint is higher. A joint's degradation rate is affected by the type of joint, the volume of traffic experienced by the joint, and the environment in which the joint is located. Marques Lima and de Brito (2010) categorize 12 different types of expansion joints from least amount of movement allowed to most, "open joints" to "preformed compression seal joints" to "multiple seal in metal runners joints." These types of joints are shown in Figure 2-6 below. Type 6 in Figure 2-6 is the elastomeric flexible strips, the same as the CDOT strip seal.

Each type of joint is susceptible to different types of degradation and defects and thus would affect the degradation rate. Additionally each joint type would have different initial, maintenance, and repair costs (Kang et al. 2007). Similarly depending on the bridge type and

location it will experience different traffic volumes, and a bridge with higher traffic volume will experience a higher rate of degradation (Marques Lima and de Brito 2010). Finally, the environment will affect the degradation rate, a dry land bound environment will cause less degradation then a wet coastal environment. Due to these many factors Marques Lima and de Brito (2010) recommend that the period between joint inspections should never exceed 15 months for a bridge with a high traffic volume.

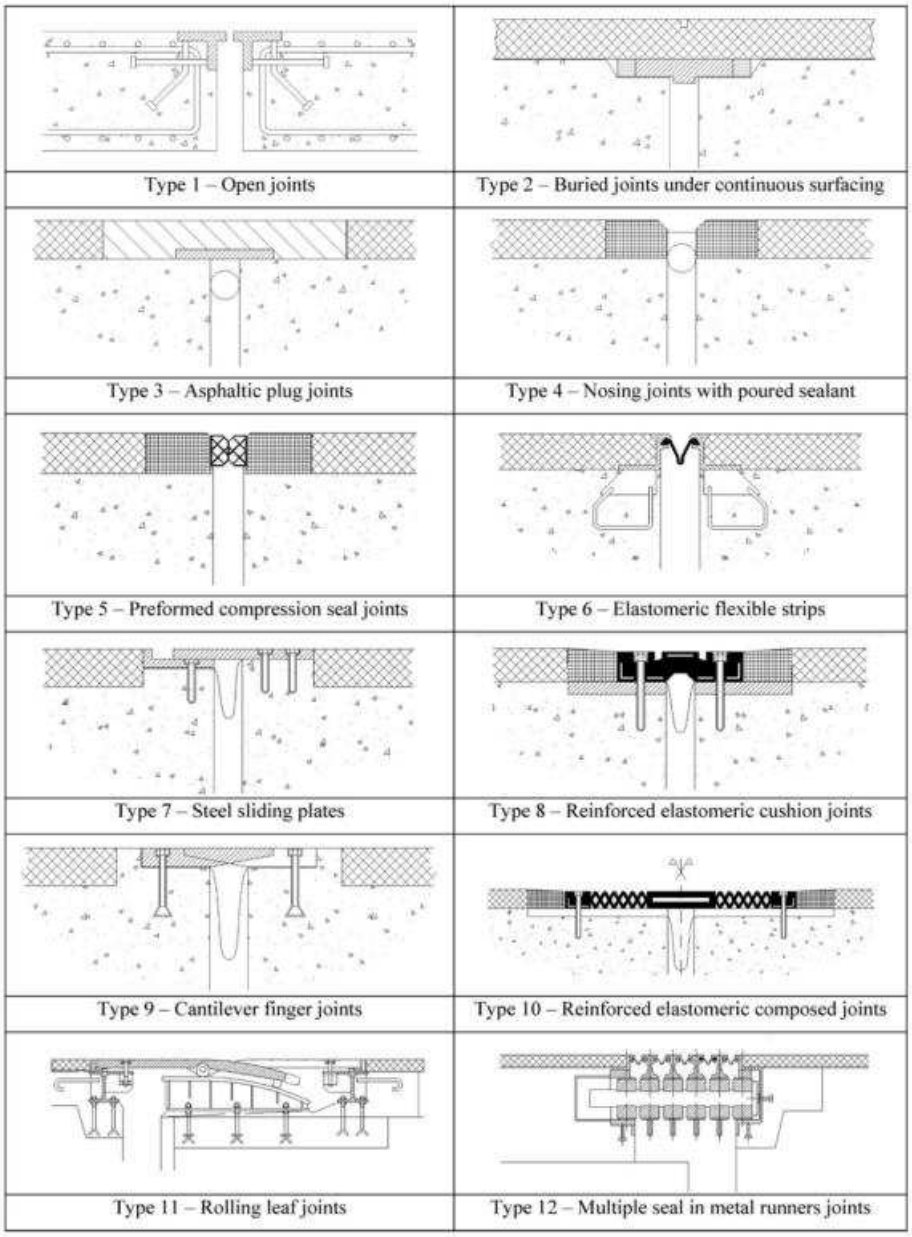

Figure 2-6 Types of Joints(Marques Lima and de Brito 2010)

Additionally, it should be noted that once one defect or type of degradation is detected matrices can be used to determine the probability of other defects occurring due to association with the first defect (Marques Lima and de Brito 2010). This is additional support for approaching bridge maintenance with a preventative approach. These defects can be due to a variety of causes, as listed in detail by Marques Lima and De Brito, in general, however, they can be due to design errors, manufacturing defects, installation error, a lack of maintenance, a sudden increase in traffic or use, a change in environmental factors, or sudden impact loads.

Marques Lima and de Brito (2010) propose a rating system for defects in expansion joints. This system determines the rating in terms of the defect's severity and thus how detrimental it is to the service of the bridge. The rating system uses Equation (2.4) below.

$$P_i = 0.2I_{ext}\,(6I_tI_{loc}C_{vt} + 5I_c) + 2I_pC_{ep} \qquad (2.4)$$

Where P_i is the rating of the defect i. Each I is an index for defect extent, service life penalty, traffic penalty, defect location, structure potential penalty, and population penalty respectively, varying from 0 up to 5 depending on the index and based on increasing severity. The C's are coefficients for traffic volume and surrounding population respectively. The numbers correspond to percent weights for the system such that if every index and coefficient where to be at critical the total rating would be 100. However in reality the highest rating would be 94 which concerns collapse or missing joints. Anything higher than 50 is considered very urgent and action should be taken immediately (Marques Lima and de Brito 2010). Similarly, if a joint is in perfect condition then the rating should be equal to zero.

The total degradation of a joint can be classified as D_x, which is the sum of defect ratings, P_i, of all defects in the joint. See Equation (2.5) below.

$$D_x = \sum_{i=1}^{n} P_i \tag{2.5}$$

This equation (2.5) would enable the comparison of multiple expansion joints in the bridge and therefore the most serious one could be repaired first.

Furthermore, when the expansion joint fails, comes to the end of its design life, or is requiring excessive and expensive maintenance and repair costs then the joint should be replaced (Savioz, P. Spuler 2014). This is a simple LCCA with fewer costs included, in it the cost of continued maintenance is compared to the cost of replacement and when the latter becomes the smaller number then replacement should occur.

The goal throughout all MR&R is to maximize the service life of the expansion joint while minimizing the cost. This fits directly into the objective of LCCA for bridges. Expansion joints are a significant part of bridge design, by increasing their life cycle while minimizing maintenance cost the overall life cycle cost can be decreased.

2.5 Current LCCA Models for Bridges

Over the last few decades several LCCA models for bridges have been developed and redeveloped. Currently there are three main types of LCCA models, deterministic, rational, and probabilistic as seen in Figure 2-7 below. Each type has advantages and disadvantages depending on whether the bridge is new or old, and depending on the available practitioner experience in this area or access to archived observed deterioration data. Furthermore, each general model type has overlapping ideas and assumptions, as well as numerous variations developed by various researchers.

The simplest type of LCCA model is a deterministic model, where each contributing cost constraint is identified, a corresponding cost value is found or estimated for each and the total is summed. The final LCC is a discrete deterministic result. This method produces an "acceptable range" but not a detailed or reliability based LCC (Basim and Estekanchi 2015). This model type does not account for uncertainties, variation, or costs due to unexpected events affecting the bridge (Reigle and Zaniewski 2002). The neglect of uncertainties in the deterministic LCCA approach can cause the results' validity to be questioned because uncertainty is a part of any future value or cost. The cost components for costs over the lifespan of the bridge or structure might be the estimated median cost due to each component (Basim and Estekanchi 2015) but an average does not account for probability due to different environments or events. The maintenance cost per year is often a rough estimate using a specified percentage of the construction cost if there is no historical data to use. Although if historical data is available that value is preferred. Some costs that are hard to estimate or predict without data and probability are neglected, these might include some or all costs associated with users (Kang et al. 2007).

Rational models for LCCA are a combination of deterministic and risk analysis. They primarily take a deterministic approach but base the cost values on recorded data of similar bridges. These costs are based on the frequency of a certain cost affecting bridges in similar situations to the one being analyzed. Marques Lima and de Brito use a rational model for their LCCA, which is described for expansion joints above in section 2.4. Their model is primarily only for MR&R costs; however the rational model could be expanded for whole bridge analysis. In general their model uses a combination of matrices and tables which contain the various bridge or joint components, their respective rating, and maintenance cost (Marques Lima and de Brito 2010).

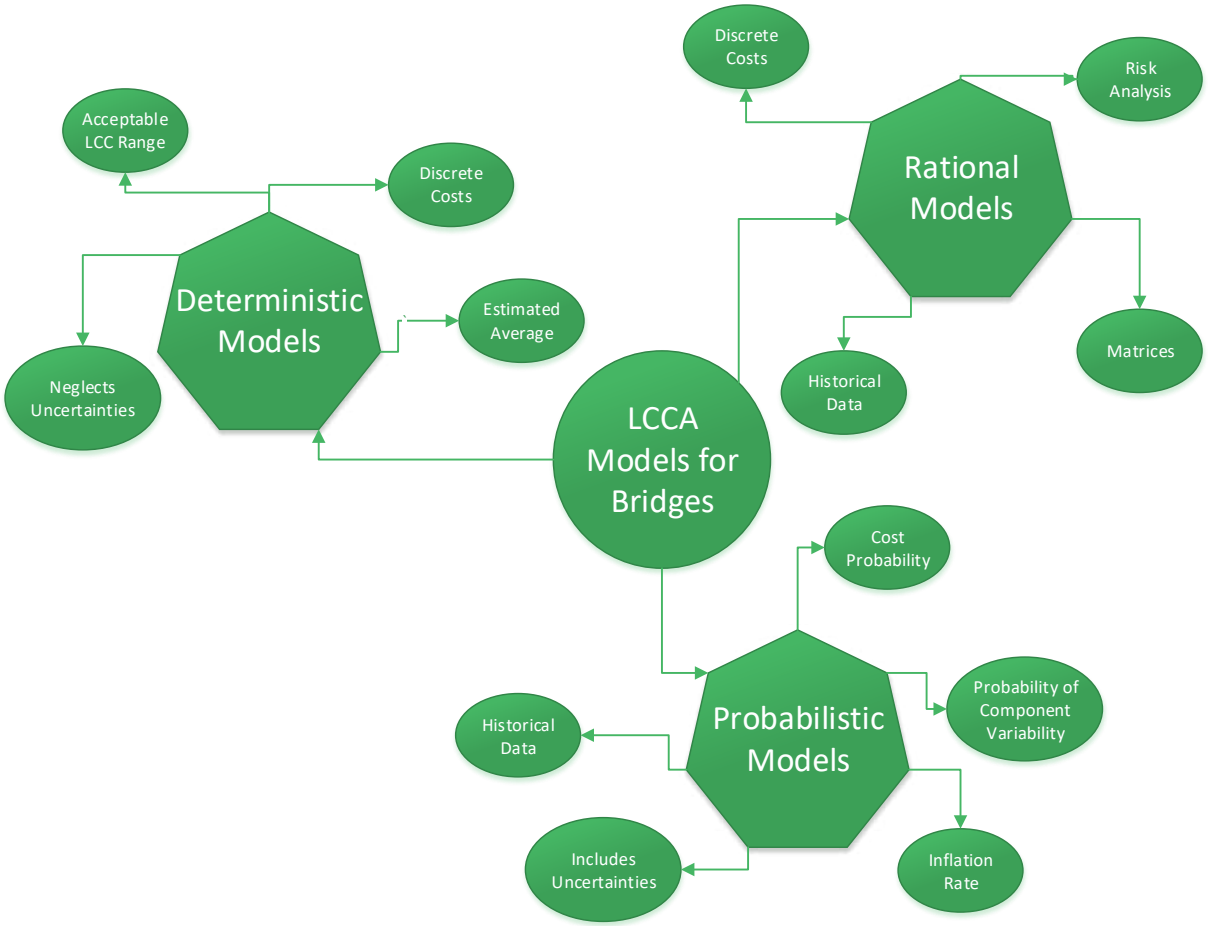

Figure 2-7 Life-Cycle Cost Analysis Models for Bridges

Probabilistic LCCA models are based on the probability of each cost occurring, a risk analysis to determine the probabilistic risk associated with each cost, and the inflation rate over the life-span of the bridge. This approach finds the variability associated with each cost component. If information and data are available, perhaps from the State Highway associate or the local Department of Transportation, then it can be analyzed to estimate the probabilities associated with each parameter. The risk of each cost could then be modeled mathematically (Agency and Severn 2000). However, if this type of data is not available or accessible then a qualitative risk assessment could be conducted (Agency and Severn 2000). By including the uncertainty of the various cost components, the decision maker can take them into account when

comparing different scenarios or designs (Reigle and Zaniewski 2002). For most probabilistic LCCA models probability distributions are used and all costs are brought back to a present worth value using basic net present worth analysis. Using a present worth analysis accounts for the monetary changes in a life cycle of various components and combining it with uncertainty analysis can provide a precise LCC (Girmscheid, n.d.).

While some probability analyses rely on analysis of bridge inspection data to form probabilities for the cost components, other LCCA models use predictive models (Reigle and Zaniewski 2002). A probability or risk based LCCA model creates a more universal model because costs for each component are going to be similar for different bridges, however, the probability will change based on the environment, location, and conditions. Therefore, if probabilities are developed for the specific situation, or design, then the LCCA can be conducted for that bridge.

In order to determine the probabilities for a LCCA all possible "hazards and accidental load scenarios" must be identified before their probability can be found (Agency and Severn 2000). If data is not available for analysis and calculation of probabilities, then a simple risk interaction matrix can be used. An example from Agency & Severn is below in Table 2-2. This matrix can then be used to analyze the hazards and risks associated with a given bridge. Agency & Severn took a 25 year old existing bridge as an example and analyze the risks with an interaction matrix as seen in Table 2-3 below. However, if a risk interaction matrix were to be used in a LCCA then the various classifications of severe, high, medium, low, frequent, occasional, remote, improbable would need to have probabilities associated with their intersections: unacceptable, tolerable with precautions, and acceptable. Furthermore, the

mitigation for each hazard would need to be quantified as a cost. These probabilities and costs could then be used in relation to the various hazards to determine the LCC in the LCCA.

Table 2-2 A Risk Interaction Matrix (Agency and Severn 2000)

Severity Category	Likelihood			
	Frequent	Occasional	Remote	Improbable
Severe	U	U	U	U
High	U	U	U	T
Medium	U	T	T	T
Low	T	T	A	A

A = Acceptable T = Tolerable with precautions U = Unacceptable/undesirable

While Agency & Severn's solution to a lack of reliable data, described above, is workable it is not as ideal nor as precise as analyzing real inspection data for probabilities. Hesham Osman in his report on "Risk-Based Life-Cycle Costs" discusses this need for reliable inspection data as one of the disadvantages of Probabilistic LCCA. He cites the need for large amounts of reliable cost and performance-related data, simulation capability and statistical manipulations as a hindrance to probabilistic analysis (Osman 2005). However, this is a limitation for him because he is focused on private sector design and building.

Federal and State agencies such as state departments of transportation have access to all of their previous bridge inspections and performance data for various types of brides in different types of locations. Therefore, if a LCCA is being carried out in the public sphere by either the State Highway Association or local Departments of Transportation or another company contracted by one of them, the data should be available for probabilistic analysis.

A newer bridge will have a higher probability of the "do nothing" action (the least severe action) being chosen because most of its deterioration is minimal and non-serious with respect to the serviceability of the bridge. The converse would be true of an old bridge which would have a higher percent of severe deterioration and thus a higher probability of needing repair or

replacement. As the bridge ages and begins to exceed 30 years in service the probability of replacement increases to 100% quickly (Mao and Huang 2015). Therefore, these probabilities can be used to determine the LCC for MR&R costs for a bridge based on its current age.

Table 2-3 Risk interaction matrix for Example (Agency and Severn 2000)

Hazard	Likeli-hood	Sev-erity	Initial Risk	Mitigation	Residual Risk
Overload	Remote	High	U	Bridge was designed to British Standards, carry out assessment to Eurocodes. From past data and bridge location, review the possibility of abnormal vehicles	T
Dispropor-tionate and progressive collapse	Remote	High	U	Assess the effects of failure of parts, such as bearings or bolts. Confirm that structure has sufficient redundancy and that requirements of Eurocode 1 are met.	T
Vehicle Impact	Occas-ional	Med-ium	T	Bridge was designed with standard UK aluminum parapet. Cary out assessment to Eurocodes and using local UK risk assessment methods for parapets.	T
Corrosion	Occas-ional	Med-ium	T	Review precious inspections. Carry out further inspections at time intervals specified in local UK requirements. If there is corrosion, determine likely loss of section for use in assessment.	A
Flooding to beam level	Remote	High	U	Bridge original designed for flood flows. Review historical river flow data. Assess structure for debris loads and water pressures if required.	T
Scouring Foundation	Remote	High	U	Review previous inspections. Cary out further inspections at low flows.	T
Settlement of foundation	Occas-ional	Sev-ere	U	Bridge originally designed for significant movements form ground settlement from mineral extraction. Review extent of current extraction and future extraction; assess effects on structure (bearings and joints in particular)	T
Seismic Effects	Remote	Med-ium	T	Bridge not designed for seismic loads, review local UK requirements. Review robustness of structure and beam seating requirements in particular	A
Fire	Remote	Med ium	T	Review likelihood of storage of hay or other flammable material under structure	A

A = Acceptable. T = Tolerable with precautions. U = Unacceptable/undesirable

The probability for each component based on deterioration and the age of the bridge can be combined to form the many MR&R costs included in the LCCA (Mao and Huang 2015). Therefore, for any bridge components the MR&R costs should be correlated to the age of the bridge, and the fact that their probability will increase as the bridge ages should be taken into consideration in any LCCA. The costs can be brought to a present value that includes that probability with respect to age.

Another one of the current LCCA approaches was developed for the National Corporative Highway Research Program (NCHRP). The Bridge Life Cycle Cost Analysis (BLCCA) methodology was described in a 2003 report by Hugh Hawk. When it was written, many states had not yet implemented any form of LCCA, the report was aimed to help more states implement LCCA approaches. While more states today are using LCCA in their decision making, the report still provides an excellent description of a LCCA model for bridges. Furthermore, the NCHRP model for BLCCA could provide a starting guide for developing a LCCA model for expansion joints in bridges. NCHRP's BLCCA model is described below.

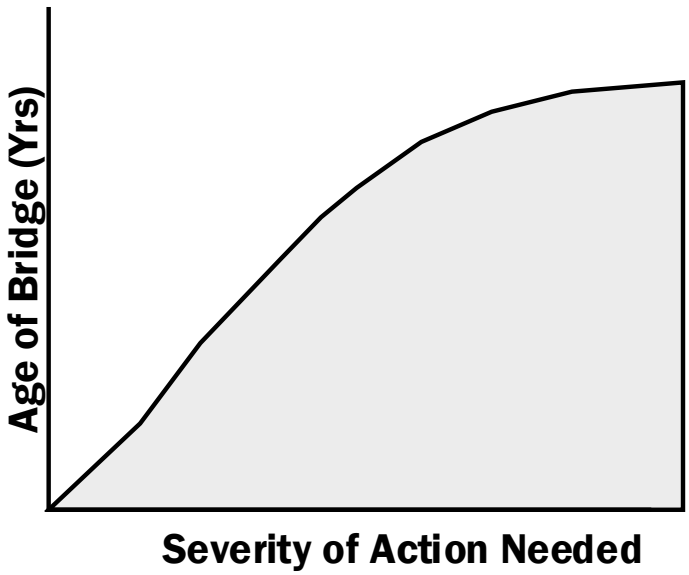

Figure 2-8 MR&R action severity vs Bridge Age

First risks and vulnerabilities must be determined for a bridge location and each of those risks assigned a cost based on the probability of it occurring and consequent costs caused by the risk. These risks and vulnerabilities could be due to overloads of traffic or equipment on the bridge, seismic events, bridge scour, partial failure, etc. (Hawk 2003). Other costs should be estimated as well. Hawk describes agency costs as including maintenance, rehabilitation, and replacement costs. Each of the agency costs is affected by material type, condition, environment and location, average daily traffic, element types, and frequency of maintenance and inspection, among others (Hawk 2003). User costs and operation costs are also directly related to agency costs and should be analyzed and determined, user costs were discussed in more detail in section 2.3 above.

The general form of the BLCCA equation is

$$LCC = DC + CC + MC + RC + UC + SV \quad (2.6)$$

Where:

LCC = life-cycle cost,

DC = design cost

CC = construction cost

MC = maintenance cost

RC = rehabilitation cost

UC = user cost

SV = salvage value

The BLCCA model's costs that take place in the bridge's future are brought to a present worth value using net present value formulas for uniform series, one time series, gradient series, or combinations depending on the nature of the cost. This would produce the present LCC for each alternative. In the BLCCA model Hawk describes predicting the distant future as impractical. Instead he proposes that a specific sequence of maintenance and rehabilitation be analyzed for LCC and then he suggests that, for analysis purposes that sequence repeats itself endlessly. Eventually the bridge is replaced and the whole LCCA is repeated. This perpetuated bridge maintenance and rehabilitation is due to most bridge design life spans being 50 years or more (Hawk 2003). Furthermore, while using probability and data for determining the components of the BLCCA equation, it is not appropriate to assume complete accuracy when approaching the end of the life span of the bridge, but by using the most current data available an acceptable confidence level might be reached.

2.6 Conclusion

LCCA is critical for cost effective bridge and expansion joint design, with cost components ranging from initial cost to maintenance and replacement costs. While there are so many factors affecting the LCC of a bridge, there are many ways to calculate that cost and perform a LCCA, from a strictly determinate analysis to an analysis based on probabilities. Each model, as discussed above, has advantages and disadvantages. However, if by taking the best parts of the various models and building a more comprehensive model for expansion joints based on determinate costs of each component and a probability of that cost being applied over the life-span of the bridge then a realistic LCC might be reached. This approach can be used to form a LCCA equation for expansion joints in bridges, however, it can also be used to form an LCCA

equation for replacing expansion joints with a continuous connection. With these two equations, for an expansion joint that has reached the end of its life-span and needs to be replaced, the LCCA can be compared for replacing the joint with a second expansion joint or for retrofitting the joint to be continuous. Then the more economical solution can be chosen based on these LCCs. The equations for each scenario are shown below as Eq. 7 and 8.

Proposed LCCA model

$$LCC_{EJ} = f\left(C_i + C_c + C_o + C_m P_m + C_r P_r + C_{cc} P_{cc} + C_u P_u + SV \right) \quad (2.7)$$

$$LCC_{RC} = f\left(C_i + C_R + C_o + C_m P_m + C_r P_r + C_{cc} P_{cc} + C_u P_u + SV \right) \quad (2.8)$$

Where:

LCC_{EJ} = Life Cycle Cost of Expansion Joint

LCC_{RC}= Life Cycle Cost of Retrofitted Continuous replacement of joint

C_i = initial cost, fixed cost

C_c = construction cost, fixed cost

C_R = retrofitting cost for continuous, fixed cost

C_o=cost of operation, fixed cost (only applicable for toll draw bridges)

$C_m P_m$=cost of maintenance (function of temp) = ($C_{mH} P_{mH}$ if Temp > 32 ˚F;

$C_{mC} P_{mC}$ if Temp < or = 32 ˚F)

$C_m P_m$= composed of maintenance costs of each part of the expansion joint

$C_r P_r$ = replacement cost (function of temp) = ($C_{rH} P_{rH}$ if Temp > 32 ˚F;

$C_{rC} P_{rC}$ if Temp < or = 32 ˚F)

$C_r P_r$ = composed of replacement costs of each part of the expansion joint

$C_{cc} P_{cc}$ = cost of capital

C_uP_u = user cost = C_dP_d+ C_vP_v+ C_aP_a

C_dP_d = driver cost

C_vP_v = vehicle operation cost

C_aP_a = accident cost

The probabilities, P, for each cost would come from an analysis of the respective Department of Transportation's bridge inspection data. The costs, C, for each component would come from the respective Department of Transportation's data, typical industry standard costs, related articles, other LCCA models, and costs for similar products or projects. These probabilities and costs could then be input into Eq. (2.7) and (2.8) to calculate the LCCAs for each case.

The LCCA for both expansion joints and for retrofitted continuous joints could be determined and the most cost effective solution chosen for any bridge scenario. While these equations are primarily designed for analyzing the LCC of joints for existing bridges, the model equations could easily be adjusted for use on new bridges. The costs and probabilities for each component would have to be adjusted for the whole bridge instead of for only the joint.

This would expand the number of components with in each overarching cost component, however the overall process and overarching cost components would remain the same.

CHAPTER 3

BRIDG C-17-AT INSTRUMENTATION PLAN, FIELD IMPLIMENTATION, AND BRIDGE DATA COLLECTION

3.1 Introduction

Two bridges were selected in consultation with the Colorado Department of Transportation (CDOT) for instrumentation and field testing to collect data pertaining to bridge behavior and assess the thermal gradient effects on expansion joints, structural behavior, and life cycle costs. The bridge was selected based on minimum curvature and skew, including at least one span with an expansion joint on either end, and simply supported. The selection process is discussed in more detail in Karly Rager's Thesis which conducted the first stage of this research (2016). Both bridges were numerically modeled with finite elements in CSiBridge. Bridges B-16-FM and C-17-AT were selected; the first is a steel super structure while the second is a reinforced concrete superstructure. Selecting one steel and one reinforced concrete bridge is critical to allow analysis and comparison of both material behaviors as to facilitate wider application of these research findings. The instrumentation plan and field implementation of bridge B-17-FM is discussed in detail in Karly Rager's Thesis (2016) and was instrumented in March 2016. Overall its instrumentation was very similar to the instrumentation of C-17-AT. This research focuses on Bridge C-17-AT, which was selected for instrumentation second and was instrumented in the field in August 2016. The instrumentation plan and field implementation of Bridge C-17-AT is detailed below in Section 3.2 as well as the process for data collection and initial data analysis. The instrumentation plan used in field can be found in Appendix B and the drawings for bridge C-17-AT can be found in Appendix A.

Data collection could be accomplished in two ways. The first method would be by manual download of data from the memory card in the data acquisition system (DAQ), which requires bringing a laptop out to the bridge and connecting it via usb/Serial cable to the DAQ before downloading the data which takes approximately one hour per week of data. Or the second method would be to install a wireless modem connected directly to the DAQ and remotely via a static IP Address download the data wirelessly to an office computer. This latter method was preferred and utilized as described in detail in the following section.

3.2 Bridge C-17-AT Field Instrumentation

Bridge C-17-AT was chosen as the concrete superstructure bridge for this research. A three span, five girders, and two expansion joint traditionally reinforced concrete bridge, C-17-AT, carries Northbound I-25 over a gravel access road that connects frontage roads. These can be seen in Figure 3-1 and Figure 3-2 below. Located approximately 30 miles south on I-25 of Colorado State University, the bride is close enough to provide easy access for field implementation and for researchers in the event of repairs or remediation needed by either the Data acquisition system (DAQ) or the sensors.

The spans are each approximately 31 ft long and 42 ft wide, with expansion joints separating the three spans. See Appendix A for drawings. Each of the five girders, as well as the deck are traditional reinforced concrete, they are also simply supported. Pier caps and columns are also reinforced concrete. Furthermore, extensive damage and corrosion and leakage from the expansion joint can be seen on the underside of the girders and expansion joints. See Figure 3-3 below.

The expansion joints are simple joint with a rubber silicone seal, however, the seal was cracked and the joint was clogged with visible clogging and deterioration on the ends. See Figure 3-4 and Figure 3-5 below showing the clogging present in the expansion joint at instrumentation.

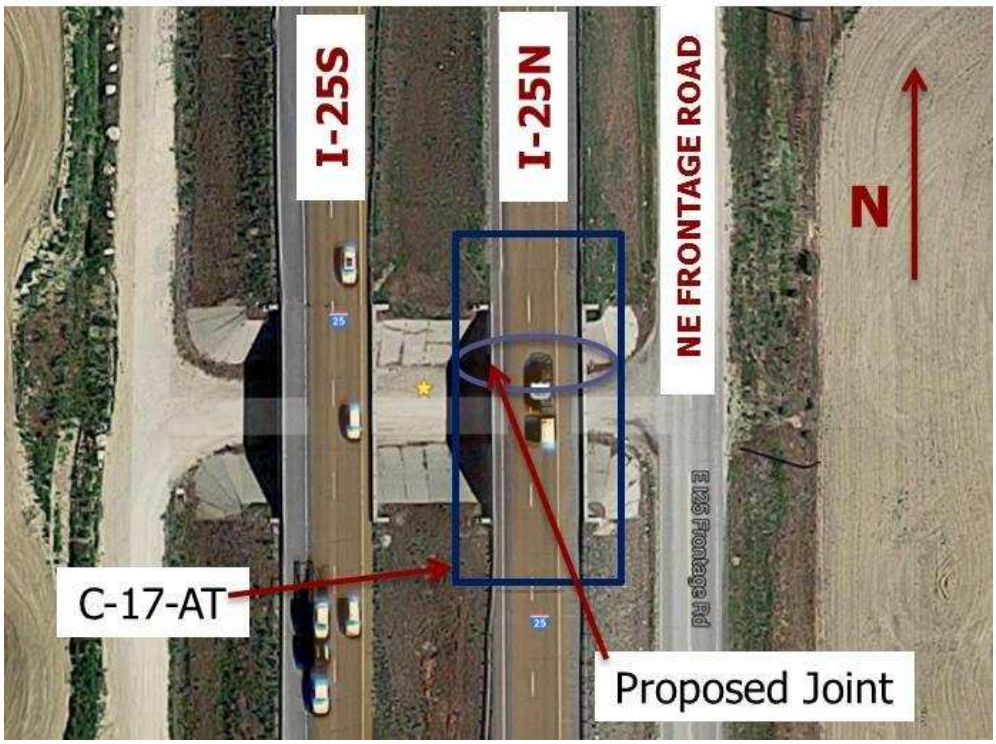

Figure 3-1 C-17-AT Overview

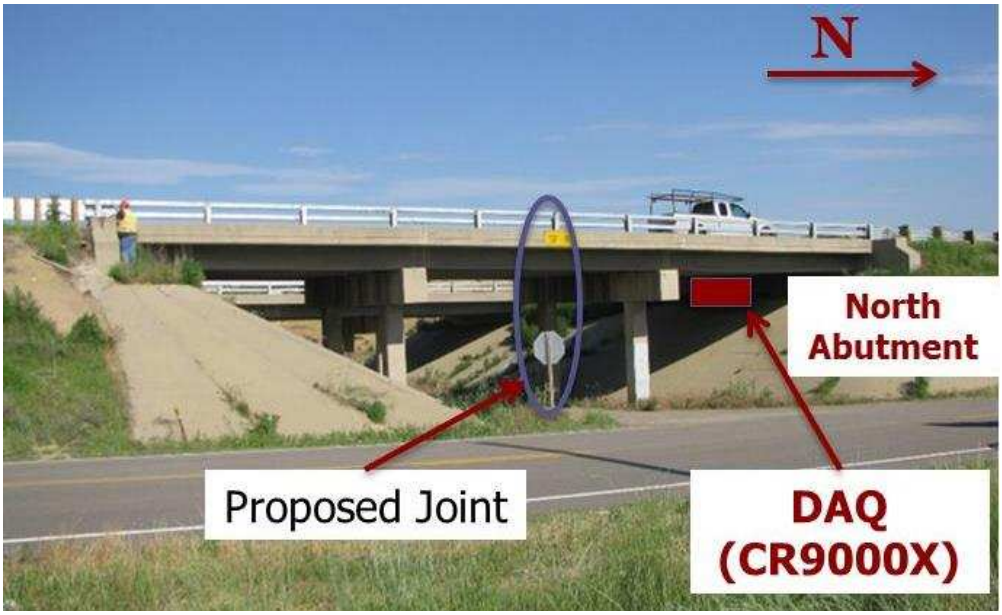

Figure 3-2 C-17-AT Sideview

Figure 3-3 C-17-AT Underside – Corrosion & Leakage

Figure 3-4 C-17-AT Expansion Joint Clogging

The northernmost expansion joint was selected for instrumentation as seen in Figure 3-1 and Figure 3-2 above. The eastern facing side of the north expansion joint was selected for the instrumentation to prevent the effects of shadowing from the southbound bridge directly to the west of the northbound bridge. By choosing the eastern facing side of the joint there is nothing blocking the sunrays from hitting the sensors on the joint and will therefore provide the most

uninterrupted thermal behavior for the sensors. Three different types of sensors were used to monitor the thermal gradient along the depth of the joint as well as the structure behavior due to thermal gradients and vehicle traffic loading on the joint. Strain gages were used to measure the strain (and by relation the stress), thermocouples were used to measure the thermal gradient, and linear potentiometers were used to measure displacement (both expansion and compression) along the depth of the joint. The placement of these sensors on the joint can be seen in Figure 3-6 below (See Appendix B for more details) and their details are discussed in Sections 3.2.1, 3.2.2, and 3.2.3 respectively.

Figure 3-5 C-17-AT Expansion Joint Deterioration

The bridge was instrumented August 22nd through the 24th, 2016. The overall instrumentation process was smooth, with only minor adjustments needed in field such as running the wires along the bridge railing instead of along the bottom of the girder. Due to the

bridge carrying northbound I-25, the running of the wires along the railing was done at night, 9pm, on August 23rd, 2016 in order to utilize a night-time construction lane closure.

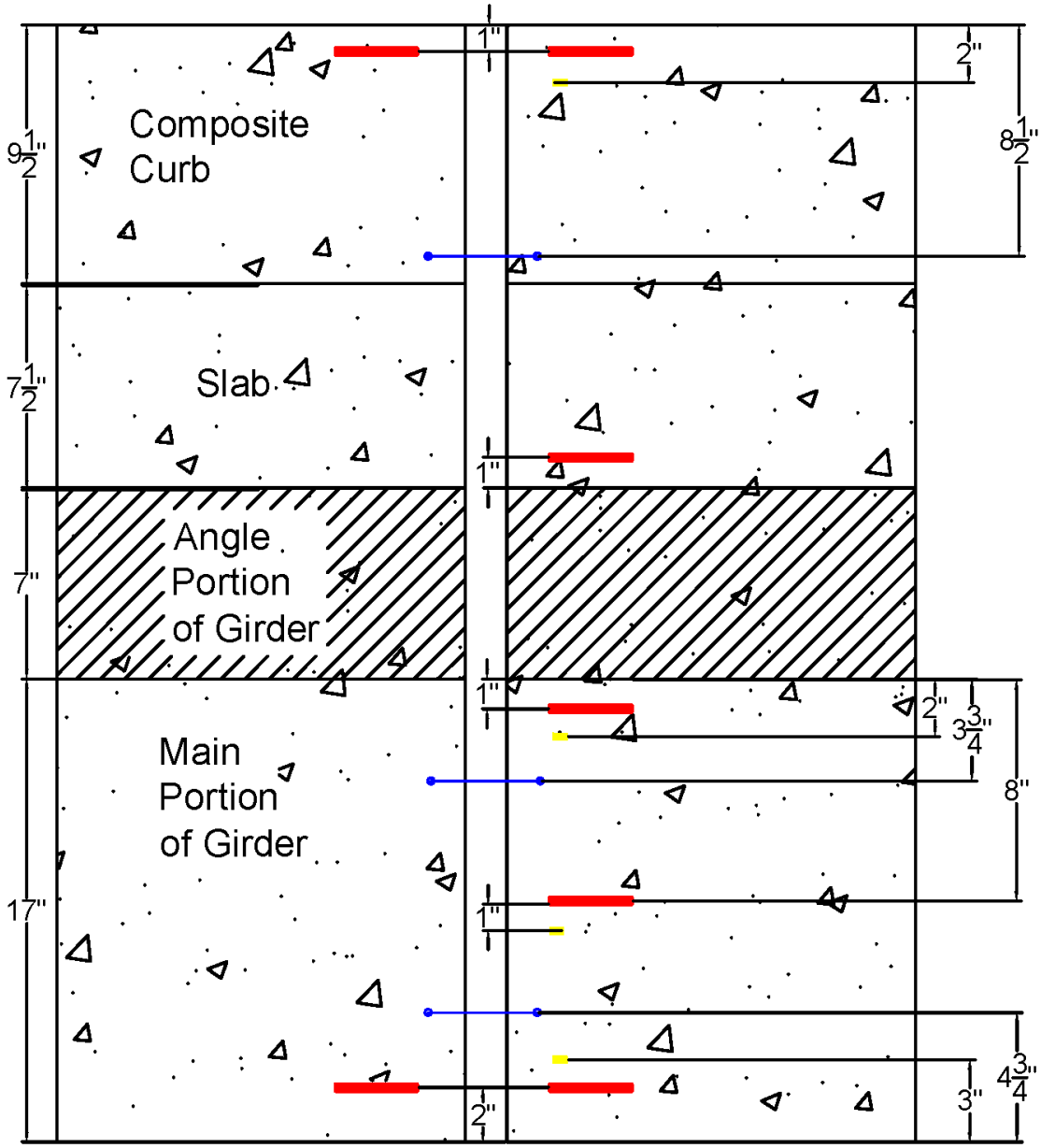

Figure 3-6 C-17-AT Expansion Joint Sensor Placement

3.2.1 Strain Gages

In order to monitor the stress and strain experienced by the joint due to both thermal and vehicle loading, seven strain gages were placed along the depth of the joint. However, due to the

nonhomogeneous nature of concrete long (30mm) 350 ohms Omega strain gages were used for C-17-AT, see Figure 3-7 below. The length of the gauge is designed to account for variability in the material's response, through averaging of the measurement along the gauge length, and thus provides a more representative strain reading.

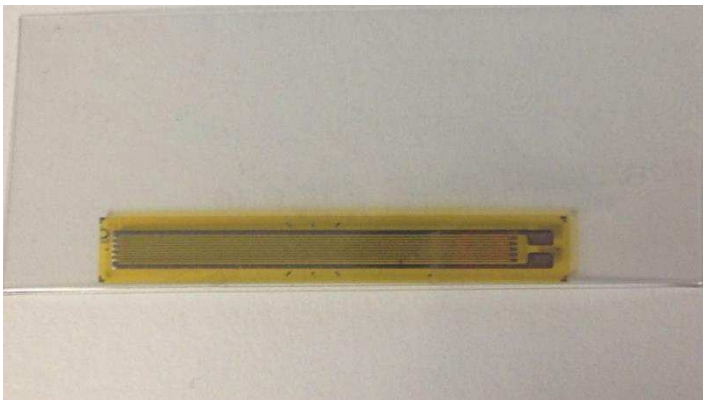

Figure 3-7 Concrete Strain Gage

Two strain gages were placed approximately one inch from the top of the slab on either side of the expansion joint to provide redundancy. One was placed approximately one inch above the bottom of the slab on the north side of the joint. One was placed on the girder approximately one inch below the slab on the north side of the joint. A fifth was placed halfway down the girder on the north side of the expansion joint. The two final gages were placed on either side of the joint approximately one inch above the bottom of the girder. These can be seen in Figure 3-6 above.

The concrete was ground smooth with a grinder before the strain gages were applied to the concrete of the slab and girders with a strong epoxy glue. The smooth surface provided by the grinder ensures full contact between the sensor and the concrete. Once glued to the slab and girders the strain gages were soldered to their corresponding labeled wires. Soldering was done in field due to the length of the strain gages. With shorter/smaller strain gages soldering can be

completed in the lab and the gages can be brought to the field already connected, however, the longer strain gages needed for the concrete are more bendable and fragile than smaller ones use for steel. Thus, soldering before application introduces unreasonable risk of damage to the strain gage. This application process can be seen in Figure 3-8 and Figure 3-9 below. Once the strain gage was soldered to the wires in the field, the resistance at the other ends of the wires was tested to ensure proper connection to the strain gage. Extra strain gages were available in the event that soldering was improper and unfixable, in which case a new strain gage would have been applied and soldered and tested. Once the strain gages were installed and tested, they were covered by an adhesive rubber protective cover that was also caulked along the edges to ensure protection.

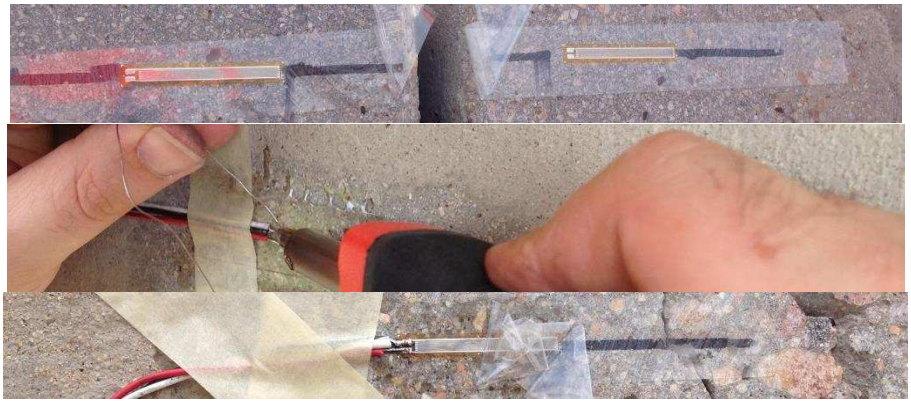

Figure 3-8 Strain Gage Application

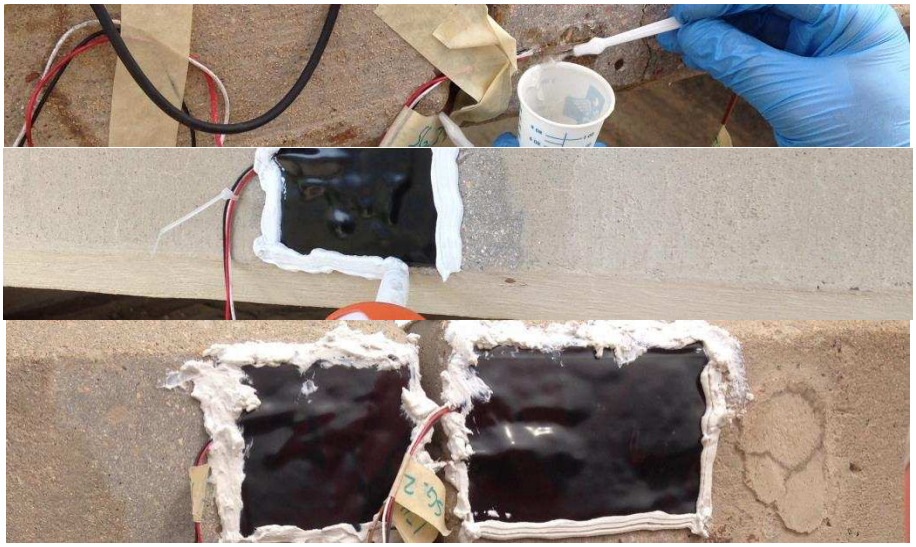

Figure 3-9 Strain Gage Protection

3.2.2 Thermocouples

Thermocouples were used to monitor the thermal distribution throughout the depth of the expansion joint. Omega type K thermocouples were chosen; they are self-adhesive and designed to resist the outdoor elements. Their flexible design allows for full contact with the material and a large temperature range of -58 to 392°F. These are the same thermocouples used for bridge B-16-FM, and have provided consistent data for that bridge supporting the decision to use the type of thermocouples for bridge C-17-AT.

Four thermocouples were used along the depth of the expansion joint to record and monitor the thermal gradient along the joint. One thermocouple was placed approximately two inches below the top of the slab, or approximately one inch below the strain gage on the north side of the joint. A second one was placed approximately two inches below the bottom of the slab on the girder (about 1 inch below the strain gage). A third thermocouple was placed at mid depth on the north girder approximately 1 inch below the mid depth strain gage. A final thermocouple was placed approximately 2 inches above the bottom of the north girder, about 1 inch above the bottom strain gage. Their placement can be seen in Figure 3-6 above.

The concrete was also ground smooth with a grinder before the thermocouples were applied by peeling off the protective cover and pressing the adhesive side to the concrete, as shown in Figure 3-10 below. Once the thermocouple is firmly attached, the wires were connected using thermocouple wire connection plugs, which were prewired to the thermocouple and the shielded wires before instrumentation. These connection plugs are specific to type K thermocouples and provide a fully secure, protected, and complete connection between the thermocouple and the wire and thus the DAQ. These connectors can be seen in Figure 3-11 below and help ensure accurate data is recorded.

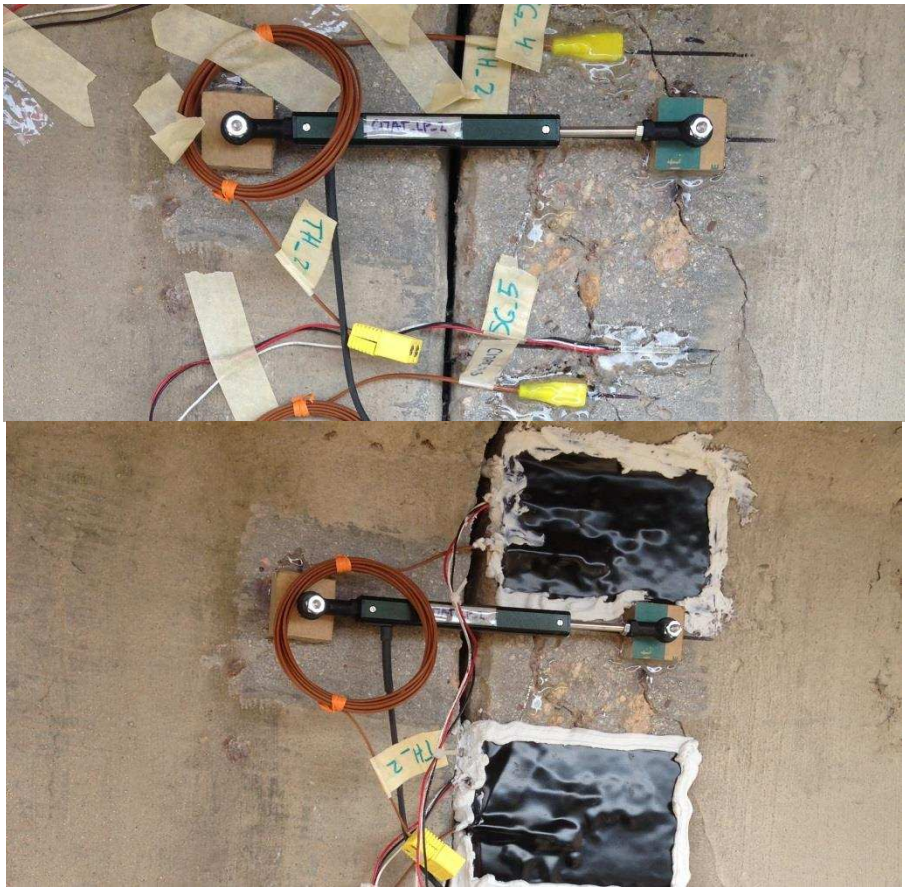

Figure 3-10 Thermocouple Application


Figure 3-11 Thermocouple Connectors

3.2.3 Linear Potentiometers

Measuring the displacement of the joint in both directions, expansion and contraction, is the primary indication of how critical the expansion joint is to the bridge as well as the effects of

clogging and thermal gradient changes on the bridge. To measure these displacements, Celesco model CLP 50 linear potentiometers were chosen. These linear potentiometers can measure up to one-inch extension and one-inch compression, for a total of two inches of displacement. The linear potentiometer in Figure 3-12 below is shown extended to its full two-inch extension. This model has a life expectancy of 25 million repetitions and is designed to resist environmental elements, including a temperature range of -40˚ to 212˚F and up to 20000 Hz of vibration. These were the same linear potentiometers that were used on B-16-FM and have provided consistent and continuous displacement data from that bridge.

Figure 3-12 Extended Linear Potentiometer

Three of these linear potentiometers are used on the north joint of C-17-AT. The first was placed across the joint at mid depth on the slab, approximately 3.75 inches below the top of the slab. The second linear potentiometer was placed across the joint on the girders approximately 3.75 inches below the bottom of the slab. The last linear potentiometer was placed across the joint on the girders 3.75 inches above the bottom of the joint. Their placement can be seen above in Figure 3-6.

In order to ensure full extension and compressibility of the linear potentiometers across the joint the linear potentiometers were mounted on mounts made of a square of Plexiglas with a bolt through the middle which was then ran through the ring on the end of the linear potentiometer and secured with a nut, see Figure 3-13 below. The concrete was ground smooth

with a grinder before the mounts were glued to the girder with the same epoxy that was used for the strain gages. When mounting the linear potentiometers, measurements were made and marked on the concrete, next the mounts were glued in placed. The epoxy only takes a couple minutes to harden and once hardened the linear potentiometers were attached and bolted in place, see Figure 3-14 below. Finally, the linear potentiometer was covered with half of a PVC pipe to the sensor from weather. The PVC pipe was only attached on one side of the joint to ensure free movement of the joint and sensor. The PVC covered linear potentiometer can be seen in Figure 3-15 below.

Figure 3-13 Linear Potentiometer Mount

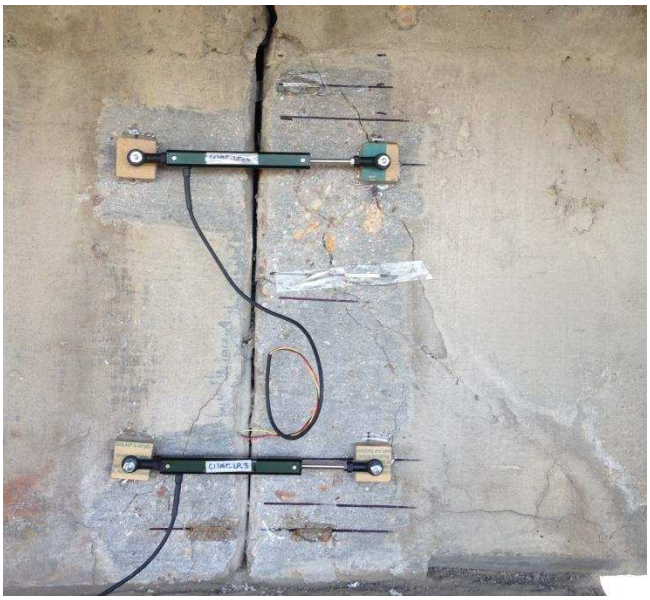
Figure 3-14 Linear Potentiometer in Place on Joint

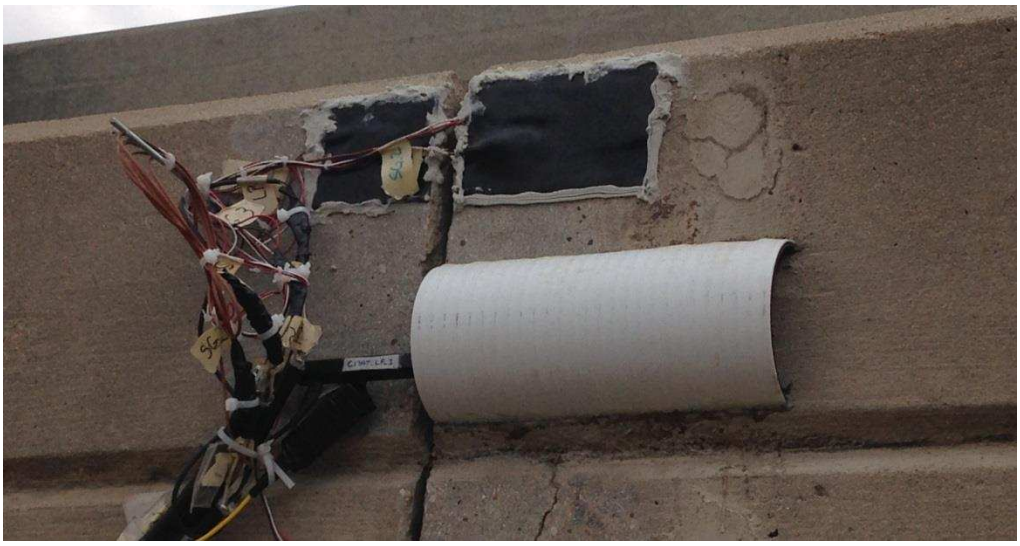

Figure 3-15 PVC covered Linear Potentiometer

3.2.4 Wires

Shielded wires were used for all sensors to protect the data from the elements and minimize noise in the data collected. Two types of shielded wires were used. Thermocouples wired over distanced greater than a few feet require shielded thermocouples wires that will transmit the temperature over the longer distances and protect it from the elements. Thus Type K Omega extension thermocouple wires were used. These wires have a polyvinyl shield, a max temperature of 221˚F, and solid wires, with a 16 AWG No, these wires can be seen in Figure 3-16 below.

Figure 3-16 Shielded Thermocouple Wire

For the strain gages and linear potentiometers, shielded wires from Allied Wire and Cable were chosen. The FR-EPR/CPE Instrumentation Cable with individual and overall shielded pairs. These wires have AWG No. 18, with two pairs of wires. The wires have copper drain wires that were grounded to minimize noise, Ethylene propylene Rubber (FR-EPR) insulation, and shields of aluminum with overall covers of chlorinated Polyethylene (CPE). The have a max temperature of 194˚F and voltage of 600V. These double shielded wires are shown below in Figure 3-17.

Figure 3-17 Double Shielded Wire

3.2.5 The Data Acquisition System

For the collection of data from the sensors a Campbell Scientific CR9000X Data Logger was chosen as the data acquisition system (DAQ). The CR9000X is a multiprocessor, high-speed, 16 channel system including digital and analog filters to eliminate noise and provide clear signals. With a measurement rate of 100,000 Hz the CR9000X provides high speed sampling capabilities which is ideal for this project in which measurements from the sensors are recorded every 5 seconds. Furthermore, data can be collected directly or remotely (with the addition of a

wireless modem) from the DAQ. This allowed us to connect the DAQ to a laptop computer in field and monitor the data as soon as the sensors were in place and wired to the DAQ. Monitoring the data on sight, it ensured that the sensors were operating correctly and allowed for an immediate review of the response of the bridge.

On-sight the CR9000X data logger was enclosed in a large steel weatherproof job box. The job box with the DAQ inside was placed on the north abutment of C-17-AT as seen in Figure 3-18 and was chained to the bearing. Figure 3-19 shows the DAQ inside the job box.

Figure 3-18 Job Box on North Abutment'

Figure 3-19 DAQ in Job Box

The wires were run from the sensors on the north joint along the top of the bridge to the job box. The wires were connected to the railing along the west edge of the bridge using zip ties and protected by halved PVC pipes to provide uniformity and security. The wires were then run through a gasket on the side of the job box and connected to the CR9000X data logger inside. The wires running along the bridge are shown in Figure 3-20 below.

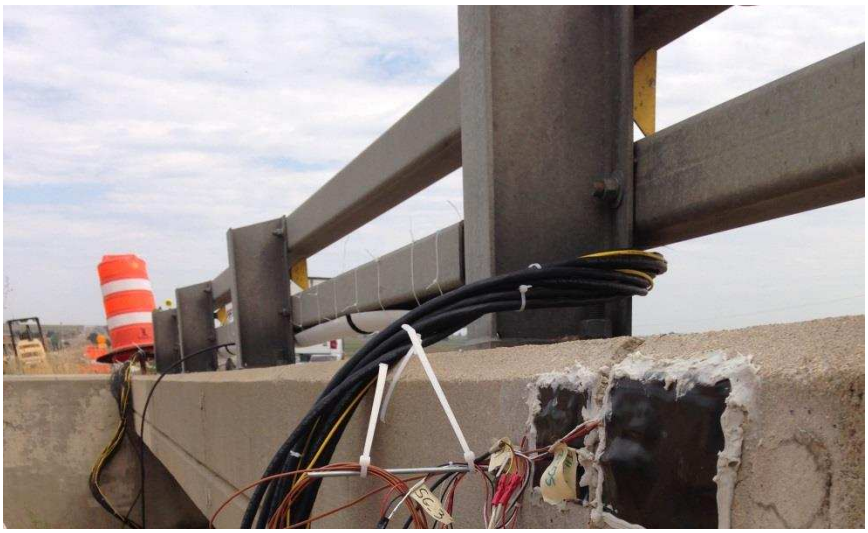

Figure 3-20 Wires Along Railing

The DAQ system is powered by a size 27 deep cycle marine battery that is charged by a 70 Watt solar panel. The battery is stored inside the job box next to the CR9000X as seen in Figure 3-19 and connected via wires to the positive and negative terminals in the CR9000X. The solar panel was installed a month and a half after sensor installation due to shipping time. During the interim period the battery was charge using a battery charger about once each week. The solar panel was placed at a 45-degree angle to maximize sunlight exposure throughout the year and was installed on the west side of the north abutment. The solar panel is wired to a charge controller which is then connected to the battery. The charge controller prevents the battery from becoming over charged. The solar panel installation is discussed in Section 3.4 below.

3.3 Remote Data Collection

Two methods were available for data collection from the CR9000X. The DAQ stores data on a 2 GB memory card, which can hold several months of data. The first method of collection would be by going out to the bridge periodically for collection by hardwiring a laptop to the DAQ and downloading the data from the memory card. The second option would be connecting a wireless modem to the CR9000X data logger and then downloading the data remotely from the DAQ to an office computer using a static IP address.

The second method was chosen as more convenient and economical. Not only would a wireless connection to the DAQ make data collection easier, it would also allow the researchers to check on the sensors remotely. This would ensure that sensors are working properly, thus allowing researchers to easily see when a sensor might need attention or mediation in field.

The Campbell Scientific RavenXTV modem was chosen for wireless data collection. This modem is designed to work with the CR9000X data logger and a Verizon IP address. A static IP address was chosen to provide easier access to the data. Once the Verizon static IP address was set up and assigned to the modem the modem was configured using provided software and was plugged into the CR9000X data logger on-sight. Figure 3-21 shows the modem connected to the data logger and Figure 3-22 show the modem's antenna attached to the side of the bridge. For collection the software RTDAQ was used to connect remotely to the CR9000X via the modem and IP address. Once connected, data can be downloaded and saved as .csv files and analyzed. Data is collected, downloaded, and converted once a week to minimize any backup of data and streamline the analysis process discussed in Chapter 4.

Figure 3-21 RavenTXV Modem

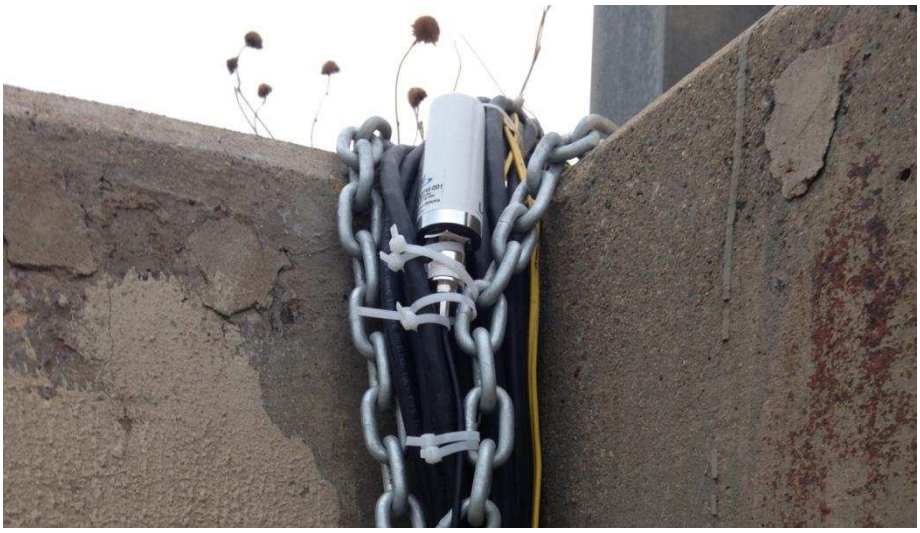
Figure 3-22 Modem Antenna

3.4 Solar Panel Installation

The location of bridge C-17-AT does not provide access to electricity, consequently alternative sources of energy for powering the CR9000X system were considered. First, rechargeable batteries were considered. These would be switched out and recharged by either CSU or CDOT personnel. The second option considered was a rechargeable battery charged by solar panel attached to the abutment. This second option proved to be both more cost and time effective because it would not require regular trips out to the bridge. The cost of the solar panel

proved to be comparable to a second rechargeable battery and significantly cut maintenance hours. The battery chosen is a deep cycle 12 Volt marine battery, a Diehard Group 27M. The solar panel chosen is a Newpowa 70-Watt panel with a 12-Volt solar charge controller to prevent over charging of the battery. The solar panel weighs 13 pounds, and is 30.48 in x 26.57 in x 1.18 in and is shown in Figure 3-23 below.

Figure 3-23 70 Watt Solar Panel

A frame to hold the solar panel at a 45-degree angle against the abutment was built out of 2x4s. Positioning the solar panel at a 45-degree angle allows for maximum sunlight ray absorption throughout the calendar year based on sun ray angles. The frame 2x4s were connected to the solar panel using screws and brackets as seen in Figure 3-24 below. The ends of the frame were attached to brackets which would be attached to the concrete abutment using screws. The in place solar panel is shown in Figure 3-25 below.

The solar panel was installed on October 8th, 2016. The panel was installed after the rest of the instrumentation due to shipping time constraints. During the interim between instrumentation and solar panel installation, the battery was picked up once every eight days to be charged and then returned to the sight. The panel was installed by using a pachometer to detect rebar in the abutment, the locations of the screws were then marked and holes drilled into the concrete. The solar panel was then put in place and the frame screwed into the concrete. Once in place, the solar panel wire was connected to the charge controller and that to the battery providing power to the DAQ.

Figure 3-24 Solar Panel Frame

Figure 3-25 Solar Panel Attached to Abutment

3.5 Summary and Discussion

The reinforced concrete bridge C-17-AT was selected for in-service instrumentation and joint assessment. The bridge was instrumented over the course of three days, with linear potentiometers, strain gauges, and thermocouples along one joint. The instrumentation processes were smooth, a solar panel was installed after the initial instrumentation to provide a source of energy for the battery powered CR9000X system.

CHAPTER 4

CONTROLLED LOAD TEST MODEL VALIDATION

4.1 Introduction

In order to validate the finite element model of bridge C-17-AT, described in Chapter 6 Section 6.2a static control load test was performed following the completion of the field instrumentation. Due to the bridge carrying northbound I-25, the load test was performed at approximately 3 AM in order to minimize the impact on drivers. The test was performed by parking a truck with known dimensions and axle weights on the bridge and strain data was collected. The test was performed in two parts, first with the front axle directly above the mid-span strain gage, and second with the back axles centered above the mid-span strain gage. The same truck loads were placed on the finite element model and the two responses were compared.

4.2 Test Vehicle Information

The truck used for the control load test was an Aspen Aerials A-40 Bridge Inspection Unit Truck, which was provided and operated by CDOT personnel. . This was the same truck that was used for sensor installation on the bridge. The axle weights and dimensions for the A-40 truck can be seen below in Figure 4-1. These axle weights are for when the inspection bucket arm is fully contracted and stowed on the bed of the truck. These axle weights are accurate to within +/- 2% of the exact weight, according to the manufacture. The position shown, with bucket arm fully contracted, is how it was parked on the bridge for the test.

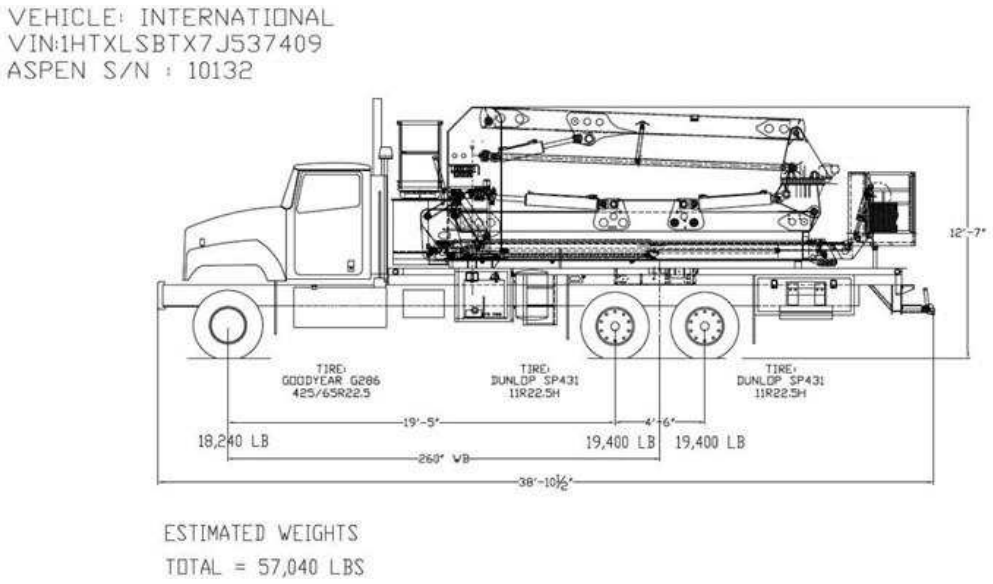

Figure 4-1 Aspen Aerials A-40 Truck with Dimensions and Axle Weights

4.3 Model and Predictions

The effect of the Aspen Aerial A-40 truck was included in the finite element model of bridge C-17-AT by inputting the axle weights as point loads representing the tires in the same location as in field test scenarios. Two scenarios were modeled separately. The first scenario had the truck parked in the west lane such that the front axle was directly above the mid-span strain gage. The second scenario had the truck parked in the west lane such that the two back axles were centered over the mid-span strain gauge.

The strain gauge at mid-span was monitored during the truck load tests and used for validating the numerical model. This strain gauge was installed about 2 inches above the bottom of the outside west girder at mid-span. The strain gauge data is measured in microstrain. In order to compare the field test data to the model for validation, the field microstrain was converted to corresponding stress values using the modulus of elasticity given by the bridge drawing

specifications, 3604 ksi. This measured and converted field stress was then compared to the stress obtained from the finite element model and the percent error was calculated.

The first scenario in the model, where the front axle is above mid-span, gives the stress at the bottom of the girder at mid-span to be 0.146 ksi. The second scenario, when the back axles are centered above mid-span, gives stress at the bottom of the girder at mid-span to be 0.349 ksi.

4.4 Results and Comparison

Each of the two scenarios of the control load test were performed for approximately one to two minutes. During each of these tests the data was collected in field at 5 second intervals from the strain gauge at mid-span. Collecting several data points over the span of the test allowed for a moving average to be applied to the data. These average strains were then converted to stress and compared to the corresponding finite element model stresses. Figure 4-2 and Figure 4-3 shows the data collected for the front axle and for the back axle tests respectively.

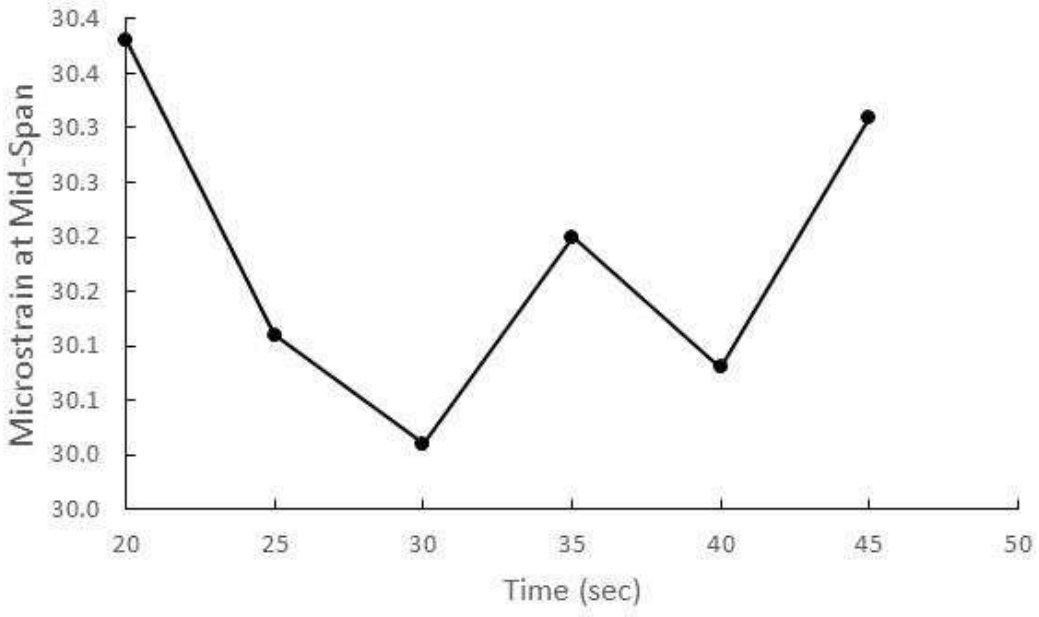

Figure 4-2 Front Axle Control Load Test Data

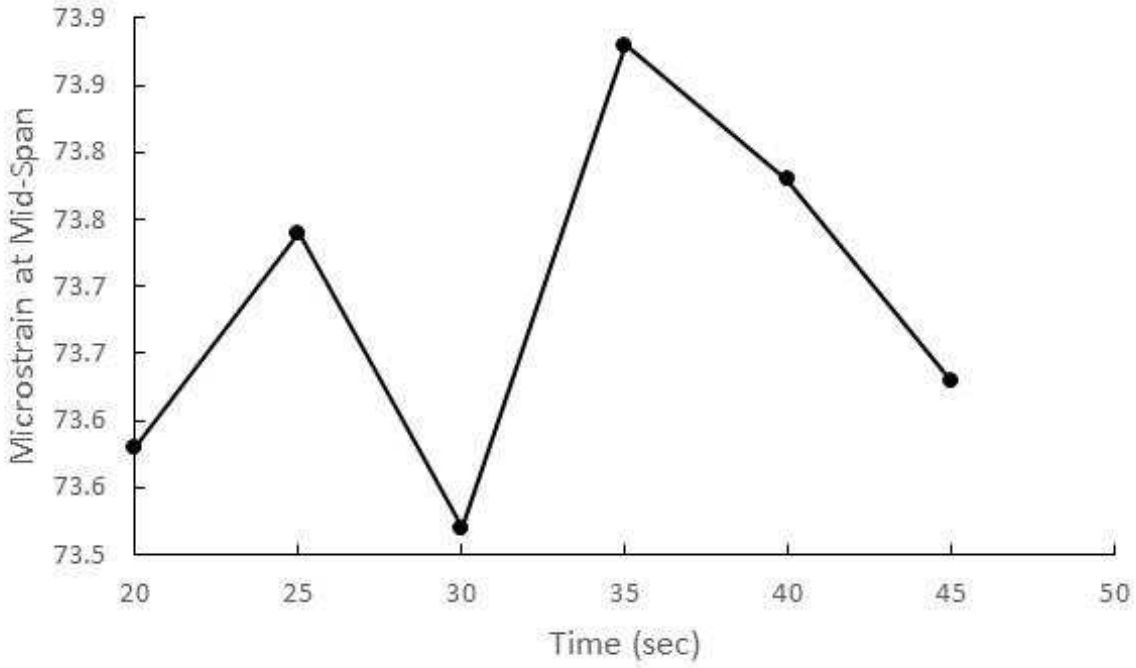

Figure 4-3 Back Axle Control Load Test Data

An average of the data collected during the field test was used to calculate the average micro strain for each of the two scenarios. The front axle scenario gave an average micro strain at mid-span of 30.18. The back axles gave an average micro strain at mid-span of 73.69. These micro strains were converted to stresses using the modulus of elasticity of the concrete, 3604 ksi. Table 4-1 below shows both the predicted stresses from the numerical model and the measured field response stresses. Table 4-1 also shows the calculated percent difference between the predicted and measured stresses. A percent difference less than 20% is considered good, and as shown good agreement was achieved between the field test and the numerical model.

Table 4-1. Comparison of Field Stress and Model Stress Predictions

	Front Axle at Mid-span	**Back Axles at Mid-span**
Predicted Stress (ksi)	0.146	0.349
Measured Stress (ksi)	0.109	0.266
Percent Difference (%)	11.5	9.74

4.5 Conclusion

The control load field test validated the finite element model's ability to predict the bridge's global behavior. The test used an Aspen Aerials A-40 Bridge Inspection Unit Truck from CDOT, which has a known weight, on the bridge and in the model. The truck was parked with each axle in turn directly over the mid-span strain gauge. The strain due to the truck's axle loads collected in the field was converted to stress and compared to the stress calculated by the model with the same axle loads applied. The two stresses showed an average agreement of about 10.5% for the two axles. This close agreement between the field test and the model solidifies the models ability to perform a parametric study and predict global joint behavior under different situations.

CHAPTER 5

INITIAL DATA ANALYSIS FOR BRIDGE C-17-AT

5.1 Introduction

The data from the bridge was downloaded weekly and a brief analysis performed using an analysis and plotting code written in RStudio (2016). The data was visualized and analyzed to determine patterns and correlations between the thermal, displacement, and strain/stress data. The analysis was conducted in order to discern how much movement, stress, and temperature change the bridge is experiencing. This knowledge is used to enhance understanding of the expansion joints on the bridge's overall health and life cycle cost. The correlations and patterns are used to draw conclusions about the impact of the clogged joint and of the thermal gradients through the depth of the bridge. The thermal gradients measured are also compared to standard thermal gradients for further analysis. This data and analysis was finally used to form recommendations for joint removal and retrofitting.

5.2 Analysis Plotting Code

The analysis code for the C-17-AT and B-16-FM data was written in RStudio in order to provide easy comparison and visualization of the data. The code was divided into three sections. The first section provided a general analysis and comparison of the sensors' data by producing a three-part graph. The second section provided a comparison of the maximum temperature difference and the stress by producing a two-part graph. The third section calculates the minimum, average, and maximum thermal gradients through the depth of the bridge and plots

them next to each other on a three-part graph for comparison to the standard temperature gradients of AASHTO and New Zealand.

The data is downloaded from the DAQ through the wireless RAVEN XTV modem as .dat files. These .dat files are then converted to .csv files and both are saved and backed up. The code works by reading in the appropriate files as .csv files. The user then selects the date range, desired sensors, and sets the plotting parameters. Next the code is run and the plots simulated. Finally, the plots are saved and analyzed.

5.3 Sensor Correlation and Patterns

Due to bridge C-17-AT's location in Colorado where there is a large range of temperatures, a maximum range of 140℉ (60℃) over the course of the year, the bridge is likely to experience significant differences in temperature (AASHTO, 2012). Thermal gradients are usually most uneven at times of heating or cooling of the bridge, especially during times of direct sunlight. Heat transfer due to direct radiation from the sun, conduction, or convection occurs every time that the ambient air temperature varies – typically every morning and evening. Multiple parameters affect how evenly the bridge loses and gains heat, including bridge orientation, length of concrete overhang, depth of girders, height of concrete slab, and girder spacing (Chen, 2008).

The coefficient of thermal expansion, commonly expressed as μ or α, describes the increase in length of a material for a given increase in temperature. A negative result for the change in length corresponds to a shortening and a positive value corresponds to an increase in length. Bending stresses can develop through the depth of the bridge due to the presence of thermal gradients causing the concrete deck and girder to expand at different rates.

The five months in which data has been collected to date on the C-17-AT bridge provide a foundation for preliminary conclusions about temperature's effect on the expansion joint and allows for comparison to theoretical expectations. The displacement experienced by the expansion joint should be closely correlated with the effective temperature experienced by that joint. This was found to be true in the research monitoring conducted by Y. Q. Ni et al. (2007) on the Ting Kau Bridge. It was also found that the correlation could be predicted using a linear regression model (Ni et al. 2007). However, only the effective temperature, which is the weighted average temperature throughout the depth of the bridge, was considered, rather than the exact temperature at each point through the depth of the bridge. The study also did not include monitoring of stress and strain at the expansion joint. When evaluating the data from C-17-AT over the course of these first five months, similar correlations are seen between the temperature, stress and displacement. Figure 5-1 below shows a two-week span of the C-17-AT data at the end of October and shows a distinct converse pattern between the temperature data plotted in (a) and the displacement data plotted in (b). As the temperature rises the displacement decreases, i.e. the girders expand and the joint closes; conversely as the temperature falls, the displacement increases, i.e. the girders contract and the joint opens further. This behavior of the joint, in conjunction with the temperature, confirms that the joint is directly affected by the changing temperature. A fainter pattern can be determined between the stress (from the strain gauges) in (c) and the temperature and displacement data. During the first half of the data set the temperatures show a greater range (about 15 degrees) and higher average compared to the second half, also during the first half the stress data shows more variance and during the second half is more constant. Additionally, the displacement changes less during the second half as well,

showing that the greater the range of temperature experience in a short time period the greater the displacement changes and the large the effect on the stresses in the bridge.

The impact of the daily temperature range can be further seen by looking at close up of the data during smaller range period and a larger range period. Figure 5-2 below shows data from C-17-AT from November 30th through December 2nd and Figure 5-3 below shows data from October 15th through October 18th. In Figure 5-2 the temperature range is only approximately 10 degrees and the displacement in (b) shows minimal change, a maximum of 0.05 inches of change in displacement. The stress also shows very little change in (c). On the other hand, looking at Figure 5-3, the temperature range is around 15 degrees and the displacement (b) shows a little more change, a maximum of about 0.09 inches and the stress (c) shows some variance. All of which indicates the importance of the temperature range on the joint and bridge's overall health.

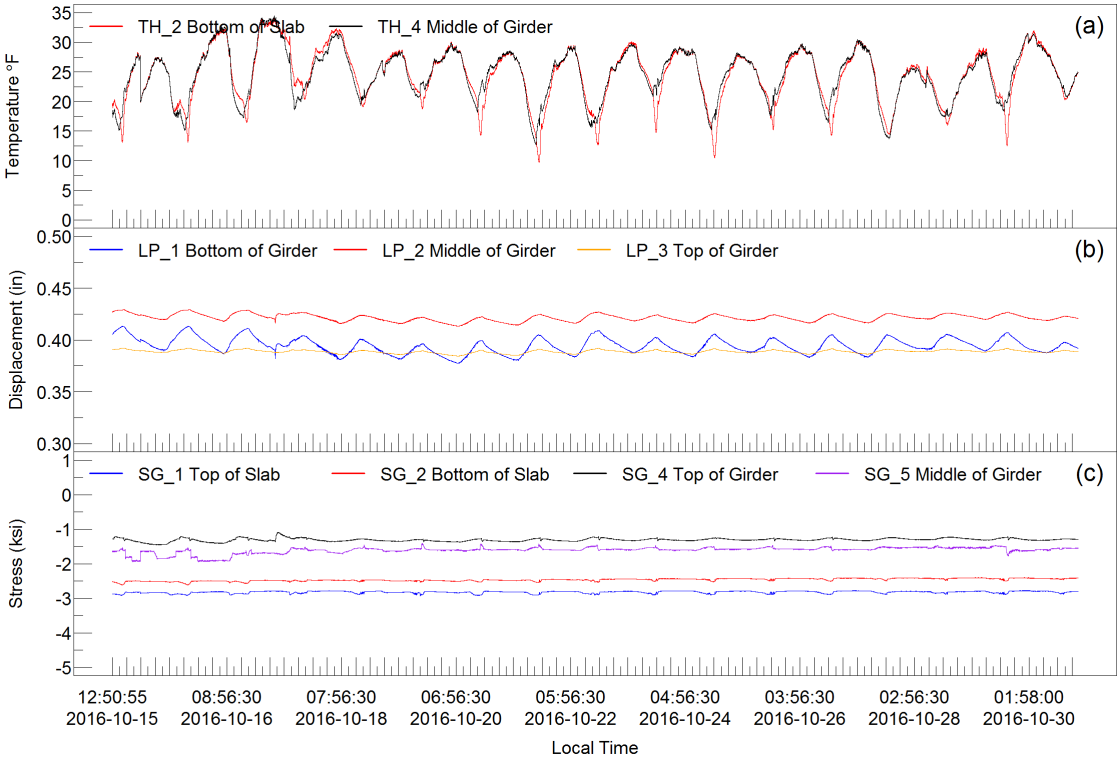

Figure 5-1 C-17-AT Bridge Sensor Data Oct.15th through Oct. 30th, 2016
(a) Thermocouple Data, (b) Linear Potentiometer Data, (c) Change In Stress Data.
Note: ℃ = (℉ – 32)/1.8; 1 in = 25.4 mm; 1psi = 6.89 kPa

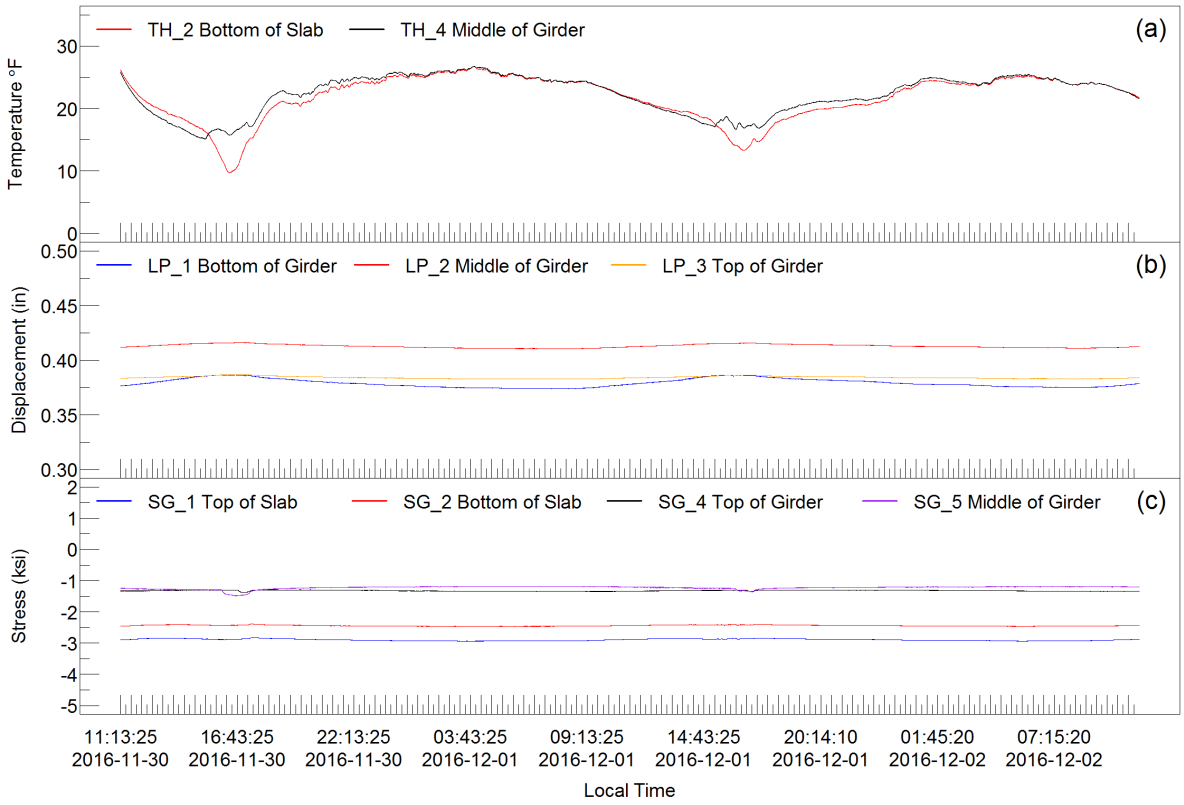

Figure 5-2 C-17-AT Bridge Sensor Data Nov.30th through Dec. 2nd, 2016
(b) Thermocouple Data, (b) Linear Potentiometer Data, (c) Change In Stress Data.
Note: ℃ = (℉ – 32)/1.8; 1 in = 25.4 mm; 1psi = 6.89 kPa

Furthermore, these patterns and relationships between temperature and joint displacement and stress can be seen more distinctly in data from the steel girder bridge, B-16-FM. The B-16-FM bridge's data shows these relationships more clearly for two reasons. First, is due to the data being collected during times of greater temperature ranges and second is due to the nature of the bridge because the girders are steel in B-16-FM, on rollers, the bridge is under more direct sunlight, and the joint is more severely clogged. Figure 5.4 below shows some data from B-16-FM that confirms the same relationships seen in C-17-AT's data above. When evaluating the middle portion of Figure 5-4 one can see that the temperature is varying very little as are the displacement and stress compared to either end of the data were significantly greater temperature ranges and variance in displacement and stress are observed.

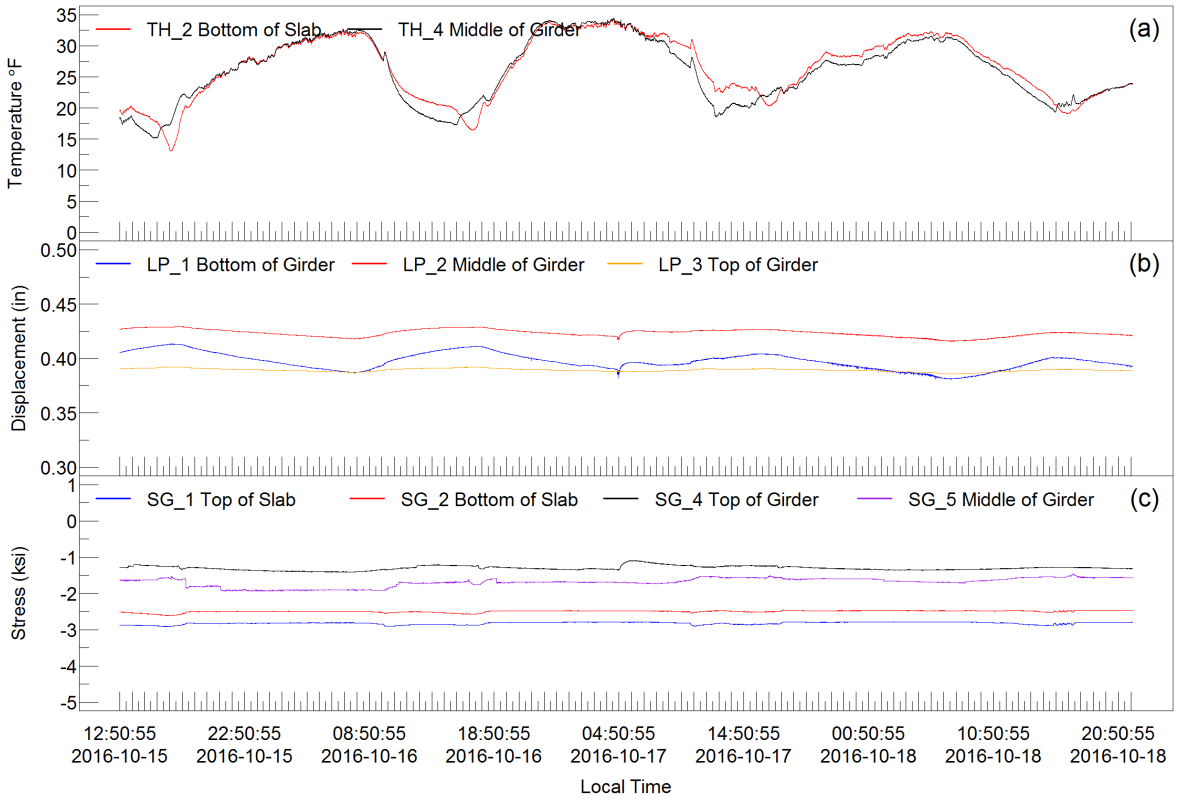

Figure 5-3 C-17-AT Bridge Sensor Data Oct.15th through Oct. 18th, 2016
(c) Thermocouple Data, (b) Linear Potentiometer Data, (c) Change In Stress Data.
Note: ℃ = (℉ – 32)/1.8; 1 in = 25.4 mm; 1psi = 6.89 kPa

From these initial correlations, it can be concluded that not only is the temperature change affecting both the expansion joint's movement but also the stress experienced in the vicinity of the joint. When the temperature has a similar daily variation of around or less 10 degrees the average stress varies by less than 0.25ksi for the concrete bridge and 3 ksi for the steel bridge and displacements vary by about 0.02 in and 0.5 inches respectively. However, when the daily temperature range changes from day to day and is larger (15 degrees or more), the joint experiences larger stress and displacement shifts. These larger daily temperature shifts cause stresses to vary by 0.25-0.5 ksi and 5-7 ksi (34450 - 48230 kPa), respectively, and displacements by about 0.05-0.09 in and 0.5 in (14 mm), respectively. While these values are still not large, if transferred to the abutment they could be significant and should be considered carefully when

discussing the possible removal of the expansion joint. Additionally, for the reinforced concrete bridge, C-17-AT, the data collected so far is for small temperature ranges and the stresses and displacements are likely to increase as the temperature range increases through the changing seasons. This is also indicated by the CSiBridge model parametric study and parts of the LCCA discussed below in Chapters 6 and 7 respectively.

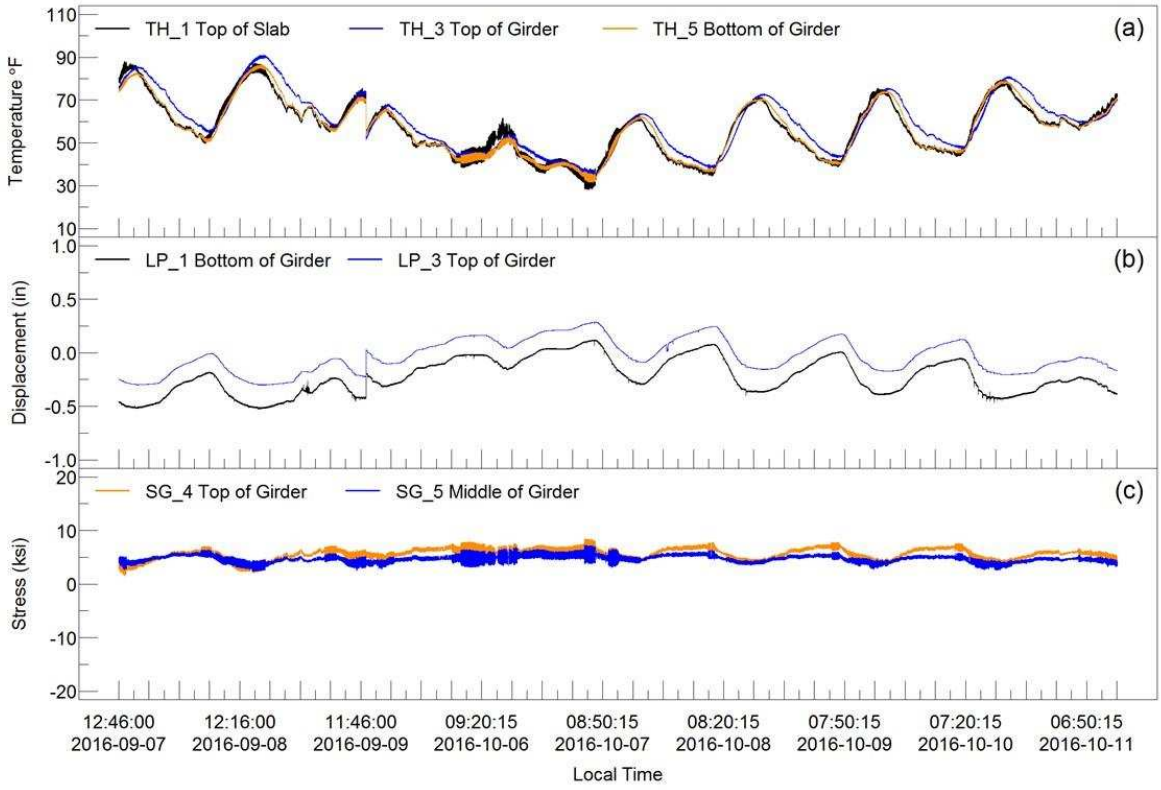

Figure 5-4 B-16-FM Bridge Sensor Data Sept. 7th through Oct. 11th, 2016
(d) Thermocouple Data, (b) Linear Potentiometer Data, (c) Change In Stress Data.
Note: ℃ = (℉ – 32)/1.8; 1 in = 25.4 mm; 1psi = 6.89 kPa

A concept worthy of recognition is the difference in timing between critical thermal movements and critical thermal stresses. The maximum bridge expansion and contraction occur at the joint during the warmest days in summer and the coolest nights in winter, respectively. However, the maximum thermal stresses due to the presence of thermal gradients through the depth of the superstructure occur during the warming of the

bridge in the early afternoon or the cooling of the bridge in the evening rather than that in the morning (Moorty, 1992). Verification of this concept and further understanding of the heating and cooling cycles on Colorado bridges can be further understood with temperature data from instrumentation of in-service bridges such as C-17-AT and B-16-FM.

Although current AASHTO provisions only require consideration of total longitudinal thermal movement based on average bridge temperatures, stresses due to temperature differentials in the cross section were shown to commonly be above +/- 5 ksi (34450 kPa) in steel box girder bridges in Texas (Chen, 2008). Though different girder material, widths, depth and bridge location would change the value of these stresses as shown above, it is clear that the significance of these stresses is worth analysing in Colorado's reinforced concrete and steel bridges.

The significance of the thermal gradient across the depth of the bridge is justified not only through the correlation between the temperature measurements and corresponding stresses, but also by calculating and comparing the maximum temperature difference. The maximum temperature differential through the depth of the bridge was calculated from the thermocouple data and compared to the stresses experienced by the bridge in Figure 5-5 below. The peaks in stress correlate with the larger magnitude temperature differences. Furthermore, the warmer the season becomes the greater the maximum difference in temperature across the girder's depth and the greater the stresses experienced.

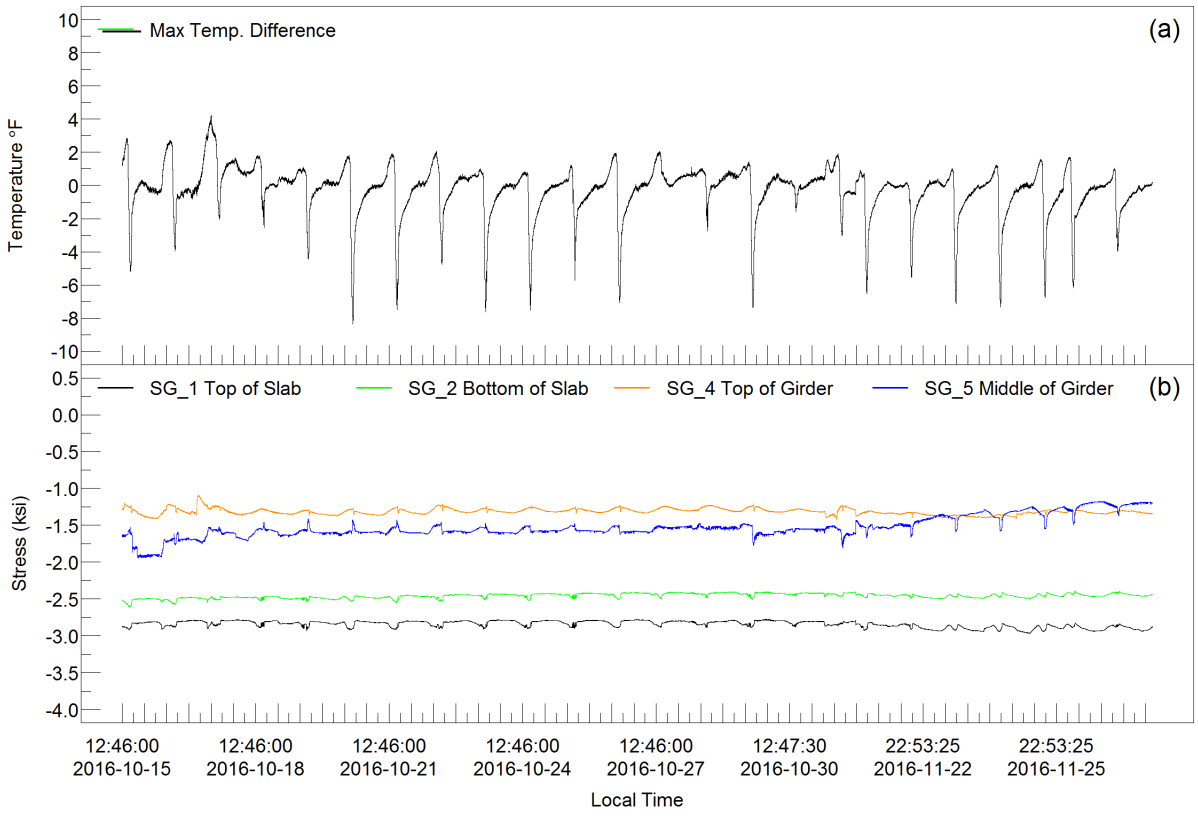

Figure 5-5 Maximum Temperature Difference Through Depth vs Stress Data.
(a) Max Temperature Difference, (b) Change in Stress Data.
Note: ℃ = (℉ – 32)/1.8; 1 in = 25.4 mm; 1psi = 6.89 kPa

5.4 Thermal Gradients and Bridge Deterioration

The next step is to compare these thermal gradients through the depth of the joint to standard design gradients. First, the temperature gradient with the minimum temperature and the average of the temperature gradients in the 10th percentile of measured temperature and second the temperature gradient with the maximum temperature and the average of the temperature gradients in the 90th percentile of measured temperature were plotted to see what shape the thermal gradient formed on the joint as seen in Figure 5-6 (c) below. The standard thermal gradients were also plotted on the depth of the girder for full comparison. What is initially apparent is that the minimum and maximum gradients have opposite shapes, as seen in Figure

5-6 (c), although the maximum temperature gradient has a more gradual slope when compared to the minimum. Nonetheless, when compared to the shape of the New Zealand and the AASHTO Standard Temperature gradients as shown in Figure 5-6 (a) and (b) respectively, they do not match (AASHTO, 2012; New Zealand, 2013).

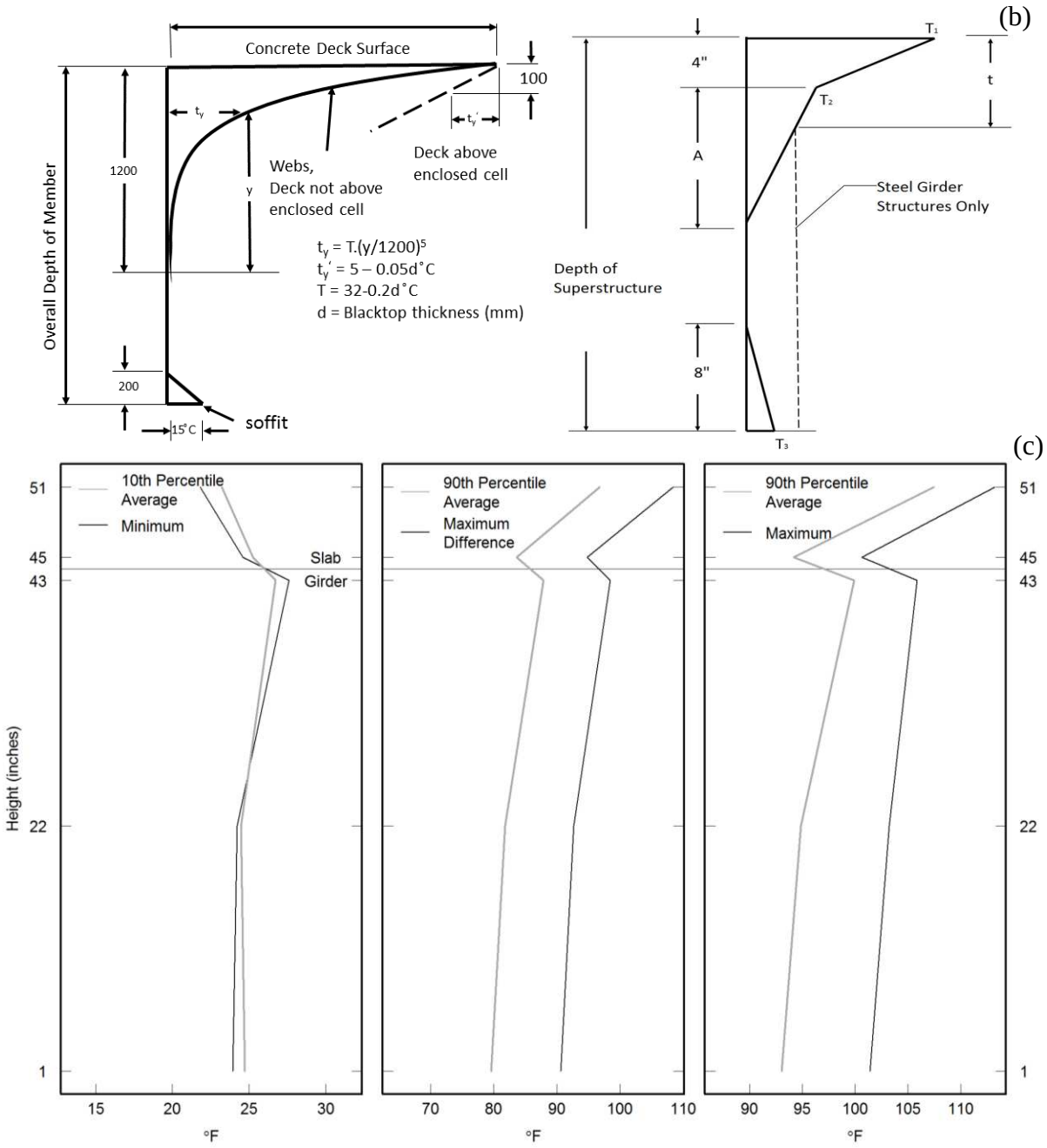

Figure 5-6 Design Standard vs. Measured Temperature Gradients. (a) New Zealand (mm) (17), (b) AASHTO (in) (1), (c) Measured Temperature Gradients. Note: ℃ = (℉ – 32)/1.8; 1 in = 25.4 mm;

The maximum gradient is the most similar to the AASHTO Standard with its positive slope in the top half. The bottom half is still, however, different than the standard. Furthermore, neither of the two gradients match the New Zealand standard, which has a more parabolic shape and a varying slope. Neither standard appears adequate for either a maximum or minimum temperature gradient on C-17-AT. This implies a need for further research into the accuracy of these temperature gradient design standards and modification for more accurate predictions. However, the comparison does indicate that the standards are in some ways conservative given that they appear to predict a higher temperature then the actual temperature being experienced by the joint.

Finally, it should be noted that the standard temperatures are to be applied on top of the temperature at which the bridge was built, while the gradients shown from the measured data are just the raw temperatures experienced by the bridge, and these gradients are only for the winter months due to limited C-17-AT data. This does not impact the ability to compare shapes of the gradients, and if anything shows that the standard gradients might be aimed at summer temperature gradients. However, even in the summer they may prove to conservative given the current observations.

While conservatism is beneficial in providing safety factors, economical design should also play a role. Furthermore, an economical design and solution is what many DOTs are most interest in when considering bridge expansion joints. Furthermore, when instrumenting bridge C-17-AT and bridge B-16-FM the severe clogging of the joints and associated deterioration in the surrounding decking and abutments was noted. The deterioration at the joints and abutments can be seen in Figure 5-7 and Figure 5-8 below for Bridge C-17-AT and Bridge B-16-FM respectively. Perhaps the greatest insight from this data is the consequences of the partially

locked joint as evident by the present stresses shown above with their correlation to the temperature experienced and the deterioration shown below. This type of deterioration, cracking and spalling, is likely in part due to the clogged joints inducing stress when the bridge tries to expand. If the joint was fully functioning, little to no stress would be present in or around the joint. The joint is not fully locked as shown by the linear potentiometers measuring displacements. While movement can initially be seen as good because it proves the joint is not fully blocked, this, in combination with the present changes in stress, indicates the potential for fatigue and deterioration.

Figure 5-7 Deterioration of C-17-AT Abutments and Joints

Figure 5-8 Deterioration of B-16-FM Abutments and Joints

With this in mind, the measured thermal gradients were utilized for the analysis of temperatures impact on abutments, assuming clogged joints, as were seen in the field. In order to perform this analysis, the maximum and minimum temperature gradients measured for each bridge was applied to that bridge's CSiBridge model. This created four models, each was run and the forces at the ends of the girders due to the thermal loading were recorded. The average force for each case, and the average temperature for each gradient was calculated as seen in Table 5-1 below. These average values were used to find a linear equation relating force to temperature for each bridge, the equations are shown below. The relationships these equations represent, while they are approximate due to the need to use averages for simplicity, they show direct relationship between the stress experienced by the bridge and abutments due to temperature and clogged joints. The equations differ by a magnitude of 10. This could be in part due to the steel data and thus thermal gradients having 6 months of data that spans winter and summer compared to the concrete bridge, C-17-AT, only have 3 months of winter data to utilize. The limited amount and type of data available for the concrete bridge C-17-AT is likely causing it to have a significantly smaller slope due to less variance in temperature limiting the simulated relationship. This is further supported when comparing the average maximum and minimum temperatures for the two bridges. C-17-AT had significantly, and unrealistically low average temperatures with a max at only 24℉. However, if until further data is obtained, the thermal gradients were assumed to uniform a greater range of temperatures could be analyzed in the models and a more realistic equation could be determined. This process is discussed and utilized in Chapter 7 below as part of the life cycle cost analysis (LCCA) for bridges with expansion joints. The analysis includes the impact of clogged joints on their abutments.

Table 5-1 Temperature and Force for C-17-AT and B-16-FM

Variable	B-16-FM	C-17-AT
Average Force – Max Temp. Gradient	31.8 ksi	1.6 ksi
Average Force – Min Temp. Gradient	7.6 ksi	0.75 ksi
Average Temperature – Max Temp. Gradient	102.8℉	37.75℉
Average Temperature – Min Temp. Gradient	23.75℉	15.25℉
Equation	Y=0.306*T	Y=0.038*T

5.5 Summary and Preliminary Conclusions

The impact of temperature, thermal gradients, and overall shifts in temperature due to changing seasons have a significant effect on bridge expansion joints in Colorado. The potential for 0.02 in of movement and 0.5 ksi in stress increase on concrete bridges regularly and 0.5 in movement and 5 ksi stress on steel bridges regularly is not negligible. Furthermore, this preliminary data on the concrete bridge C-17-AT only accounts for mid-winter and does not account for the hottest or coldest days of the year which can cause the greatest movement in the expansion joint. This fact should be kept in mind when considering these preliminary findings and their application. However, these limited observations do imply that if CDOT is interested in removing an expansion joint, the bridge superstructure and retrofit option would need to support the movement of the bridge and the potential for abutment stresses due to movement. These displacements do not appear so great as to require the use of an expansion joint. On the other hand, more data at different times of the year is needed for a more definite recommendation.

Removing the joint would eliminate the concentrated stresses which could prevent possible fatigue cracking at joints. This would not eliminate the stresses introduced at the abutment and could introduce more. In the event of joint removal, the abutments would need to be analyzed and reinforced to support these stresses due to the temperature gradients and thermal

contraction and expansion. Nonetheless, the impact and potential benefits of constructing a bridge without deck joints or bearings or eliminating all deck joints and bearings by retrofitting an existing bridge is significant. The behaviors of interest and parameters influencing them are numerous and vary for new construction and existing bridges. These parameters and costs are analyzed further in Chapter 7. Additionally, based on the comparison of thermal gradients with standard gradients further research is needed to determine a more accurate standard for temperature gradient prediction. This would not only help predict stresses around a joint due to thermal gradients, but also benefit abutment design for continuous or retrofitted bridges. All of which could potentially lead to a more economical and safe design. Finally, more scientifically verified information on the response of reinforced concrete and steel bridges and development of well-understood replacement connections would assist in furthering the concept of deck joint replacement and, therefore, decrease maintenance costs and increase the durability of bridges' superstructures.

CHAPTER 6

PARAMETRIC STUDY

6.1 Introduction

Below describes the numerical model and parametric study performed using the CSiBridge three-dimensional numerical model of C-17-AT, which was validated using the control load test discussed in Chapter 4. The objectives of the parametric study were to consider the different code based thermal gradients and the effects of these thermal loads on the joint and bridge performance. The behavior of the bridge under different amounts of joint clogging while under thermal loads was also examined. Different joint elimination scenarios were also examined to provide DOT engineers with the implications of different joint removal alternatives. Three joint removing connections, three thermal load scenarios, and three joint clogging scenarios were analyzed.

6.2 CSiBridge Finite Element Numerical Model

The finite element model of bridge C-17-AT was developed by Kalry Rager along with a finite element model of the steel bridge B-16-FM during the first stage of this study. The finite element software chosen was CSiBridge which is used by many practicing engineers. The software was created by the same developers as SAP2000 and was chosen by CDOT due to its heavy presence in private consulting.

The finite element model was built using thin shell elements for the girders and slab, as seen in Figure 6-1. The thin shell elements were assigned dimensions and area section properties

to match the properties of bridge C-17-AT. Rebar was included for both compressive and tensile reinforcement in the girders and for two-way slab action in the concrete deck. For concrete properties, the compressive strength of 4000 psi concrete was defined along with a modulus of elasticity of 3604 ksi. The shell elements were meshed at six inch intervals to provide uniform response and minimize computational time.

Composite action was obtained using short frame elements connecting the girders to the slab, these short frame elements were assigned Grade 50 steel properties with a modulus of elasticity of 29000ksi. These elements represented the shear studs used in traditional reinforced concrete construction to connect girders to slabs. The stiff links are shown as blue lines connecting the a node on the girder to a node on the slab in Figure 6-2 below. These stiff link shear studs were sized so that their cross-sectional area matched that of the shear connectors detailed in the construction documents in Appendix A.

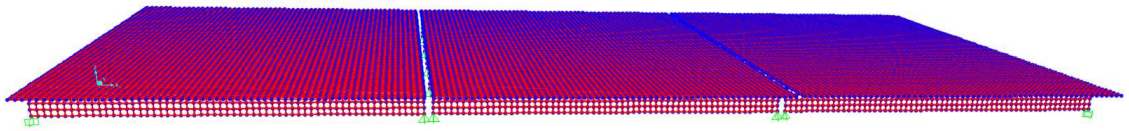

Figure 6-1 C-17-AT Finite Element Model.

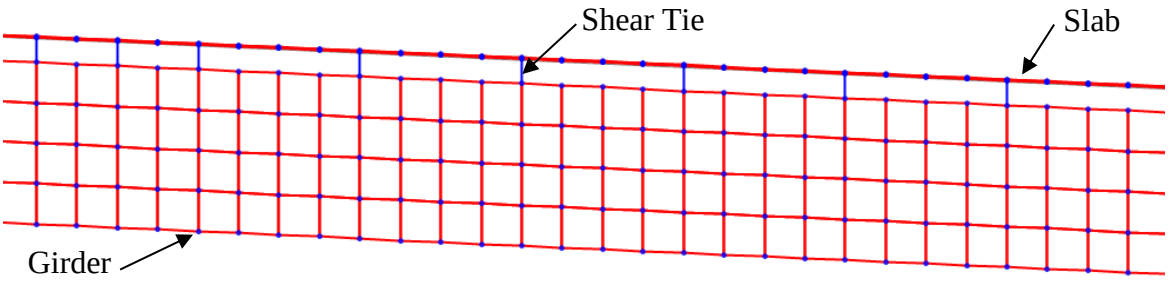

Figure 6-2 C-17-AT Finite Element Model Ties Between Girder and Slab

Several loading scenarios were analyzed. Self-weight dead loads, point loads, and uniform loads were applied for the first verification stage. Theoretical calculations were also made using these same loads and composite beam theory in order to perform the initial verification. The second verification stage is discussed in Chapter 4 and used a CDOT A-40 truck's axle loads on the instrument bridge and in the finite element model. The strong agreement between the theoretical calculations, within 10%, the field tests, within 15%, and the CSiBridge finite element model provide the confidence needed for the parametric study to be completed.

The boundary conditions for the bridge were fixed at the abutment ends due to bridge C-17-AT being monolithic with the abutment. At the pier caps, due to the presence of bearing pads, the connection is not a true pin. Instead the bearing was retained as a spring boundary connection fixed in the vertical direction and with a spring stiffness value of 45 kip/in due to friction in the horizontal and transverse directions. The friction resulted from the interaction between the concrete girders and the neoprene bearing pads on the pier caps.

6.3 Joint Retrofitting Options Analyzed

There are multiple alternatives for connecting two spans after the removal of a joint, this parametric study focuses on past alternatives that have been considered and utilized by transportation agencies. This allows for the results to be related to typical field practices among DOTs. The three connection types chosen were 1) Deck Only, 2) Girder Only, and 3) Deck and Girder Full-Moment Splice. Localized stresses in the girder and deck were examined for each connection type.

To model the deck only connection, the slab was connected in the finite element model using the same slab type of shell elements. The girder was connected similarly, by

connecting the girder sections with the same shell elements. The full moment splice was achieved by connecting the slab and girders with their respective shell elements. Standard Thermal Gradients Applied

In order to assess the superstructure's response to different thermal loading scenarios in the modelled bridge, while also looking at the effects of removing joints, three vertical thermal distributions were utilized. Two of these distributions had a gradient through the depth of the bridge while the third had a uniform thermal distribution. The first thermal gradient considered was adopted from the AASHTO LRFD Bridge Design Specifications and the second thermal gradient considered was based on the New Zealand bridge design code. This New Zealand code was selected because a previous study conducted by French et al. (2013) showed reasonable agreement between this fifth order gradient curve and the field-measured thermal loading on the bridge studied. Finally, a uniformly distributed temperature change of 50^{O}F was applied. The uniform temperature distribution entailed an increase of 50^{O}F, which was applied to the entire cross-section along the length of the spans in order to determine how thermal stress from a uniform thermal gradient compares to varying vertical thermal gradients. An increase of 50^{O}F was chosen because all bridges in Colorado experience this temperature change over the course of one year. The AASHTO and New Zealand thermal gradients are shown in Figure 6-3 below.

The temperatures were applied to the bridge model using a piece-wise thermal gradient method modelled after an example entitled *Temperature Changes and Fabrication Errors* in the textbook Matix Analysis of Structures by Aslam Kassimali (2012). The piece-wise approximation divides the girder and slab into elements and each element is assigned a single temperature based on the equivalent piece-wise distribution of the thermal gradient. For the model of C-17-AT the bridge's depth is divided into 5 shell elements including the slab

thickness. The piece-wise approximations for the AASHTO, New Zealand, and Uniform thermal gradients are shown below in Figure 6-4.

(a)

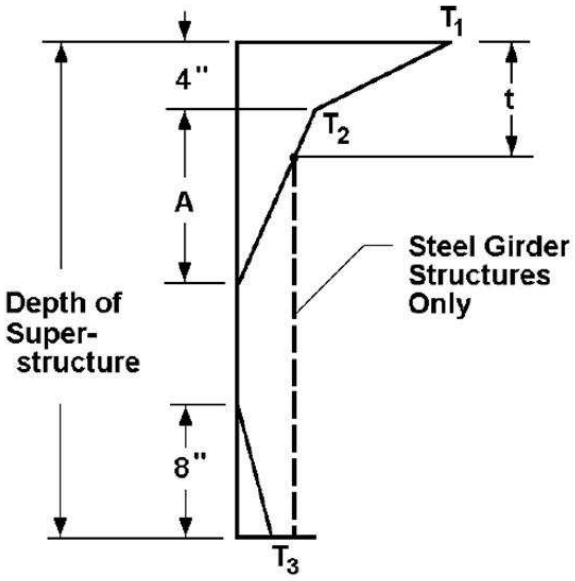

(b)

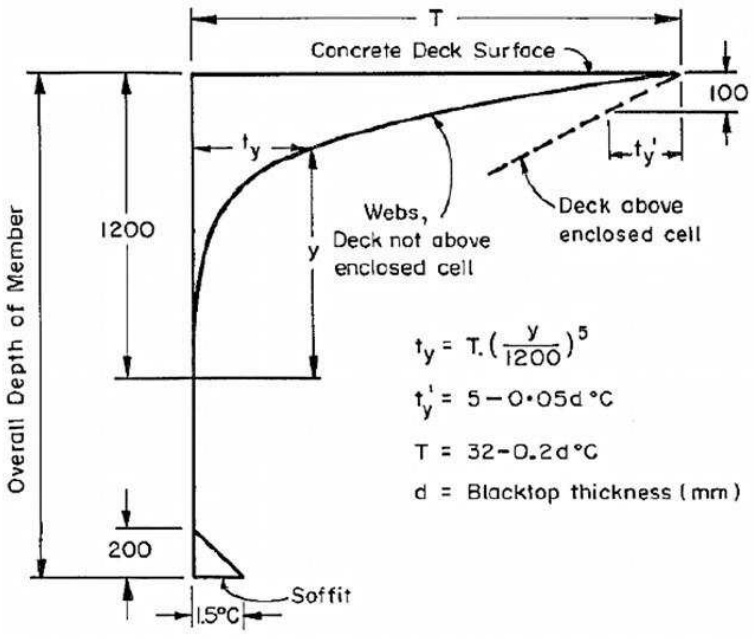

Figure 6-3 (a) AASHTO Thermal Gradient, (b) New Zealand Thermal Gradient.

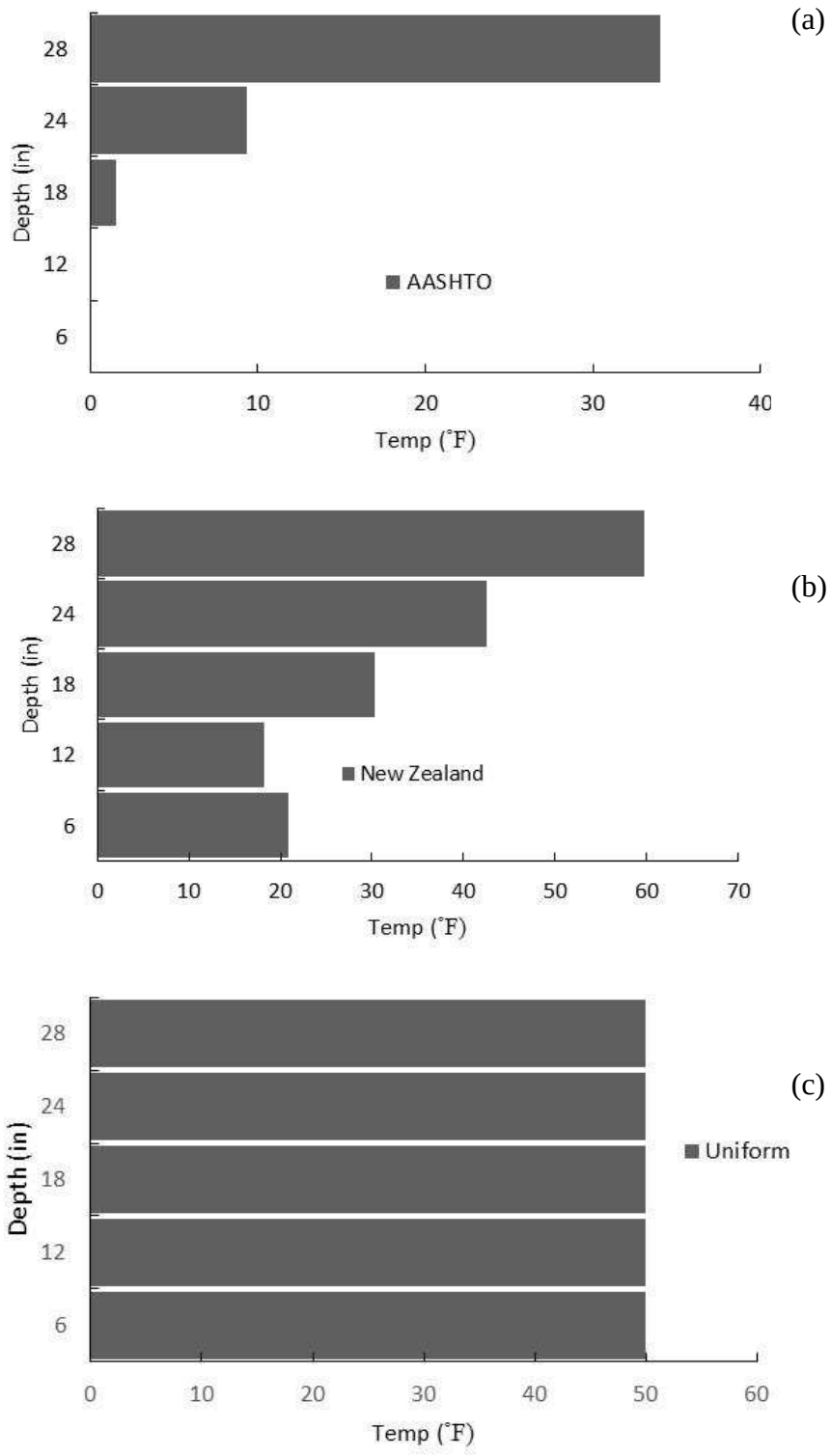

Figure 6-4 Piece-wise Approximation: (a) AASHTO Thermal Gradient, (b) New Zealand Thermal Gradient, (c) Uniform Gradient

6.4 Joint Clogging Stiffness Considered

Past research has identified that joints are often clogged with debris soon after being placed into service (Chen, 2008). In order to model this clogging in CSi Bridge, axial stiffness coefficients were assigned to links connecting the slabs across the joints. These axial stiffness coefficients were calculated based on the moduli of elasticity of soil types that commonly clog joints, sand and gravel. Stiffness values (k) are typically calculated as EA/L, where E is the modulus of elasticity, A is the area, and L is the length of the element.

The soil volume clogging the joint is the structural element considered for the axial stiffness. Gravel as a typical modulus of elasticity of 150 MPa (22 ksi) and sand has a modulus of elasticity of 50 MPa (7 ksi) (Briaud 2013). The length of the clogging debris was taken as the joint opening which was 0.125 inches (L) as measured in the field. Axial stiffness was determined for each soil type and a blend. The stiffness placed evenly across the joint by placing links every six inches in the transvers direction. This assumes that the joint is evenly clogged along its length, and consequently assumes no torsional effects. The axial stiffness coefficients were taken as 30 kip/in for gravel filled joints, and 10 kip/in for sand filled joints, and 20 kip/in for a joint that is clogged with a mixture of gravel and sand. The same methodology was used in analyzing the steel bridge as outlined in Rager (2016).

6.5 Parametric Analysis Matrix

The effects of the different combinations of connection type, clogging material, and thermal gradients on local and global performance were examined using a parametric study matrix shown in Figure 6-5 below. The two types of joint alterations, clogging and connection

type, were analyzed with each of the three thermal gradients. All analysis were conducted using the finite element model of C-17-AT and the results are discussed below in Section 6.6.

Thermal Gradients	Stiffness of Clogging Links Across Joints			Connection Retrofit	
	10 kip/in	20 kip/in	30 kip/in	Deck Only	Deck and Girder
AASHTO	x	x	x	x	x
New Zealand	x	x	x	x	x
Uniform (+50˚F)	x	x	x	x	x

Figure 6-5 Parametric Study Matrix

6.6 Analysis Results and Implications

The results and implications of the parametric study analysis are divided into two sections: those associated with clogged joints and those associated with the retrofit connection types. The results from the clogged joints are presented as line graphs because the stiffness assigned to the two-joint links are continuous quantitative variables. However, the retrofit connection types are discreet qualitative variables and are therefore presented as bar charts for comparison.

In order to analyze the different connection types and clogged joint stiffness and their effect on global and local bridge behavior three different load scenarios were examined: thermal gradient load only, truck load only, and thermal gradient and truck loads combined. The truck load used was an AASHTO HS2044 truck as shown in Figure 6-6 below.

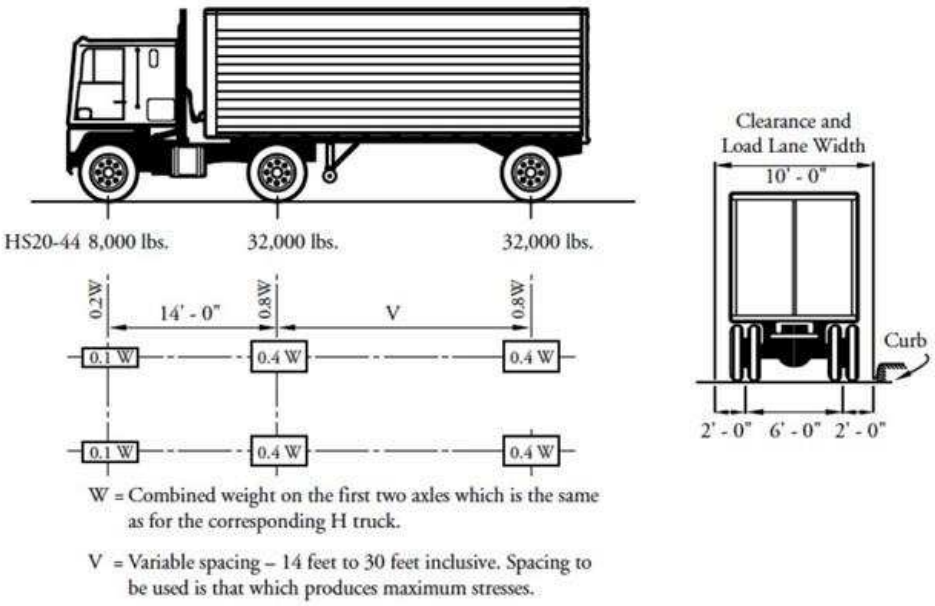

Figure 6-6 AASHTO HS20-44 Truck (Precast/Prestressed Concrete Institute, 2003)

The location of the truck was determined by performing an influence line analysis to find the location that produced the maximum moment demand. This location was found to be where the front axle is over the bearing near the beginning of the span and the back two axles are placed 14 feet apart (V=14 feet). In the remainder of the chapter, truck loading refers to this location of the AASHTO HS20-44 truck on the bridge.

6.6.1 Clogged Joint Results and Implications

The effects of clogged joints in the parametric study on the bridge as analyzed using the truck loading, thermal gradients, and values for link stiffness (k = 10 kip/in, 20 kip/in, 30 kip/in) described above. The analysis was performed considering only the thermal and truck loads, the dead load due to self-weight of the bridge was neglected.

First, the maximum stress in the bottom of the girder at the ends and at the mid-span due only to each of the three thermal gradients was determined for each of the three link stiffness

values. Figure 6-7 and Figure 6-8 show these results for the girder ends and girder mid-span. The model experienced a maximum compressive stress of 0.217 ksi in the girders at mid-span, with a 10 kip/in link stiffness and the AASHTO thermal gradient load. The maximum tensile stress in the bottom of the girders was 0.026 ksi in the girders at mid-span, with a link stiffness of 30 kip/in and the Uniform thermal gradient load.

The maximum loads experienced in the girders due to all thermal gradient loads occur at mid-span. At the bottom ends of girders the AASHTO thermal gradient gives compressive stress around zero due to no temp load applied at the base of this gradient. The AASHTO thermal load gives the largest compressive stresses at the girder bottoms at mid-span due to the larger moment induced by the gradient. New Zealand is the middle loading gradient with the Uniform thermal load mirroring the AASHTO gradient giving the largest compressive stress at the bottom of girder ends and the least at mid-span.

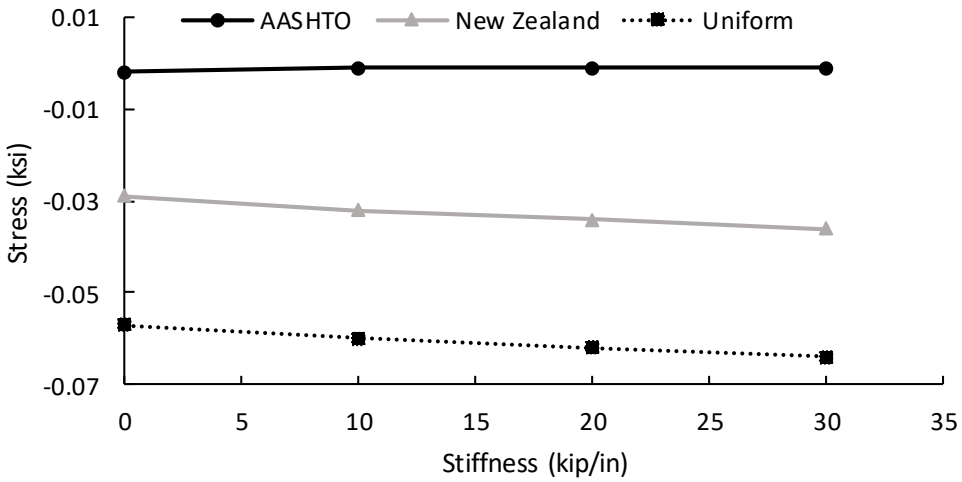

Figure 6-7 Maximum Stress in Bottom of Girder at End

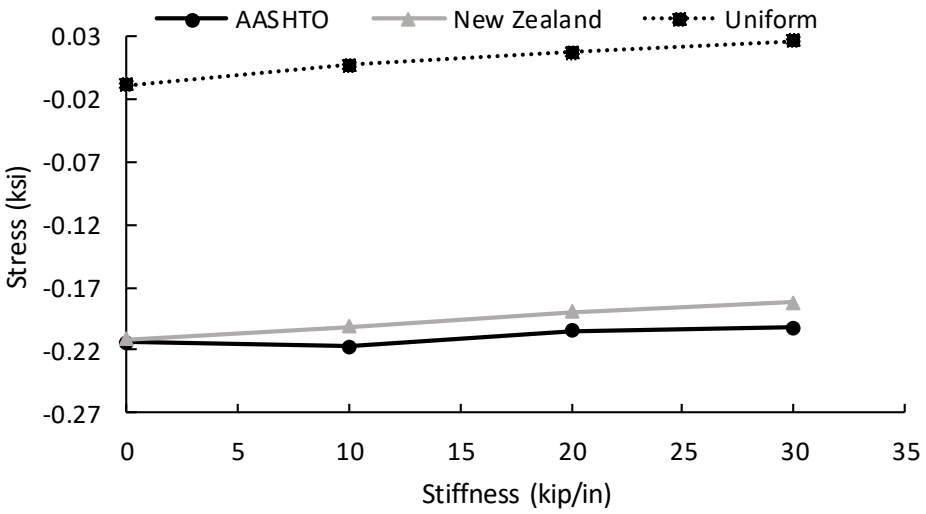

Figure 6-8 Maximum Stress in Bottom of Girder at Mid-span

The maximum in the top of the girder was also analyzed at both mid-span and at the ends due to each of the thermal gradients for each of the link stiffness values, shown in Figure 6-9 and Figure 6-10 below. The maximum tensile stress for each link stiffness value was produced due to the AASHTO thermal gradient load induced moment at mid-span in the top of the girders. This is expected since AASHTO had the highest temperature load difference between top and bottom of the girder. Whereas the maximum tensile stress was at each of the link stiffness values was produced by the Uniform thermal gradient load in the girder at mid-span. Overall, comparing the two standard thermal gradients, AASHTO appears to have the more conservative gradient due to the larger difference in temp between top and bottom despite New Zealand applying a greater maximum temperature at the top.

In all four figures the clogged joints, symbolized by the link stiffness values, do not show a significant impact on the global or local demand on the bridge superstructure. Both the stresses at the top and bottom of the girders showed relatively small changes in compressive and tensile stress under each thermal gradient load as the stiffness increased. The maximum stress range on

the girders for the different stiffness values were 0.02, 0.05, and 0.06 ksi for AASHTO, New Zealand, and Uniform thermal gradients respectively, all less than 0.1 ksi difference.

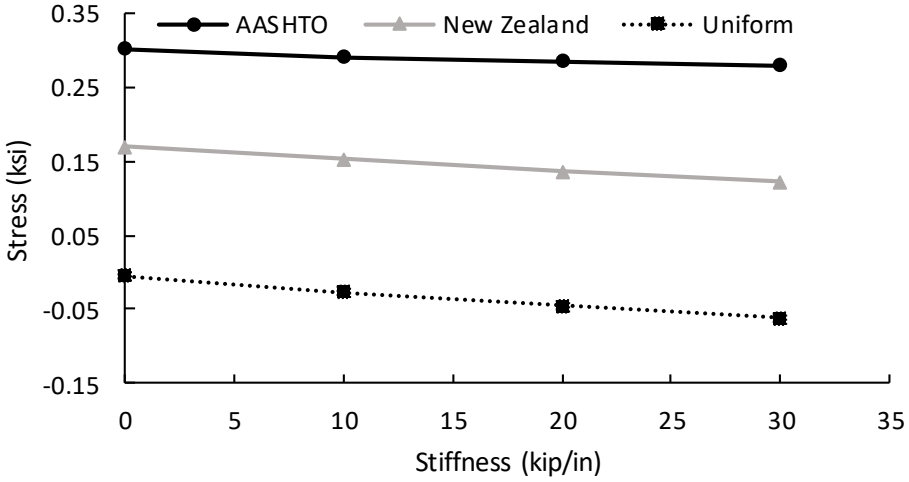

Figure 6-9 Maximum Stress in Top of Girder at Mid-span

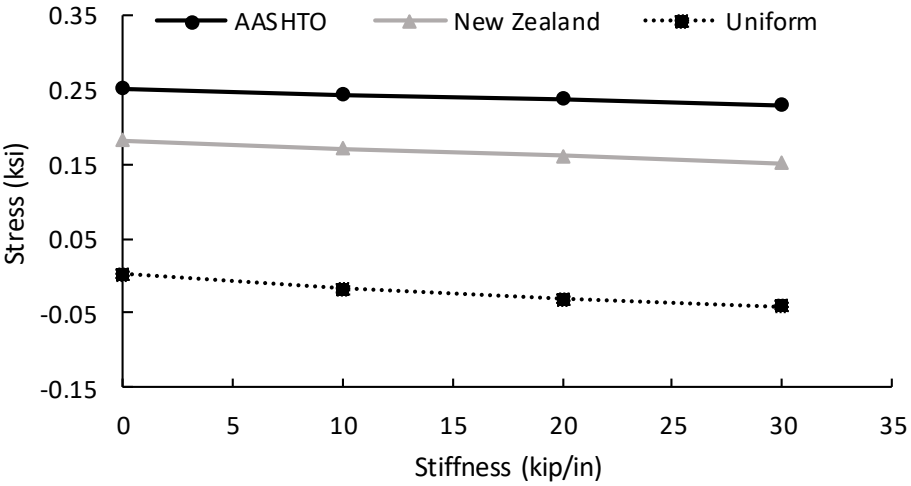

Figure 6-10 Maximum Stress in Top of Girder at the Ends

With the clogging stiffness established as not having significant impacts on the bridges behavior a truck load was added to the analysis. The HS20-44 truck was examined first with only the truck and second combined with the thermal gradient loads. Figure 6-11 below show the results of the model with the truck loading and clogging stiffness. The truck load's moment demand on the bridge decreases slightly due to the clogged joints modeled by the link stiffness

values because the simulated clogged joints hold the concrete in a negative moment region. Consequently, some moment is transferred in this negative moment region and the positive moment region's moment demand will decrease slightly unlike in an unclogged joint. This overall decrease is only about 0.0257 ksi which is only 0.4% of the moment demand with an unclogged joint and as such is insignificant, reinforcing the insignificance of the stiffness of the clogged joint.

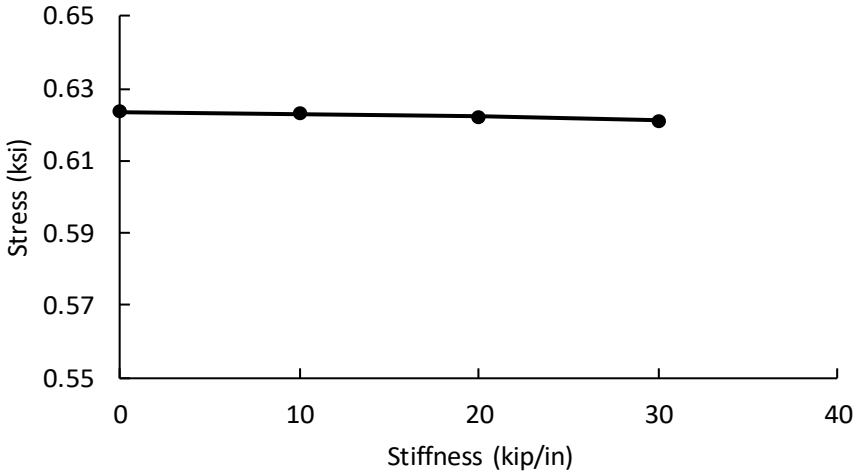

Figure 6-11 Stress Demand in Bottom of Girder at Mid-span due to Moment resulting from the Truck Load

Next, the analysis of the thermal and truck loading combined was conducted and the results are shown below in Figure 6-12. The Uniform thermal gradient showed the most obvious change between just the thermal load and the thermal load and truck load, with an increase of about 0.6 ksi. This is likely due to the Uniform gradient having almost no stress at this location by itself and thus was the addition of the truck load was close to total. The New Zealand and AASHTO gradient moved from compression to tension with an average stress change of about 0.6 ksi as well, moving from abou -0.22 ksi to 0.38 ksi. Indicating that the truck load counteracts the thermal load on the bridge.

Additionally, similar to when examining the thermal gradient loads only, the combined loads showed negligible changes in stress relative to the increase in clogged link stiffness. The maximum stress range on the girders for the different stiffness values were 0.012, 0.026, and 0.03 ksi for AASHTO, New Zealand, and Uniform thermal gradients respectively.

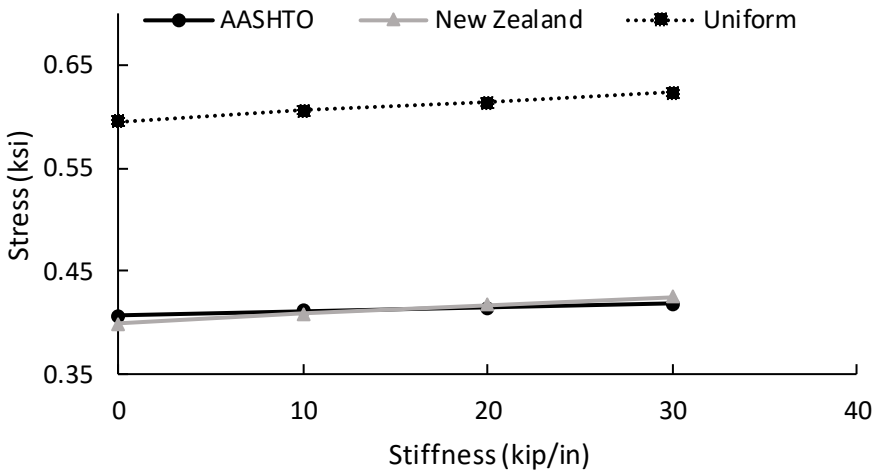

Figure 6-12 Moment Demand Due to Thermal and Truck Load in Bottom of Girder at Mid-span

6.6.2 Joint Retrofit Connection Results and Implications

First, the maximum stress at the bottom of the girders near the bearings due only to the thermal gradients was determined for each connection type. Figure 6-13 below shows these stress values. The stresses induced by the AASHTO recommend thermal gradient is a lower tensile stress when compared to the New Zealand Gradient, whereas the Uniform thermal gradient gives the largest compressive stresses. This is to be expected because the uniform thermal gradient is a uniform temperature increase of 50˚F throughout the depth of the structure. Therefore, the temperature load at the bottom of the girder for the uniform gradient of 50˚F is significantly larger than the 20.82˚F and 0˚F for the New Zealand and AASHTO recommended thermal gradients respectively. This larger temperature load will cause greater thermal expansion of the concrete and consequently greater compressive stresses. Conversely, the AASHTO

recommend thermal gradient has the lowest temperature load at the bottom of the girder and therefore it is reasonable that it should produce lower compressive stresses when the bridge is only exposed the thermal loads with the two retrofit options. The Deck Only connection produces lower stresses than the Full Moment Splice connection for all three thermal gradients. The significant difference is likely due to the boundary conditions on the bridge; the abutment connections for the superstructure are fixed conditions. Thus when the deck is connected the joints are now transferring a little of the moment capacity contained in the fixed ends through to the center span. However, when the deck and girders are connected in a Full Moment Splice that entire moment can be carried throughout the length of the bridge, across all spans, significantly increasing the moment capacity. This allows a negative moment region across the supports and increases the moment capacity and thus the stress in the girders. For the AASHTO and New Zealand thermal gradients, the Full Moment Splice increases the tensile stress significantly. This is likely due to the lower temperature loads at the bottom of the girder when compared to the top. The difference, of 30-40˚F, creates significantly greater compression in the top versus the bottom and induces a moment that the Full Moment Splice allows to be carried, increasing the stress.

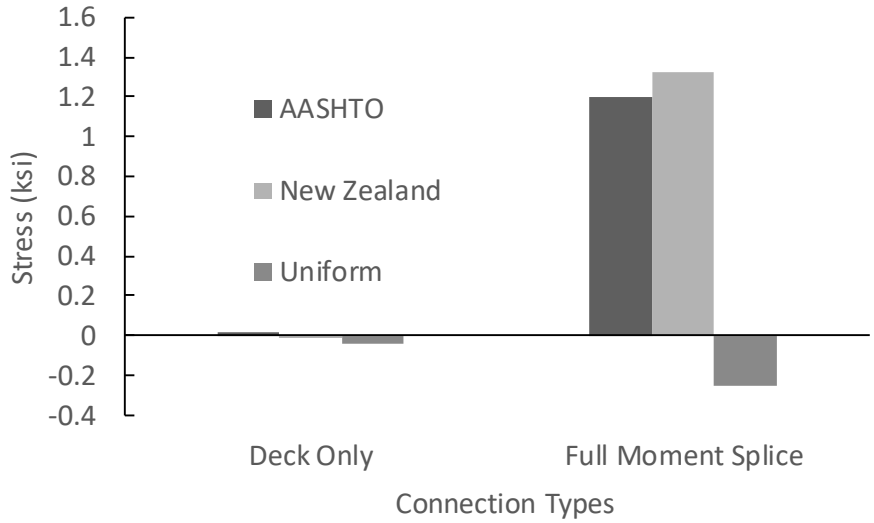

Figure 6-13 Maximum Stress at Bottom of Girder due to Thermal Gradients Only

In order to fully evaluate a potential increase in the span's moment capacity for the two retrofit connection types considered, the analysis was performed for only the truck load with each of the connection types. The stress values due to the truck loading are shown below in Figure 6-14. The maximum stress at the bottom of the girders near the bearings was measured to gauge the moment demand for each connection type. When the Deck Only connection was examined the truck load induced a tensile stress in the girders of 0.06 ksi, whereas when the Full Moment Splice was examined the truck load induced a greater compressive stress of 0.46 ksi. This change from tensile to compressive stress indicates an increase in moment capacity of the superstructure, corresponding to a 75 % decrease in moment demand.

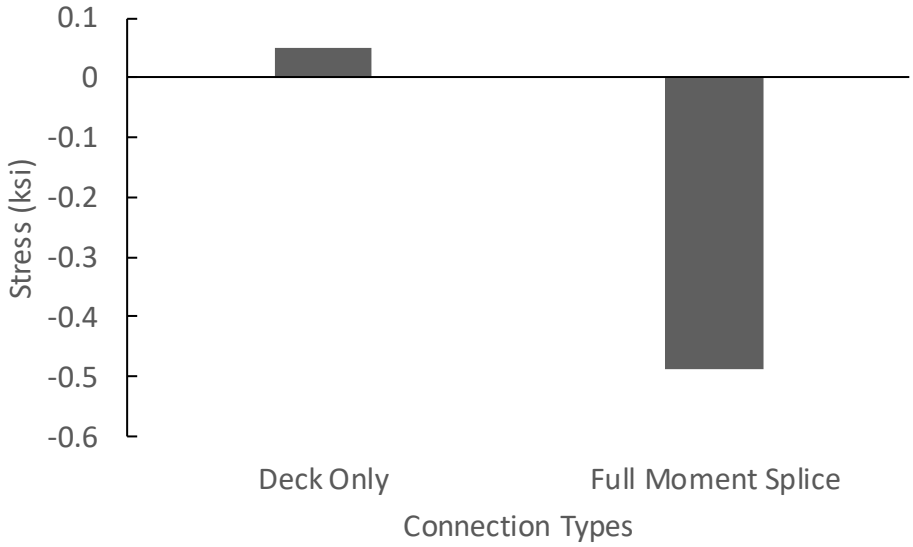

Figure 6-14 Maximum Stress at Bottom of Girder due to Truck Loading Only

Once thermal gradient loads and truck loading scenarios were analyzed separately, analysis was completed for combined thermal and truck loading for both connection types. The stress at the bottom of the girders near the bearings due to both loads are shown in Figure 6-15 below. Comparing Figure 6-13 and Figure 6-14 with Figure 6-15 it is evident that under the Deck Only connection the stresses increased in tension. Under the Uniform thermal gradient and

deck only retrofit connection, the truck load caused the stress to switch from compressive to tensile. On the other hand, the truck load in the Full Moment Splice connection decreased the tensile stress under the AASHTO and New Zealand thermal gradients, and increased the compressive stress when the Uniform thermal gradient was applied. This change in stress illustrates how the connection type for joint retrofitting influences global moment demand on the bridge when considering thermal gradients. The Truck load counteracts the thermal loads once again, and the full moment splice increases the bridge's moment capacity significantly compared to the deck only connection.

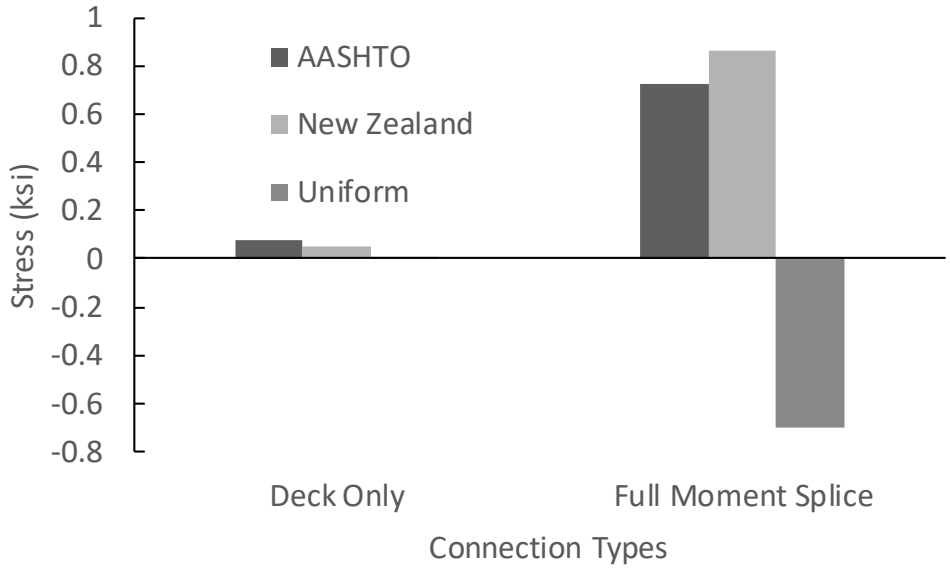

Figure 6-15 Maximum Stress at Bottom of Girder due to Thermal Gradients and Truck Load Combined

6.7 Conclusion

These parametric study results illustrate the differences between the thermal gradients and joint retrofit connection types considered. The thermal gradients when subjected to different joint clogging stiffness values showed relatively little change in stress as the stiffness increased. At mid-span the AASHTO thermal gradient showed the greatest stresses, while at the girder ends

the Uniform thermal load showed the greatest stress. Applying a standard truck load to the bridge counteracted the stresses and moments induced by the thermal loads.

When applied to the different connection types the thermal gradients and truck load's impact on the bridge's moment capacity was examined. The New Zealand thermal gradient showed the greatest difference in stress load for the two different connection types. This can be connected to the fact that the New Zealand thermal gradient has the greatest temperature at the top of the gradient creating a difference of about 40˚F between top and bottom, and inducing significant expansion at the top with the potential for moment transfer when fully connected. A decrease in moment demand was observed when the Full Moment Splice connection was used under only truck loading. However, the moment capacity and demand increased when the truck load was combined with the AASHTO and New Zealand thermal gradients and a Full Moment Splice was utilized. This increase in demand is influenced by the fixed ends of the bridge at the abutments which allow for moment transfer throughout the length of the bridge when a Full Moment Splice connection is used. With the full moment splice connection giving the greatest increase in moment capacity the full moment splice will be assumed for the retrofit to continuous analysis in the Life Cycle Cost Analysis in Chapter 7.

CHAPTER 7

LIFE CYCLE COST ANALYSIS

7.1 Introduction

Many Departments of Transportation (DOTs) are looking for a better way to address deteriorating expansion joints on highway bridges. Many of the bridges built after The Federal Aid Highway Act of 1956 were designed with expansion joints because expansion joints provided an easy way to design simply supported bridges before the era of structural analysis software (Federal Highway Administration n.d.). Bridge expansion joints create a break in the structural continuity of a bridge. They are located at abutments and at the ends of individual spans over piers. They are designed to absorb thermal movements of the bridge between two bridge elements. These simply supported expansion joint bridges could be designed and analyzed quickly by consulting engineers and firms providing an easy solution to the rapidly expanding highway system. At the time, detailed knowledge about the maintenance requirements and costs of these types of bridges was not known leading to this design boom and leaving the country with a plethora of expansion joint bridges, many of which are still in use today (Tsiatas and Boardman 2002).

Notably, expansion joints, and bearings, require regular and frequent maintenance throughout their life-span in order to function properly and thus inhibit damage to the bridge superstructure (Hawk 2003). A clogged joint can induce un-designed for stresses into the girders and abutments. A leaking joint can cause corrosion of the superstructure below, primarily the pier caps (Lam et al. 2008). Deicing salts and chemicals used in colder regions increase the likelihood of corrosion beginning in the superstructure if a leaking joint is present. Additionally,

the location of a bridge in the mountains, where chains are used on vehicles, can cause deterioration that is more extensive. These issues are what caused expansion joints to be named by the American Association of State Highway and Transportation Officials (AASHTO) as the second most common bridge maintenance issue behind concrete bridge decks (AASHTO, 2012).

Most DOTs do not have the resources or personnel-time to conduct preventative maintenance, such as joint cleaning and seal repair on their bridge joints leading to deterioration spreading until replacement is needed. These preventative maintenance actions would need to be done every few months due to the fact that a joint becomes clogged after just a few weeks. The required frequency as well as the restrictions and precautions necessary when washing/cleaning a joint due to the risk of contaminating the environment with chlorides and other automotive chemicals, is what makes preventative maintenance beyond a DOTs resources.

The cost and time intensive nature of bridge expansion joint maintenance, as well as the consequences of deteriorating joints on the bridge superstructure have gained the attention of bridge engineers and managers. With the rise of structural analysis software modern bridge design is moving away from the use of expansion joints. In most modern bridge designs joints are completely eliminated or kept to a minimum, such as in semi-integral bridges which have joints only at the abutments. While new bridges seek to eliminate joints and their associated problems, DOTs are still left with a significant inventory of older bridges with many joints, and the need to make decisions about what to do with the joints. For example, could it be more cost effective to remove all joints and retrofit the bridge to be continuous instead of continuously replacing joints on a 7-10 year cycle? To answer this question a life cycle cost analysis (LCCA) is utilized to examine the most cost effective solution for dealing with expansion joint deterioration in existing bridges.

LCCA involves determining all costs associated with a piece of infrastructure over its remaining design life. Depending on if the structure is new or existing these costs can range from design and construction, maintenance and user costs, to environmental and vulnerability costs (Frangopol and Liu 2007; Marques Lima and de Brito 2010; Hawk 2003; Safi, Sundquist, and Karoumi 2015; Kim et al. 2010; Hatami and Morcous 2014; Reigle and Zaniewski 2002). Once all costs have been adjusted for a common reference point or present value they are quantified and the total calculated. This total cost for an infrastructure's relevant analysis period or remaining design life is the life-cycle cost (LCC) and can then be compared to the life-cycle cost of other designs or alternatives for the same piece of infrastructure. LCCA becomes an effective way to compare designs and support the choice of a particular design or alternative as the most economic cost overall even if individual or upfront costs are high (Hatami and Morcous 2014). This can be particularly helpful when talking to the public or working in public design, maintenance, and construction (Al-Wazeer, Harris, and Nutakor 2005).

The following paper addresses the question of what to do about existing expansion joints in bridges by utilizing a LCCA. The LCCA looks at two alternatives and works to determine what costs should be included in the analysis.

7.2 Life Cycle Cost Analysis (LCCA) Model

The goal of this paper is to present and examine a LCCA that can be used to determine if it is more cost effective to continue replacing bridge expansion joints as they deteriorate (i.e.***no change*** to current practice) or to ***retrofit*** joints to be continuous. The approach is intended to be applicable to any existing steel girder/concrete deck bridge; the characteristics of one typical northern Colorado steel plate girder bridge with reinforced concrete abutments, deck, and pier

caps are used as an example. The example bridge is located in Northern Colorado and has three 75 ft. spans with five 44 in. steel plate girders each, An important step in conducting a LCCA is determining the appropriate costs to include in the analysis. Four different LCCA Cost Scenarios are examined, each successive Cost Scenario including more costs due to expansion joint damage. The scenarios are as follows: Cost Scenario 1) considers costs directly associated with expansion joints only; Cost Scenario 2) considers expansion joints and pier caps; Cost Scenario 3) considers expansion joints and abutment damage; and Cost Scenario 4) considers expansion joints, pier caps, and abutment damage. Pier caps and abutments are identified for inclusion because they are considered to be the parts of the superstructure most vulnerable to expansion joint damage. The Cost Scenarios assume that a damaged joint is both clogged, inhibiting movement, and leaking water and chlorides to the superstructure below, and that when a damaged joint is in need of repair or replacement it is unlikely to be repaired promptly causing problems for abutments and pier caps.

For each Cost Scenario the first alternative is the current practice of replacing the joints after failure without maintenance, also known as the do nothing or no change to current practice alternative. The second alternative is retrofitting the joints to be a full moment splice after failure and accounting for cracking of decking and thermal loading. Within each alternative and the differences in results between two general locations, mountains and plains, will also be examined. Figure 7-1 shows the flow chart of cost scenario to alternative to topographic location.

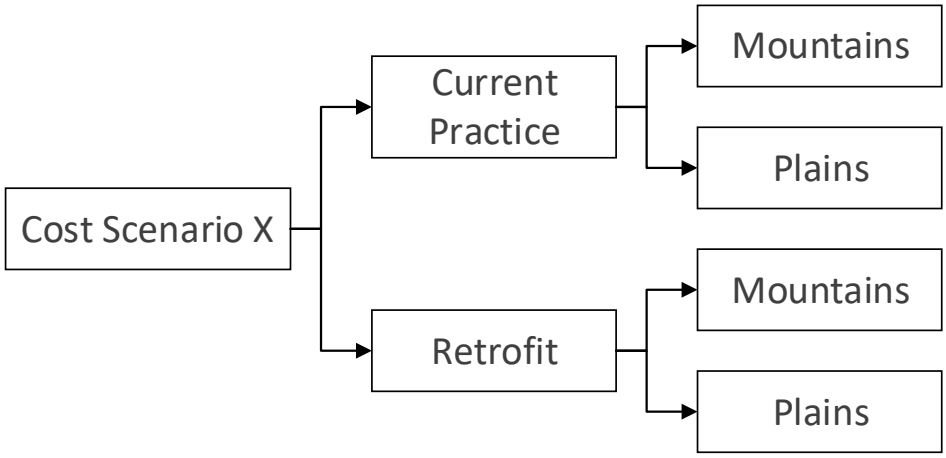

Figure 7-1 LCCA Cost Scenario

7.3 Life Cycle Cost Analysis (LCCA) Equations and Variables

If all parts, consequences, and alternative actions on a structure, in this case bridge, can be expressed monetarily then the best combination of actions or alternatives can be determined, as the combination that minimizes the total life cycle cost (LCC) of keeping the bridge in service. If each of the parts, consequences, and alternatives are quantified there is also present a probability that that consequence or action will occur causing that cost to become real.

There are two general LCC equations serving as the basis for this paper, one for each alternative. These general equations, shown below, include all possible parameter costs, where Eq. (7.1) is the LCC for no change to current practice and Eq. (7.2) is the LCC for joint retrofitting.

$$LCC_{NC} = C_i + C_{cm} + C_o + C_m P_{m+} C_r P_r + C_{cc} P_{cc} + C_u P_u - SV \quad (7.1)$$

$$LCC_{JR} = C_i + C_{cm} + C_R + C_s + C_o + C_m P_{m+} C_r P_r + C_{cc} P_{cc} + C_u P_u - SV \quad (7.2)$$

Where C_i, C_{cm}, C_o, C_R, and C_s are the initial, construction, operation, retrofitting, and crack sealing (if retrofit) costs. $C_m P_m$, $C_r P_r$, $C_{cc} P_{cc}$, and $C_u P_u$ are the maintenance, replacement, cost of capital and user costs and their respective probabilities of occurrence. The maintenance

term is composed of three parts, $C_mP_m = C_cP_c + C_{pcr}P_{pcr} + C_{abtr}P_{abtr}$, the joint maintenance (cleaning), pier cap repair/maintenance, and abutment repair/maintenance costs and associated probabilities. Finally, SV is the salvage value of the structure at the end of its life span.

While some of these costs and probabilities are obtainable or calculable based on information from CDOT or testing, some are more ambiguous or not applicable to this particular LCCA. The initial and construction costs are not applicable as this paper focuses on maintenance and repair decisions for existing bridges only. The operation cost does not apply since this analysis is not focusing on drawbridges or other bridges with daily operations. The user costs and costs of capital are more ambiguous; they are an indirect cost, a cost of time and convenience to the using public and cost of initial investment, things that are not easily quantifiable and as such are left out. Finally, because this paper focuses on the impact of expansion joints on the LCC of a bridge the salvage value is not directly impacted and will show little variation under different joint alternatives, for these reasons it is also left out of the analysis.

The adjusted equations are shown below as Eq (7.3) and (7.4). Depending on the cost scenario and alternative different terms within these general equations will be eliminated or included as illustrated in Table 7-1. Additional terms will multiply costs in order to account for the number of joints or linear feet of joint on the bridge.

$$LCC_{NC} = C_cP_c + C_{pcr}P_{pcr} + C_{abtr}P_{abtr} + C_rP_r \quad (7.3)$$

$$LCC_{JR} = C_cP_c + C_{pcr}P_{pcr} + C_{abtr}P_{abtr} + C_rP_r + C_R + C_s \quad (7.4)$$

Table 7-1. Costs Included in the Cost Scenario Equations

Cost Scenario	Joint Costs, C_cP_c, C_rP_r, C_R, C_s	Pier Cap Costs, $C_{pcr}P_{pcr}$	Abutment Costs, $C_{abtr}P_{abtr}$
1	Yes	No	No
2	Yes	Yes	No
3	Yes	No	Yes
4	Yes	Yes	Yes

Data collection and analysis were conducted to identify values for each of the variables indicated in equations (7.3) and (7.4). The costs associated with expansion joints, pier caps, and abutments are shown in Table 7-2. The costs were obtained from the CDOT business website from the 2014, 2015, and 2016 cost data books (Colorado Dept. of Transportation 2016). These costs were taken as present value costs. According to the Federal Highway Administration, when performing a LCCA and working with present and future costs discount rates instead of inflation rates should be used (FHWA, 2002). As present value costs the interest rate used to bring these costs to future values throughout the LCC and the discount rate used to bring them from future value back to present value were assumed to offset each other providing conservative costs for the LCCs.

Table 7-2 Known Variables (Colorado Dept. of Transportation 2016)

Variable	Value
Cost of Cleaning a Joint (C_c)	\$20/LF
Cost of Replacing a Joint (C_r)	\$350/LF
Cost of Removing/Retrofitting a Joint (C_R)	\$205/LF
Cost of Sealing Cracks (C_s)	\$0.75/LF
Cost of Repairing Damaged Abutments (C_{abtr})	\$1800/item[a]
Cost of Repairing Damaged Pier Caps (C_{pcr})	\$2000/item[a]

[a] These are estimates from CDOT, the costs are variable and site specific. Costs depend on amount of damaged material and ease of access, both depend on extent of damage, traffic, and location of bridge.
[b] Average life spans of bridge joints are based on CDOT personnel experience.

Other terms in the LCCA equation depended on agency practice or were bridge dependent. Values for these variables are shown in the Test Matrix in Table 7-3. Case A represents CDOT general practices, according to CDOT personnel in the Division of Project Support, and assumptions based on those practices. Because Case A considers estimates and assumptions, Cases B and C consider two additional variations. Case B looks at increasing the

time until joint replacement. Case C examines the effects of increasing the remaining design life of the bridge, i.e. extending the period of analysis. Those values that are assumed are listed first, as noted in the table, with the bridge dependent variables following. The agency practice values are values that would vary depending on the exact DOT district practices. Bridge dependent variables include the remaining design life of the bridge, the number of joints and abutment joints, the width of the bridge/length of the joint, and the compressive strength of the reinforced concrete abutment.

For the LCC discussion and analysis, the LCCs from Case A are presented in tables for comparison and discussion, with the LCCs from Cases B and C used for comparison when applicable.

Table 7-3 Test Matrix

Variable	**Case A** Common CDOT Practice	**Case B** Longer Joint Replacement Time	**Case C** Longer Remaining Design Life
Prompt joint replacement (t_{rp}) [a]	0.5 yrs.	1 yrs.	0.5 yrs.
Max time to replace joint (t_{rpmax}) [a]	3.5 yrs.	4 yrs.	3.5 yrs.
Frequency of joint cleaning (t_c) [a]	0.5 yrs.	0.5 yrs.	0.5 yrs.
Probability of joint cleaning (P_c) [a]	0.0000001	0.0000001	0.0000001
Remaining design life (DL)	30 yrs.	30 yrs.	50 yrs.
Number of joints total (N)	4	4	4
Number of abutment joints (N_b)	2	2	2
Width of bridge (w)	7.3 m (24ft)	7.3 m (24ft	7.3 m (24ft
Abutment compressive strength (f)	27.5MPa(4ksi)	27.5MPa(4ksi)	27.5MPa(4ksi)

[a] Assumed values based on CDOT general practices and discussions

7.4 Cost Scenario Equations, Variables, and Calculations

Each cost scenario adapts the two basic equations to its particular analysis of costs and variables. The following describes the equations particular to each cost scenario and how the

different variables are calculated. Calculations for each cost scenario were conducted in MATLAB using the costs in 2 and agency practices in Table 7-3, as seen in Appendix C.

7.4.1 Cost Scenario 1

For Cost Scenario 1 equations (7.3) and (7.4) were modified to equations (7.5) and (7.6). The probability for cleaning is assumed to be nearly zero as seen in Table 7-3 because CDOT and other DOTs do not have the personnel or resources to clean/maintain expansion joints.

$$LCC_{NC} = C_c P_c * n * d + C_r P_r * n \tag{7.5}$$

$$LCC_{JR} = C_c P_c * (n_b \text{ or } 0) * d + C_r P_r * (n_b \text{ or } 0) + C_R * (N_j \text{ or } N) + C_s * (n_j \text{ or } n) * d/2 \tag{7.6}$$

Where d is the number of times a joint would be cleaned or sealed if done every 6 months over the remaining design life, N_j, N_b, and N are the number of bridge joints, abutment joints, and total number of joints respectively. n_j, n_b, and n are the length of interior joints, length of abutment joints, and total length of joints respectively.

The probability of replacement of an expansion joint, P_r, was calculated based on the joint lifetimes obtained from CDOT personnel in the Division of Project Support, which were provided as discrete ranges for the two locations. The joints located in the plains have a joint life spans of seven to ten years and joints located in the mountains have an joint life span of three to six years. These joint life spans were assumed to fall in a normal distribution with the median joint life being the most probable and the extremes the least probable for each range. The probability that a joint will fail after a given life span was calculated, and is shown below in Table 7-4. In addition to the time until joint failure and its associated probability the time until replacement needed to be addressed as well. The time from failure to replacement was assumed for Case A to be from 0 to 3.5 years, where anything within the first half a year would be

considered prompt. When calculating the LCC a while loop was used, within which the joint life and time from failure to replacement were both selected from a distribution based on location and Agency Practice Case. For each loop, the probability corresponding to the joint life in years selected in that loop was used in adding the joint replacement cost to the LCC equation. The selected years were added up until the remaining design life was reached ending the loop and giving the LCC for that location, alternative, Agency Practice Case and Cost Scenario. In this way the LCC could then be calculated for each alternative and location combination within Cost Scenario 1.

Table 7-4 Probability of Joint Failure in Plains/Mountains

Variable	Probability
Probability of Failure Every 7 Years (P_7)/ Probability of Failure Every 3 Years (P_3)	0.176
Probability of Failure Every 8 Years (P_8) / Probability of Failure Every 4 Years (P_4)	0.336
Probability of Failure Every 9 Years (P_9) / Probability of Failure Every 5 Years (P_5)	0.352
Probability of Failure Every 10 Years (P_{10}) / Probability of Failure Every 6 Years (P_6)	0.136

7.4.2 Cost Scenario 2

Cost Scenario 2 takes the equations from Cost Scenario 1 and adds the costs due to pier cap corrosion due to leaking joints as shown in equations (7.7) and (7.8) below.

$$LCC_{EJ} = C_cP_c *n*d + C_{pcr}P_{pcr}*N_j + C_rP_r*n*t \quad (7.7)$$

$$LCC_{RC}= C_cP_c *(n_b \text{ or } 0) *d + C_rP_r*(n_b \text{ or } 0)*t + C_R*(N_j \text{ or } N) + C_s*(n_j \text{ or } n) *d/2 \quad (7.8)$$

In addition to the variables determined for Cost Scenario 1 a probability for corrosion damage to pier caps during the remaining design life of the bridge is needed. To estimate this probability, the effect of water containing de-icing salts that is leaked by the damaged joint directly onto the pier caps below needs to be considered. Once leaking begins chlorides are able

to build up on the surface of the pier over time, and diffuse through the concrete to the rebar. When the internal chloride concentration reaches a threshold value at the level of the rebar, it is assumed that corrosion of the rebar begins. The concentration of chlorides present on the pier cap is dependent on the length of time the joint is leaking and the location of the bridge, i.e. how heavily de-icing salts are used. The threshold concentration needed to start corrosion of the rebar is determined by the concrete mix, clear cover, and type of rebar used (e.g. traditional bare bars, epoxy coated, stainless steel). The threshold concentration and time to reach the threshold concentration were determined using the software Life-365 developed under the American Concrete Institute (ACI) Committee 365 "Service Life Prediction" and sponsored by ACI, the National Institute of Standards and Technology (NIST), and ASTM International (ASTM) in 1998.

Life-365 is a LCC and service life prediction tool for reinforced concrete structures exposed to chlorides. The version used for this research is Version 2.2.2 released July 2013. The Life-365 software does not account for carbonation induced corrosion as it has a low probability of occurrence and is often associated with poor quality concrete (Life-365^{TM} Consortium III. 2014). The software analysis is composed of four main steps: predicting the corrosion initiation period, predicting the propagation period, estimating the frequency and promptness of repair, and estimating the LCC.

For this research, results from the first two steps were utilized to determine the time and concentration needed to corrode the rebar in bridge pier caps. The initiation period is estimated using a simplified method based on Fickian diffusion. This method only requires a few inputs from the user as discussed below. Furthermore, the model assumes that diffusion is the dominant mechanism at play and that there are no cracks in the concrete in question. The diffusion

coefficient used is a function of time, temperature, and concrete mix composition. The equations for the diffusion coefficient can be found in the Life-365 Users Manual Section 2.1.1 (Life-365^{TM} Consortium III. 2014).

Life-365 uses the type of structure, the geographical location, and the environmental exposure input by the user to calculate the maximum chloride surface concentration corresponding to the threshold chloride content at the level of the rebar and time to reach that concentration. The temperature profile uses compiled meteorological data based on the geographical location input by the user. The user can also manually input a temperature profile. The user can also define the concrete mix composition and type of rebar present.

For the LCCA of leaking expansion joints in Colorado, Life-365 was utilized to determine the time and chloride concentration at which corrosion is expected to begin and until the rebar becomes too corroded to function. Urban bridges were selected as the structure type, the location chosen was Denver, CO, the temperature profile for that location was used, and a basic concrete mixture without special additives was assumed. Once these inputs were in place the model was run. The model produces a graph of chloride surface concentration vs. time in years as seen in Life-365 is a LCC and service life prediction tool for reinforced concrete structures exposed to chlorides. The version used for this research is Version 2.2.2 released July 2013. The Life-365 software does not account for carbonation induced corrosion as it has a low probability of occurrence and is often associated with poor quality concrete (Life-365^{TM} Consortium III. 2014). The software analysis is composed of four main steps: predicting the corrosion initiation period, predicting the propagation period, estimating the frequency and promptness of repair, and estimating the LCC.

For this research, results from the first two steps were utilized to determine the time and concentration needed to corrode the rebar in bridge pier caps. The initiation period is estimated using a simplified method based on Fickian diffusion. This method only requires a few inputs from the user as discussed below. Furthermore, the model assumes that diffusion is the dominant mechanism at play and that there are no cracks in the concrete in question. The diffusion coefficient used is a function of time, temperature, and concrete mix composition. The equations for the diffusion coefficient can be found in the Life-365 Users Manual Section 2.1.1 (Life-365^{TM} Consortium III. 2014).

Life-365 uses the type of structure, the geographical location, and the environmental exposure input by the user to calculate the maximum chloride surface concentration corresponding to the threshold chloride content at the level of the rebar and time to reach that concentration. The temperature profile uses compiled meteorological data based on the geographical location input by the user. The user can also manually input a temperature profile. The user can also define the concrete mix composition and type of rebar present.

For the LCCA of leaking expansion joints in Colorado, Life-365 was utilized to determine the time and chloride concentration at which corrosion is expected to begin and until the rebar becomes too corroded to function. Urban bridges were selected as the structure type, the location chosen was Denver, CO, the temperature profile for that location was used, and a basic concrete mixture without special additives was assumed. Once these inputs were in place the model was run. The model produces a graph of chloride surface concentration vs. time in years as seen in Figure 7-2 , this graph was used to develop a linear relationship between chloride concentration and time. This relationship was then used to determine the concentration at a given time based on the total length of time the joint remained damaged and leaking.

The probability calculations followed the flowchart shown in Figure 7-3. which is assumed to begin after a pier cap has be repaired. The process is followed until the threshold corrosion concentration is reached. Once this threshold is reached corrosion of the rebar in the pier cap will begin. The time until the threshold is reached was found using distributions for how long it will take the joint to fail, based on topographical location, and for the joint to be replaced after failure, 0 to 3.5 years for the typical practices case, A. The corrosion process was simulated 500, 1000, and 2000 times to determine the time to pier cap corrosion. A cumulative distribution function for time to pier cap corrosion was fit to each set of simulations, and they are plotted in Figure 4. All three cumulative distributions are very similar, with the 500 simulations distribution being slightly more variant. Consequently, the 1000 simulation was chosen for the final LCCA calculations to maximize agreement and minimize run time.

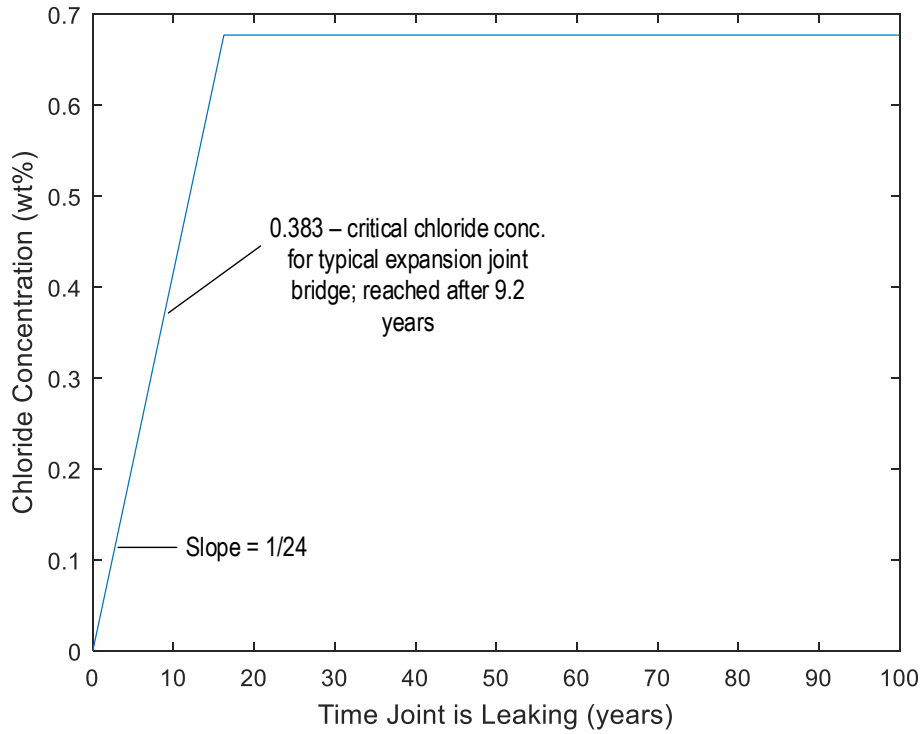

Figure 7-2 Life 365 Chloride Surface Concentration Vs. Time (years) for Colorado

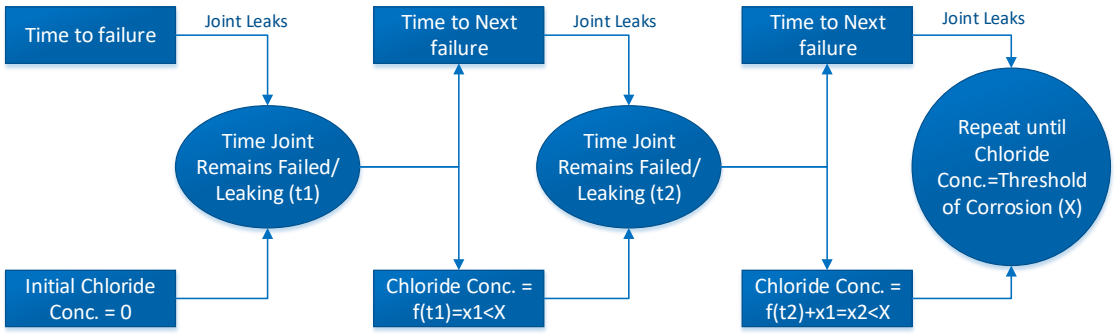

Figure 7-3. Corrosion of Pier Cap Flow Chart

The cumulative probabilities were used for the LCC in order to account for the likelihood of corrosion beginning during the remaining design life of the bridge, assuming the initial chloride concentration is zero, due to recent repair or cleaning of the pier cap. If the bridge has not recently had its pier caps repaired, then the number of years since the last pier cap replacement is added to the remaining design life for the corrosion probability selection. Looking at the probabilities in Figure 4, with an initial concentration of zero there is no significant likelihood of corrosion beginning within the first 30 years where the probability is about 4%, however, after that the probability increases rapidly. Additionally, corrosion was assumed to happen once during the remaining life span of the bridge due to the length of time it takes to initiate corrosion. Nonetheless once the pier cap is repaired the build-up of chlorides begins again. However, it should be noted that if an existing bridge is analyzed an initial chloride concentration may already exist on the pier cap. This would cause corrosion to begin earlier than predicted when an initial value of zero is assumed. The probability used in the LCC equations is the one corresponding to the remaining design life of the bridge. The corrosion costs and probabilities were only used in the LCC for the no change to current practice (i.e. continual joint replacement) alternative, because if the joints are retrofit they cannot leak and the likelihood of pier cap corrosion due to leaking joints vanishes.

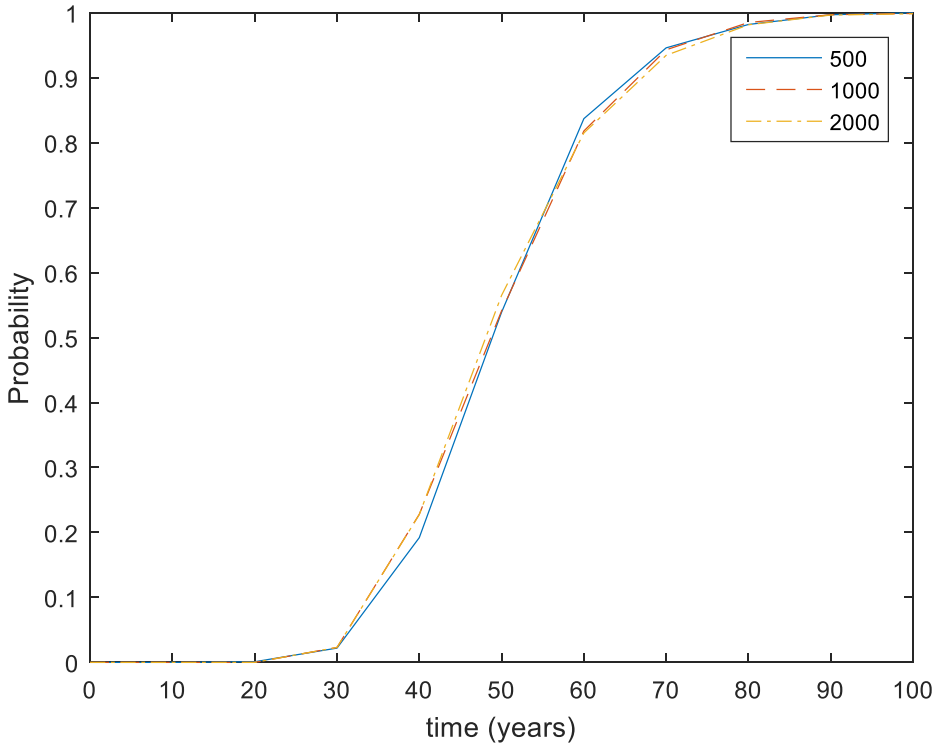

Figure 7-4. Corrosion Cumulative Probability for 500,1000, & 2000 Simulations

7.4.3 Cost Scenario 3

Cost Scenario 3 takes the equations from Cost Scenario 1 and adds the costs due to abutment damage due to clogged joints as shown in equations (7.9) and (7.10) below.

$$LCC_{EJ} = C_cP_c *n*d + C_{abtr}P_{abtr}*N_b + C_rP_r*n *t \quad (7.9)$$

$$LCC_{RC}= C_cP_c *(n_b \text{ or } 0) *d + C_{abtr}P_{abtr} *N_b + C_rP_r*(n_b \text{ or } 0)*t + C_R*(N_j \text{ or } N) + C_s*(n_j \text{ or } n) *d/2 \quad (7.10)$$

In addition to the variables determined for Cost Scenario 1 a probability for abutment damage during the remaining design life of the bridge is needed. The probability of damage to abutments depends on the joints being fully clogged and the temperature change causing bridge expansion, which would exert a force on the abutments. If the force exerted on the abutments is

greater than the compressive strength of the abutments, then damage can occur in the form of cracking and spalling. However, this is not as assured a measure of damage as corrosion in the pier caps, because damage to the abutment also depends on the stiffness of the soil behind the abutment and the temperature gradient through the depth of the bridge. The thermal gradient through the depth of the bridge can create stronger compression forces at the top or bottom and even apply a slight moment if the difference between top and bottom stresses is large enough. However, this analysis uses an average temp, which does neglect the potential impact of a gradient. Therefore, this analysis is more approximate. Additionally, according to CDOT personnel, abutment damage is less frequent and less severe compared to pier cap corrosion, but when it does occur it is costly to repair.

Given these assumptions and criteria a CSiBridge model of the steel plate girder bridge was run under average temperature increases of 10 ˚C (50˚F), 23.9 ˚C (75˚F), and 37.8 ˚C (100˚F). These temperature increases are assumed to be in addition to the temperature at which the bridge was constructed. After the analysis was conducted forces at the bottom end of the bridge's girders were recorded, as shown in Table 7-5 below. The forces indicated a direct linear relationship with the temperature as expected. The average temperatures and the corresponding forces for the bridge are used to develop a linear equation. This equation will calculate the force on the abutment given a temperature applied to the bridge. This equation is also found in Table 7-5.

Table 7-5. Temperature Increase & Corresponding Abutment Force – Steel Bridge

Scenario	Force and Equations
Uniform – 10 ˚C (50 ˚F)	82 MPa (11.9 ksi)
Uniform – 23.9 ˚C (75 ˚F)	121 MPa(17.6 ksi)
Uniform – 37.8 ˚C (100 ˚F)	164 MPa(23.8 ksi)
Equation – Uniform Temp.	F =3.8*T ˚C +69Mpa (F=0.238*T ˚F)

For the analysis in MATLAB a distribution of temperatures experienced by the bridge was generated based on the temperature history given for Colorado in Life-365. The temperature history in Life-365 has a mean of 10.1 ˚C (50.2˚F) a median of 9.89 ˚C (49.8˚F) and a mode of 3.98 ˚C (39˚F), 50% of the temperatures are below the mean and 50% are above, and it plots in a bell curve. All of these statistics, except the mode, indicate a normal distribution, and with the mode only being slightly less than the mean and median, a normal distribution was assumed. The distribution of temperature represents the change in temperature experienced by the bridge and has a minimum temperature of -17.8 ˚C (0˚F) and a maximum temperature of 37.8 ˚C (100˚F). The abutment concrete strength was assumed to be 27.5 MPa (4 ksi), this could be adjusted for any bridge. Using a sample temperature size of 1000 normally distributed temperatures the force was calculated for each temperature to determine if it could induce crushing. Due to abutments being a series system with the reinforced concrete abutment and the soil behind, there are two outlets for the stress based on the soil strength. These two outlets are either crushing the abutment or causing some form of deformation depending on the stiffness of the soil. The unknown stiffness of the soil and thus the likelihood of one outlet controlling was accounted for using a reduction factor. The reduction factor was taken as 0.75 and can be adjusted for stronger or weaker soil. The number of times the force exceeded the compressive strength divided by its safety factor and multiplied by the reduction factor was then used to determine the probability of abutment damage

7.4.4 Cost Scenario 4

For Cost Scenario 4 the variables and probabilities in Cost Scenarios 2 and 3 were combined and used in equations (7.11)(7.11) and (7.12) below. Note that the retrofit equation, (7.12), does not include a term for pier cap corrosion costs because all joints above the pier caps

would be retrofit to be continuous and would not leak chlorides assuming no cracking or that cracks are sealed promptly.

$$LCC_{EJ} = C_cP_c *n*d + C_{pcr}P_{pcr}*N_j + C_{abtr}P_{abtr}*N_{b+} C_rP_r*n*t \quad (7.11)$$

$$LCC_{RC}= C_cP_c *(n_b \text{ or } 0) *d + C_{abtr}P_{abtr} *N_b + C_rP_r*(n_b \text{ or } 0)*t + C_R*(N_j \text{ or } N) + C_s*(n_j \text{ or } n) *d/2 \quad (7.12)$$

7.5 Results

The MATLAB code developed to compute the LCCs was run for each cost scenario and alternative agency practice combination shown in Table 2. The results of these analyses were compiled and plotted in order to determine the most cost efficient solution for existing bridge expansion joints.

7.5.1 Cost Scenario 1 Results

Cost Scenario 1 examines the LCCs for existing bridge joints only, without considering costs associated with damage to the bridge's superstructure. Following are the LCCs and discussion for both alternatives and the topographical locations. The LCC for alternative 1, joint replacement otherwise known as the "no change" alternative, accounts for cleaning costs if $P_c >$ 0, and replacement costs. The LCC for alternative 2, joint retrofitting to continuous, is calculated in two different ways. First, 2A, the LCC is calculated for if abutment joints are replaced after each failure and mid-span joints are retrofit to continuous after the first failure. By leaving the abutment joints in place there remains an outlet for thermal expansion and contraction stresses, however, this also leaves open the possibility of abutment damage. This is then compared to the second variation, 2B, where the LCC is calculated for if all joints are retrofit after their initial failure, which does not leave an outlet for thermal expansion and contraction stresses. These

LCCs account for cleaning cost, replacement cost, retrofit cost, and cost of sealing cracks that develop where joints were retrofit. The cracks are assumed to need sealing once every three years. The LCC for each case is listed in Table 7-6 below. For the mountain location the LCCs for both of the retrofit option variations, Alternative 2A & B, are almost half that for the no change option, Alternative 1. This is a more significant difference compared to the variation between the plains location options. In the plains, where joints have a much longer average design life the two options are very close in cost. The retrofit, Alternative 2A, LCCs are slightly less than the no change option, with the retrofit all joints option being about $2000 less. However, compared to the $20,00-$30,000 difference for mountain bridges $2000 is not very significant.

Consequently, when only considering the costs due to the joints themselves, as in Cost Scenario 1 here, there is a significant cost benefit to retrofitting the joints if the bridge is in the mountains and an insignificant benefit if the bridge is in the plains.

The significant variable change between agency practice Case A and Case C is the remaining design life of 30 and 50 years respectively. This change in design life increases the mountain LCCs for Cost Scenario 1 by about $2,000 and increases the plains LCCs by about $10,000. This additional cost indicates the importance of the remaining design life of a bridge in deciding whether or not to retrofit the bridge to remove all joints. The significant difference between Cases A and B is the increase in time it takes to replace joints after failure. In Cost Scenario 1 this difference causes the Case B LCCs to be less than Case A because joints are not replaced as frequently.

Table 7-6. LCC for Cost Scenario 1

Variable	LCC ($) - **A**	LCC ($) - **B**	LCC ($) - **C**
LCC for Alternative 1 - Mountains	45,427	38,170	47,309
LCC for Alternative 2A – Mountains – leave abutment joints	32,734	29,105	33,794
LCC for Alternative 2B – Mountains – retrofit all joints	20,040	20,040	20,280
LCC for Alternative 1 - Plains	29,568	27,686	39,514
LCC for Alternative 2A – Plains – leave abutment joints	24,804	23,863	29,897
LCC for Alternative 2B – Plains – retrofit all joints	20,040	20,040	20,280

7.5.2 Cost Scenario 2 Results

Cost Scenario 2 examines the LCCs for existing bridge joints and their impact on pier caps, taking the costs considered in Cost Scenario 1 and adding the costs to repair pier cap damage due to corrosion.

For Case A, a remaining design life of 30 years is assumed. Assuming a chloride concentration starting at zero (perhaps representative of a recently repaired pier cap) 30 years gives a cumulative probability of corrosion of only 2.67%, as seen in Figure 7-4, Consequently, the LCCs for continuing routine joint replacement, shown in Table 7-7, are not much more than those for Cost Scenario 1 shown in Table 7-6. The increase in cost is no more than $10 for Cases A and B but it is $5,000 for Case C where the remaining design life is 50 years. A simple increase in remaining design life to 50 years increases the cumulative probability of corrosion to 54.33% and increases the Cost Scenario 2 LCCs as shown in Table 7-7.

LCCs for Alternative 2A & 2B, retrofitting joints to be continuous, in Cost Scenario 2 are identical to Alternative 2A & 2B in Cost Scenario 1 because once the joints are retrofit they cannot leak chlorides onto the pier caps and cause corrosion. Comparing Alternative 2A to Alternative 1, the LCCs shown in Table 7-6 decrease by roughly $15,000 for mountain locations

and roughly $5,000 - $15,000 for plains locations, indicating a distinct benefit to retrofitting and avoiding pier cap corrosion damage as well as joint replacement costs.

Table 7-7. LCC for Cost Scenario 2

Variables	LCC ($) – **A**	LCC ($) – **B**	LCC ($) - **C**
LCC for Alternative 1 - Mountains	45,438	38,183	54,292
LCC for Alternative 2A – Mountains – leave abutment joints	32,734	29,105	33,794
LCC for Alternative 2B – Mountains – retrofit all joints	20,040	20,040	20,280
LCC for Alternative 1 - Plains	29,575	27,696	45,347
LCC for Alternative 2A – Plains – leave abutment joints	24,804	23,863	29,897
LCC for Alternative 2B – Plains – retrofit all joints	20,040	20,040	20,280

7.5.3 Cost Scenario 3 Results

Cost Scenario 3 examines the LCCs for existing bridge joints and their impact on abutments, taking the costs considered in Cost Scenario 1 and adding the costs due to abutment damage.

The Alternative 1 LCCs calculated including abutment damage and assuming joint replacement showed similar results to the Cost Scenario 1 Alternative 1 cases for plains and mountain locations. These LCCs are shown in Table 7-8. For Alternative 1 including the abutment costs in Cost Scenario 3 increases LCCs on average by roughly $70,000 for the mountain locations and $50,000 for the plains locations compared to Cost Scenario 1. The plains cases show generally lower costs due to longer average joint lives as expected.

The Alternative 2A LCCs calculated including abutment damage assuming between-span joint retrofitting showed similar results to the Cost Scenario 1 Alternative 2A cases for plains and mountain locations. For Alternative 2B, if the abutment joints were retrofit to be continuous as full moment splices accounting for thermal loading then the LCC would be the same as the all joint retrofit LCC in Cost Scenario 1 Alternative 2B. These LCCS are shown in Table 7-8. .

Overall, Cost Scenario 3 Alternative 2A LCCs are about $10,000 for the mountains and $5,000 less for plains compared to those for Alternative 1, indicating a significant cost benefit to retrofitting the bridge joints.

Table 7-8**.** LCC for Cost Scenario 3

Variables	LCC ($) - **A**	LCC ($) - **B**	LCC ($) - **C**
LCC for Alternative 1 - Mountains	118,840	99,857	123,770
LCC for Alternative 2A – Mountains – leave abutment joints	106,150	90,792	110,250
LCC for Alternative 2B – Mountains – retrofit all joints	20,040	20,040	20,280
LCC for Alternative 1 - Plains	77,354	72,432	103,370
LCC for Alternative 2A – Plains – leave abutment joints	72,590	68,608	93,756
LCC for Alternative 2B – Plains – retrofit all joints	20,040	20,040	20,280

7.5.4 Cost Scenario 4 Results

Cost Scenario 4 examines the LCCs for existing bridge joints considering costs due to the joints, pier caps, and abutments. This provides the most comprehensive comparison of expansion joint alternatives. The LCCs are shown in Table 7-9.

For the Case A presented in Table 7-9 the LCCs for the retrofit, Alternative 2A, options are about $10,000 less than Alternative 1 options for bridges located in the mountains and about $5,000 less for bridges in the plains. Furthermore, Alternative 2B gives LCCS that are $70,000 less than Alternative 1 for the mountain locations and $50,000 less for plains locations leading to the conclusion that retrofitting all joints is the most cost effective solution if thermal loads are accounted for at the abutment retrofit locations. Looking at the overall trend, it clearly indicates a benefit in LCC if joints are retrofit for bridges in the mountains, and a moderate benefit if bridges are in the plains. However, when only considering the costs of the joints, retrofitting all joints or just mid-span joints do not show a significant difference in cost.

Table 7-9. LCC for Cost Scenario 4

Variables	LCC ($) - **A**	LCC ($) - **B**	LCC ($) - **C**
LCC for Alternative 1 - Mountains	118,850	99,871	130,750
LCC for Alternative 2A – Mountains – leave abutment joints	106,150	90,792	110,25
LCC for Alternative 2B – Mountains – retrofit all joints	20,040	20,040	20,280
LCC for Alternative 1 - Plains	77,361	39,380	109,210
LCC for Alternative 2A – Plains – leave abutment joints	72,590	41,874	93,7560
LCC for Alternative 2B – Plains – retrofit all joints	20,040	20,040	20,280

These patterns and benefits in cost are further illustrated in Figure 7-5. Figure 7-5 shows the Total LCCs for both mountain and plains for the general steel girder bridge used as a base example. The figure shows a significant decrease in LCC for the retrofit option compared to the replacement option. Not only will retrofitting reduce the costs of replacing the joints but, it will also significantly decrease the costs due to leaking joints initiating corrosion in pier caps and abutment damage.

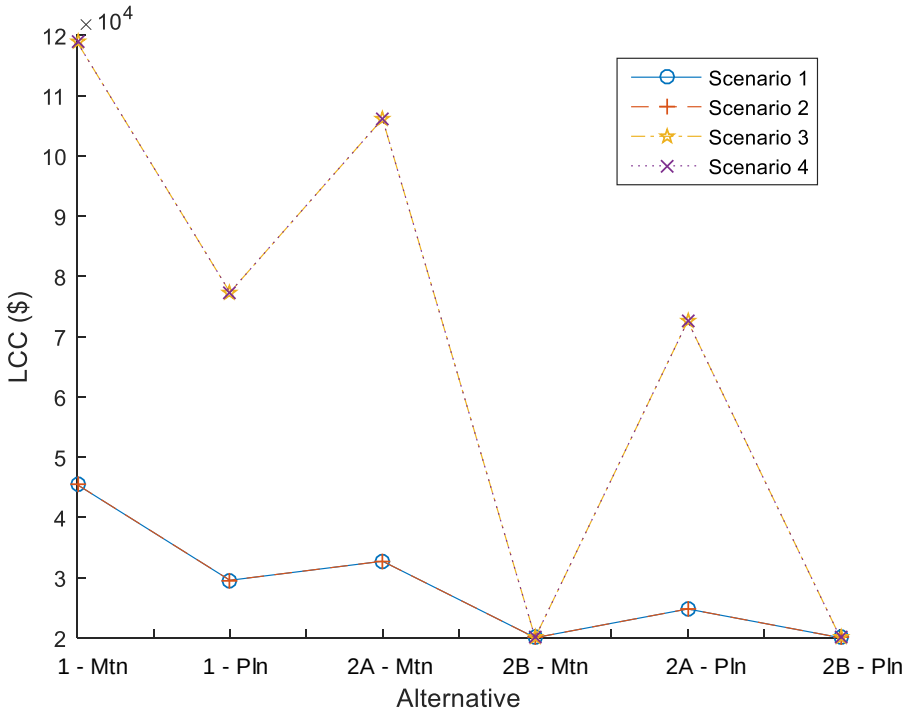

Figure 7-5. Total LCC Retrofit vs. Replacement – Case A

While the LCCs for one bridge might not seem significant over the course of 30 to 50 years in comparison to a DOTs budget or the overall cost of constructing a bridge, DOTs have far more than one bridge in their districts. Depending on the districts size and population concentration the number of bridges can vary greatly. CDOT has roughly 8,500 bridges within their jurisdiction according to CDOT personnel. Figure 7-6 shows the number of bridges versus the LCC for each Alternative within Cost Scenario 4 using Case A. If there are about 8,000 bridges in a district then the total LCC, assuming the bridges are roughly comparable in size and design, is about $950 million for Alternative 1, about $850 million for Alternative 2A, and about $160 million for Alternative 2B. Providing a difference in cost between Alternative 1 and 2B of roughly $790 million.

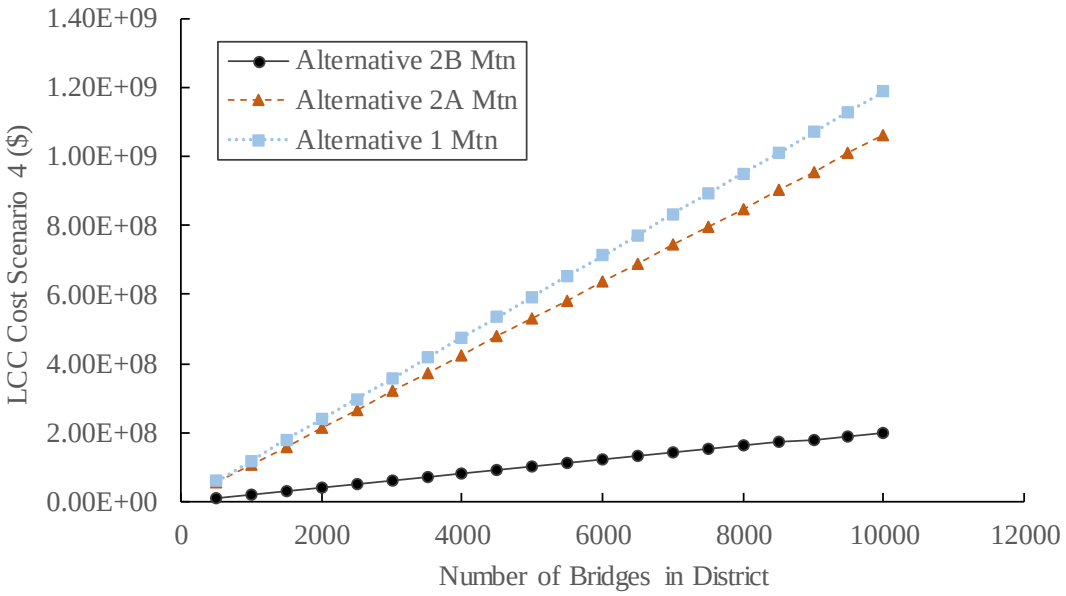

Figure 7-6. Number of Bridges vs. LCC for Cost Scenario 4– Case A

7.6 Conclusion

In conclusion, expansion joints have a significant impact on the LCC of any existing bridge. The number of joints, location, and remaining design life of the bridge affect the overall LCC. Clogged joints at abutments can cause cracking and damage to the abutment.

Corrosion of pier caps can also significantly increase the LCC if a bridge has leaking expansion joints. However, this is only a significantly probable problem for bridges who are in service for more than 30 years if they are starting at an initial chloride presence of zero. If the bridge has not recently had its pier caps repaired then the number of years since the last pier cap replacement is added to the remaining design life for the corrosion probability calculation. The longer the bridge is experiencing leaking joints repeatedly the more likely corrosion will occur. This is a much more likely and costly impact on the overall bridge than abutment damage for longer service bridges. Furthermore, it is almost entirely preventable by retrofitting the bridge joints and retrofitting the abutments or leaving the abutment joints in place to account for thermal expansion.

Retrofitting of the bridge joints while leaving the abutment joints in place creates a semi-integral bridge design and is the second most cost effective solution based on this LCCA. Allowing abutment joints to remain and serve as some expansion absorption and thermal stress mediators is reasonable for existing bridges with longer design lives and does not require that the full moment splice retrofit account for thermal loads. Furthermore, by removing the bridge expansion joints the more significant costs due to pier cap corrosion and the costs of replacing the joints are removed and replaced by much less significant costs of sealing cracks periodically. Crack sealing already takes place periodically for any bridge deck and thus this cost would not require additional bridge maintenance trips by CDOT personnel. Nonetheless, if thermal loads

are accounted for in the retrofit design then removing all expansion joints is the most cost efficient solution for existing bridges with expansion joints.

CHAPTER 8

SUMMARY AND CONCLUSIONS

8.1 Summary

In order to conduct a life cycle cost analysis (LCCA) to compare joint maintenance options and expand knowledge of thermal gradient effects on expansion joints in existing bridges, several tasks were conducted for the completion of this thesis. First, an extensive literature review was conducted to further understanding of current research into LCCA for expansion joints on existing bridges. From this literature review, general LCC equations were generated for existing bridges with expansion joints and for retrofitting bridges to remove joints. Furthermore, a in service simply supported reinforced concrete bridge was selected and instrumented at an expansion joint for long-term monitoring of joint movement, member stresses and thermal gradient. A load test was also conducted to calibrate a three-dimensional finite element model of the bridge built in CSiBridge using shell elements.

The concrete bridge was instrumented with thermocouples, linear potentiometers, and strain gauges similar to the steel plate girder bridge instrumented for Karly Rager's thesis work which was the first stage of this project (2016). These sensors provide thermal loading data throughout the depth of the bridge at the expansion joint. The strain gauges provide information of local behavior and performance at the joint. The linear potentiometers provide information on joint movement both contractive and expansive throughout the day and changing seasons. The thermocouples indicate the thermal gradient present through the depth of the bridge at any given moment and can be compared to standard design thermal gradients. A strain gauge installed at

girder mid-span was used for the finite element model calibration; agreement within 10% was achieved.

Once calibrated this model was also used to conduct a parametric study in order to gain further understanding of joint behavior under different thermal gradient loads and joint clogging stiffness. This parametric study also examined two different retrofitting scenarios, a deck splice and a full moment splice. The full moment splice provided a larger reduction in moment demand, while clogging stiffness had little effect on bridge behavior.

The data collected from the bridge was analyzed to determine if patterns and relationships are present between the different variables of movement, temperature, and stain/stress. The displacement correlated well with the temperature changes, showing a reactionary pattern. As the temperature increased the joint displacement decreased (due to girder expansion) and vice versa. The strain showed a more muted response to the temperature changes, however, it was no less apparent.

Finally, a LCCA was conducted using MATLAB as the main coding tool and data from CDOT, LIFE 365, and the CSiBridge models. This analysis examined costs associated with bridge expansion joints alone as well as those costs to the bridge superstructure, such as the bridge abutments and pier caps, due to failing expansion joints. The analysis accounted for the bridge's remaining design life, material and location, where appropriate. The analysis was conducted for three different test scenarios, each varying different parameters in order to provide a more comprehensive analysis. The analysis found that retrofitting all joints except abutment joints to be continuous was the most cost effective in most cases, assuming expansion joints will not be cleaned and maintained regularly.

8.2 Significance and Further Research

The significance of this work includes the results of the data collection and analysis, the parametric study, and the LCCA findings. The daily temperature changes, thermal gradients, and overall shifts in temperature due to changing seasons have a significant effect on bridge expansion joints in Colorado. The potential for 0.01 in of movement and 0.5 ksi in stress increase on concrete bridges consistently and 0.5 in movement and 5 ksi stress on steel bridges regularly could be significant if fully transferred to the abutments. The preliminary data on the concrete bridge C-17-AT presented in this thesis only accounts for mid-winter and does not account for the hottest or coldest days of the year with the most movement. However, these limited observations do imply that if CDOT is interested in removing an expansion joint, the bridge superstructure and retrofit option would need to support the movement of the bridge. Additionally, more data at different times of the year is needed for a more definite recommendation.

The parametric study and data analysis of thermal gradients indicate a stark need for further research into thermal gradients experienced by bridges. The current standards of AASHTO and New Zealand thermal gradients appear overly conservative and in need of refinement regarding shape compared to the measured data. Improving standard thermal gradients could also improve the cost effectiveness of new designs.

Finally, the LCCA concluded that retrofitting all joints to be continuous full moment splices that account for thermal loading would provide the most cost effective design by decreasing joint replacement costs, abutment damage, and pier cap corrosion. Further research could expand on this LCCA by examining environmental impacts and costs to users due to deteriorated expansion joints.

REFERENCES

AASHTO LRFD Bridge Design Specifications. (2012).

Agency, Highways, and River Severn. 2000. “Assessment of Composite Bridges,” 219–30.

Al-Wazeer, Adel, Bobby Harris, and Christopher Nutakor. 2005. “Applying LCCA to Bridges.” *Public Roads* 69 (3): 9–9.

Basim, Mohammad Ch., and Homayoon E. Estekanchi. 2015. “Application of Endurance Time Method in Performance-Based Optimum Design of Structures.” *Structural Safety* 56. Elsevier Ltd: 52–67. doi:10.1016/j.strusafe.2015.05.005.

Board, Capital Development. 1998. “Life Cycle Cost Analysis Service.” *World Pumps* 1998 (376): 4. doi:10.1016/S0262-1762(98)90545-4.

Briaud, L. (2013). *Geotechnical Engineering: Unsaturated and Saturated Soils.* Wiley, New YorkCDOT. (2012). *Bridge Design Manual*.

CDOT. 2015. “Bridge Expansion Device (0-4).” Colorado Dept. of Transportation. (2016). “Engineering Estimates and Market Analysis.” <https://www.codot.gov/business/business/eema> (Jan. 19, 2017).

Chen, Q. (2008). “Effects of Thermal Loads on Texas Steel Bridges.”

Federal Highway Administration. (n.d.). “History of the Interstate Highway System.” <http://www.fhwa.dot.gov/interstate/history.htm> (July. 8, 2016).

French et al. (2013). “Investigation of Thermal Gradient Effects in the I-35W St. Anthony Falls Bridge.” *J. Bridge Engineering* 18(1), 890-900

Frangopol, D M, and M Liu. 2007. “Structure and Infrastructure Engineering: Maintenance, Management, Life-Cycle Design and Performance.” *Structure and Infrastructure Engineering: Maintenance, Management, Life-Cycle Design and Performance*. doi:10.1080/15732479.2013.769013.

Girmscheid, G. n.d. “Probabilistic Risk-Based LC NPV Model.” Zurich, Switzerland.

Goh, K. C., and J. Yang. 2014. “Managing Cost Implications for Highway Infrastructure Sustainability.” *International Journal of Environmental Science and Technology*, 2271–80. doi:10.1007/s13762-014-0572-5.

Hatami, Afshin, and George Morcous. 2014. “Life-Cycle Cost Analysis for Bridge Managment An Application to Nebraska Bridges.pdf.” ASCE.

Hawk, Hugh. 2003. *Bridge Life-Cycle Cost Analysis*. Edited by Transporation Research Board. Washington D C: National Cooperative Highway Research Program.

Kang, J, S Lee, T Hong, K.-J. Koo, C.-T. Hyun, and D Lee. 2007. “Life-Cycle Cost Analysis in Bridge Structures: Focused on Superstructure.” *5th IABMAS Workshop on Life-Cycle Cost Analysis and Design of Civil Infrastructure Systems, LCC05*. London: Taylor & Francis Group. http://www.scopus.com/inward/record.url?eid=2-s2.0-84863266867&partnerID=40&md5=a7c7295395f718eee0e37cfdfb29a443.

Kassimali, A. (2012). Matrix Analysis of Structures, 2nd Ed., Cengage Learning, Independence, KY

Kim, Sang-Hyo, Jun-Hwan Kim, Chi-Young Jung, and Jin-Hee Ahn. 2010. “Life-Cycle Cost Analysis of a TPSM Applied Continuous Composite Girder Bridge.” *International Journal of Steel Structures*. doi:10.1007/BF03215824.

“LIfe Cycle Cost Optimisation in Highway Concrete Bridges Management.pdf.” n.d.

Life-365™ Consortium III. (2014). “Life-365™ User Manual.” < http://www.life-365.org/download/Life365_v2.2.1_Users_Manual.pdf> (Feb. 20, 2017).

Mao, Shiang, and Rong-Yau Huang. 2015. “Lifecycle Assessment of Maintennace Repair and Rehabilitation Costs a Deterioration Modeling Approach for Bridge Components.” Journal of the Chinese Institute of Civil and Hydraulic Engineering.

Marques Lima, Joao, and Jorge de Brito. 2010. “Managment Systems for Expansion Joints of Road Bridges.pdf.”

Osman, Hesham. 2005. “Risk-Based Life-Cycle Cost Analysis of Privatized Infrastructure.” *Transportation Research Record*. doi:10.3141/1924-24.

Ozbay, Kaan, Dima Jawad, Neville A. Parker, and Sajjad Hussain. 2004. “Life Cycle Cost Analysis: State-of-the-Practice vs State-of-the-Art.” Washinton D.C.: National Academy of Science.

Rager, Karly. 2016. "Joint Elimination retrofits and Thermal Loading Analysis In Plate Girder Bridge Using Health Monitoring and Finite Element Simulations." Colorado State University.

Reigle, Jennifer A., and John P. Zaniewski. 2002. “Risk-Based Life-Cycle Cost Analysis for Project-Level Pavement Management.”

Riedel, Thorsten, Nicole Tiemann, Michael G. Wahl, and Tony Ambler. 1998. “LCCA-Life Cycle Cost Analysis.”

RStudio. "RStudio." < https://www.rstudio.com/> (Feb. 10, 2016)

Safi, Mohammed, Håkan Sundquist, and Raid Karoumi. 2015. “Cost-Efficient Procurement of Bridge Infrastructures by Incorporating Life-Cycle Cost Analysis with Bridge Management Systems,” 1–12. doi:10.1061/(ASCE)BE.1943-5592.0000673.

Savioz, P. Spuler, T. 2014. “Minimally Invasive Maintenance Refurbishment Options for Bridge Expansion Joints.” Leiden: The Netherlands: CRC PRess/Balkema.

University, Standford. 2005. “GUIDELINES FOR October 2005,” no. October.

APPENDIX A.

BRIDGE DRAWINGS

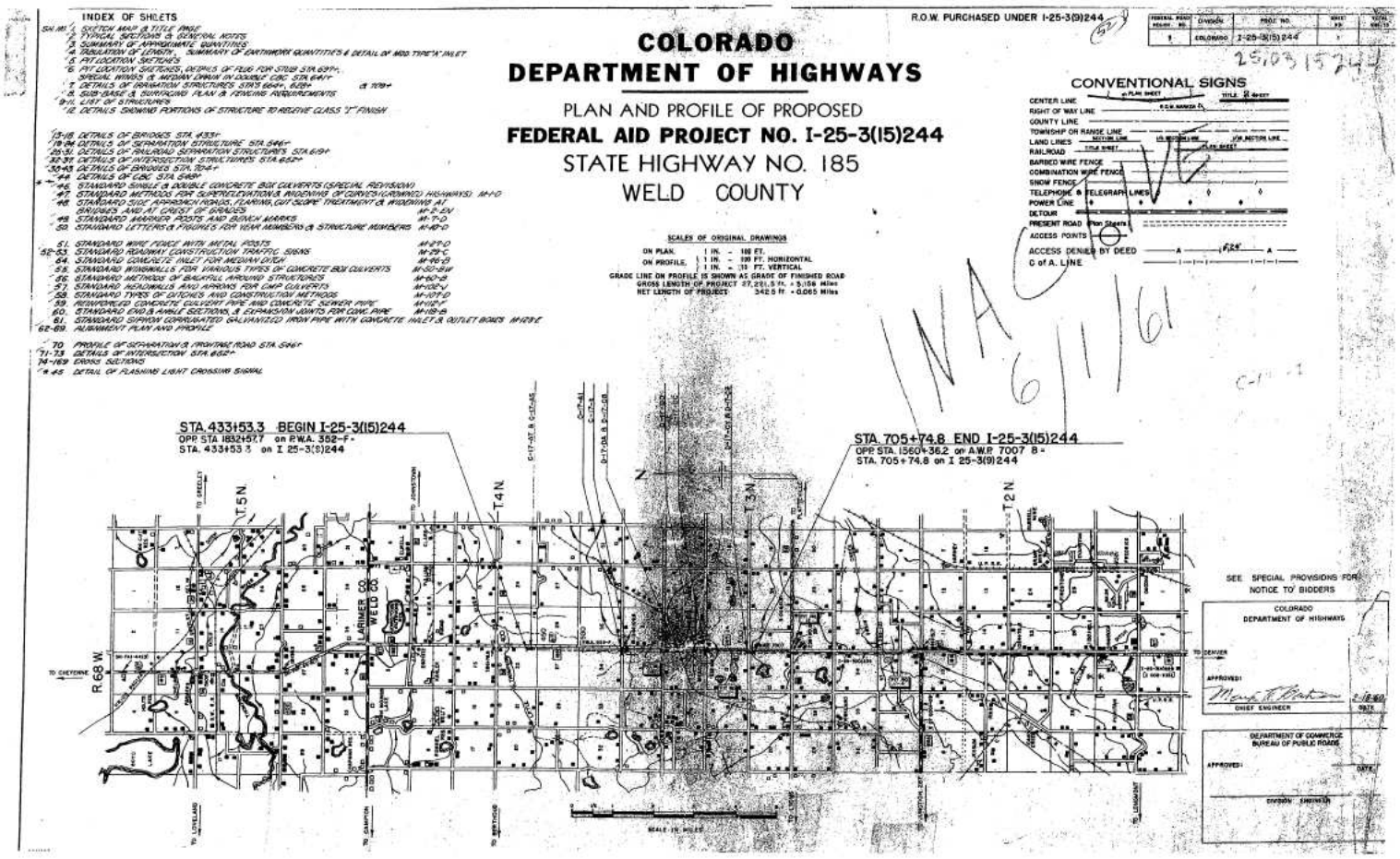
INDEX OF SHEETS
R.O.W. PURCHASED UNDER I-25-3(9)244
COLORADO
DEPARTMENT OF HIGHWAYS
PLAN AND PROFILE OF PROPOSED
FEDERAL AID PROJECT NO. I-25-3(15)244
STATE HIGHWAY NO. 185
WELD COUNTY
CONVENTIONAL SIGNS
SCALES OF ORIGINAL DRAWINGS
STA. 433+53.3 BEGIN I-25-3(15)244
STA. 705+74.8 END I-25-3(15)244
T.5N.
T.4N.
T.3N.
T.2N.
R.68 W.
SEE SPECIAL PROVISIONS FOR NOTICE TO BIDDERS
COLORADO DEPARTMENT OF HIGHWAYS
DEPARTMENT OF COMMERCE BUREAU OF PUBLIC ROADS

Rev. 3-18-60 Gird. Stats. Note P.C.

Fed. Road Dist. No.	Division	Project No.	Sheet No.
9	COLO.	I-25-3(15)244	13

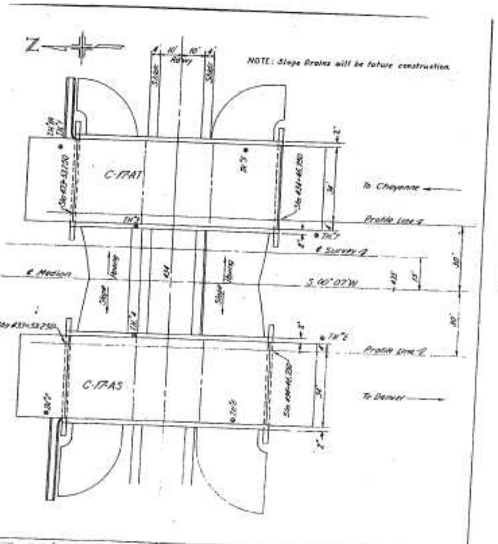

SUMMARY OF QUANTITIES			STRUCTURE Nº C-17-AS							STRUCTURE Nº C-17-AT						
Item	Description	Unit	Super-structure	Abut. Nº 1	Pier Nº 2	Pier Nº 3	Abut. Nº 4	Total	Two ② Approach Slabs	Super-structure	Abut. Nº 1	Pier Nº 2	Pier Nº 3	Abut. Nº 4	Total	Two ② Approach Slabs
14	Unclassified Structural Excavation (Bridge)	Cu. Yd.		10	29	29	10	78			10	29	29	10	78	
16	Structure Backfill (Class 1)	Cu. Yd.			23	23		46				23	23		46	
18	Station Yard Overhaul	Sta. Yd.						800							800	
18	Yard Mile Overhaul	Yd. Mi.						410							410	
46	Class "D" Concrete	Cu. Yd.	151.2	19.7	20.3	20.8	16.0	228	48	151.2	19.7	20.3	20.8	16.0	228	48
47	Reinforcing Steel (Includes 1½% for overrun)	Lb.	40,440	800	3,925	3,980	800	49,945	8,720	40,440	800	3,925	3,980	800	49,945	8,720
48	Structural Steel (Includes ½% for paint)	Lb.	6,855	645			645	8,145		6,855	645			645	8,145	
61	Steel Piling (10 BP 42)	Lin. Ft.		230	152	112	150	664			220	208	152	170	750	
65	Concrete Slope & Ditch Paving (with wire mesh)	Cu. Yd.		38			38	76			38			38	76	
②	½" Expansion Joint Material (Type B)	Sq. Ft.							2							2

~~3.9 Cu. Yd. for slope drain @ Abutment Nº 1 each Structure (future Construction)~~

① To be included in the bid price for Item 46

② Approach Slab quantities not included in Bridge Totals. (Future Construction)

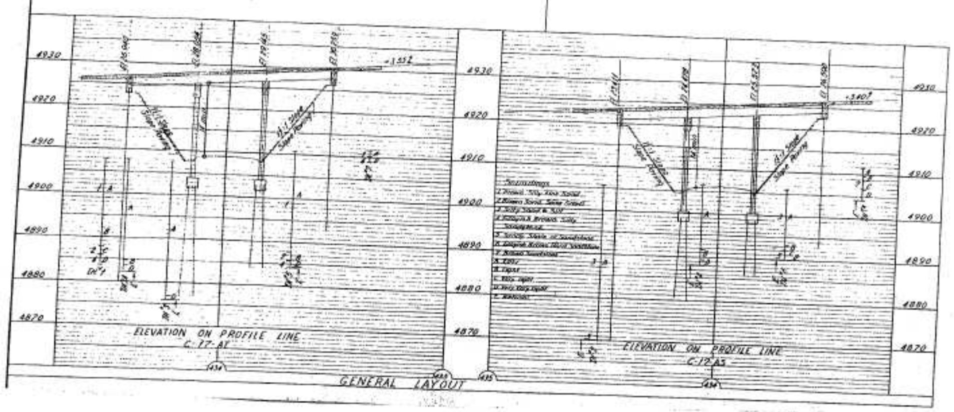

GENERAL NOTES

LOADING DATA INTERSTATE ALTERNATE

DESIGNING DATA

COLORADO DEPARTMENT OF HIGHWAYS

2-Concrete Slab & Girder Bridges with 3 Simple Spans @ 30' 38' Rdwy. 2 Curbs No Skew

General Layout, Notes and Summary of Quantities

Across Access to Service Road Sta. 433+53.250 to 434+46.750

Designed by | Made by | Approved by | Bridge Engineer

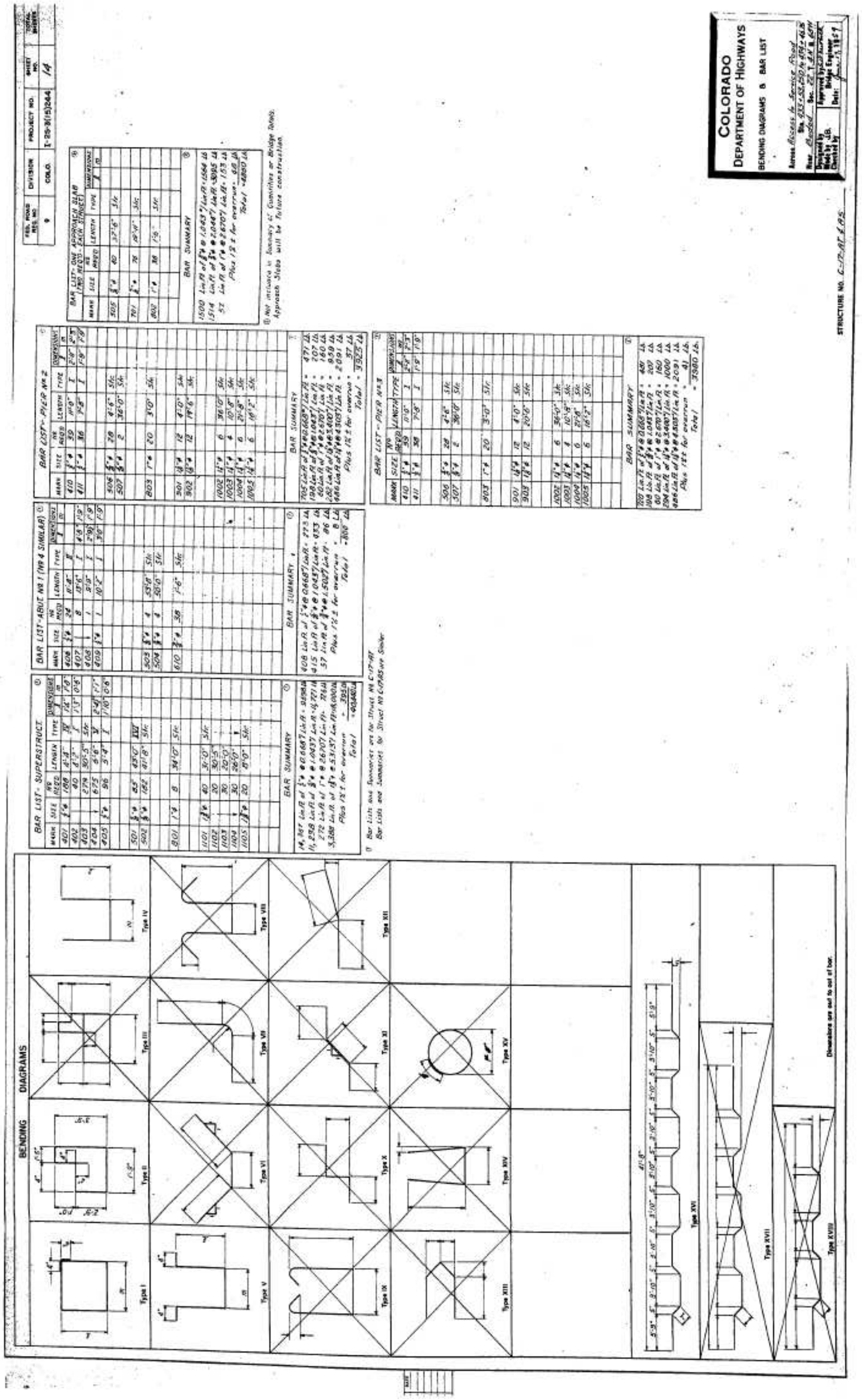
BENDING DIAGRAMS
Type I
Type II
Type III
Type IV
Type V
Type VI
Type VII
Type VIII
Type IX
Type X
Type XI
Type XII
Type XIII
Type XIV
Type XV
Type XVI
Type XVII
Type XVIII
BAR LIST - SUPERSTRUCT.
BAR SUMMARY
BAR LIST - PIER No 2
BAR LIST - PIER No 3
COLORADO
DEPARTMENT OF HIGHWAYS
BENDING DIAGRAMS & BAR LIST

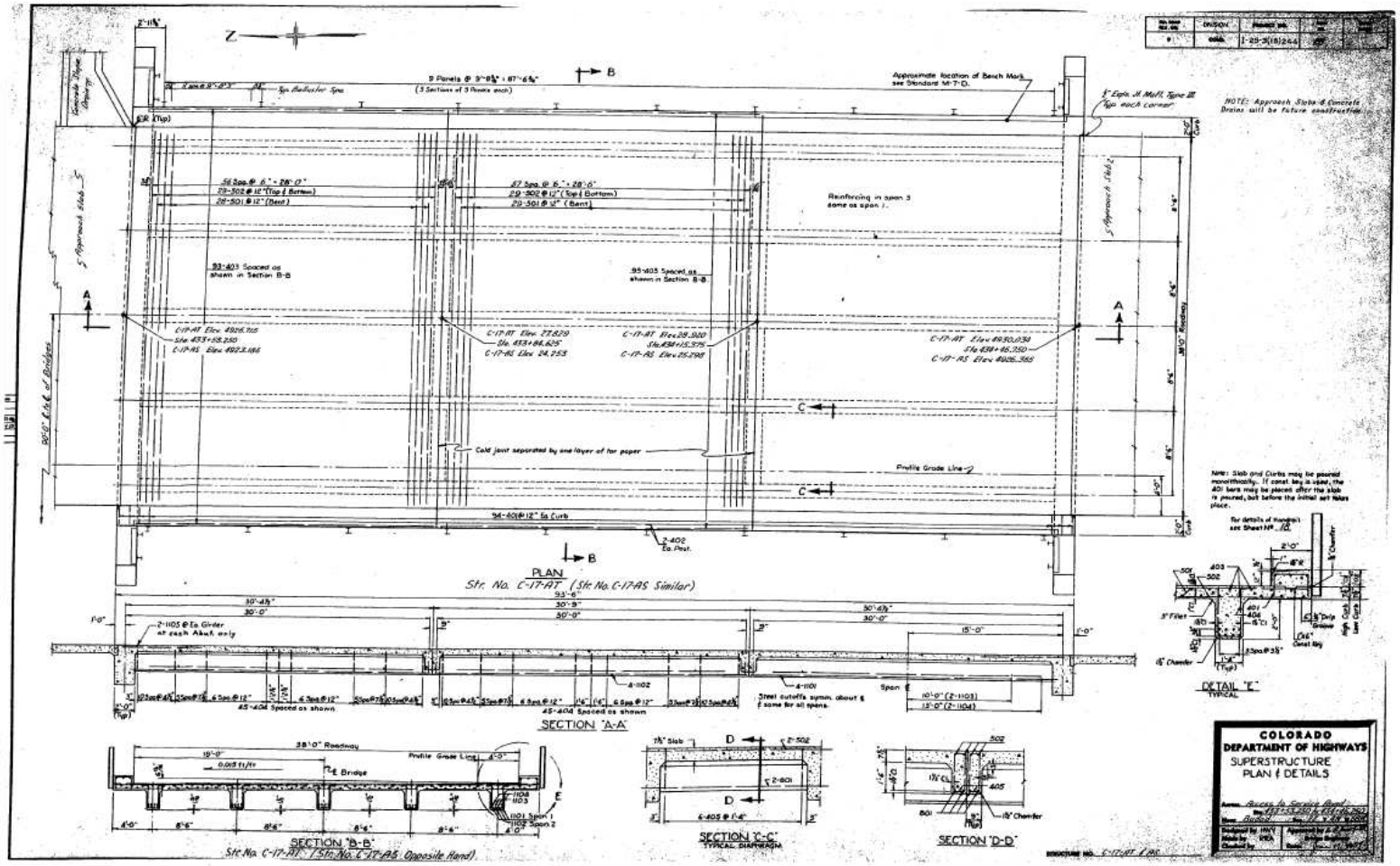
PLAN
Str. No. C-17-AT (Str. No. C-17-AS Similar)
SECTION "A-A"
SECTION "B-B"
Str. No. C-17-AT (Str. No. C-17-AS Opposite Hand)
SECTION "C-C"
TYPICAL DIAPHRAGM
SECTION "D-D"
DETAIL "E"
TYPICAL
COLORADO
DEPARTMENT OF HIGHWAYS
SUPERSTRUCTURE
PLAN & DETAILS

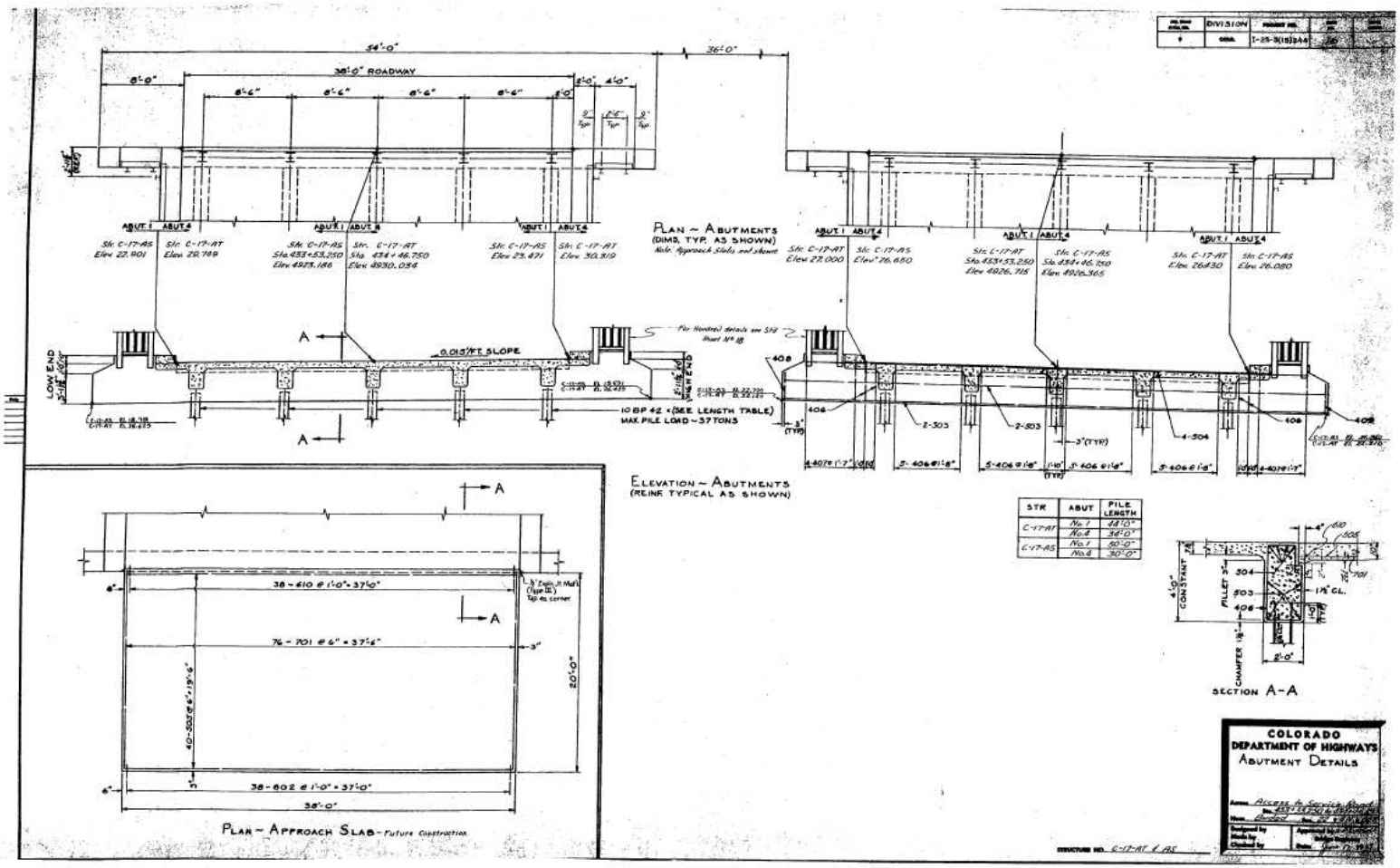
PLAN ~ ABUTMENTS
(DIMS. TYP. AS SHOWN)
ELEVATION ~ ABUTMENTS
(REINF. TYPICAL AS SHOWN)
PLAN ~ APPROACH SLAB ~ Future Construction
SECTION A-A
COLORADO
DEPARTMENT OF HIGHWAYS
ABUTMENT DETAILS

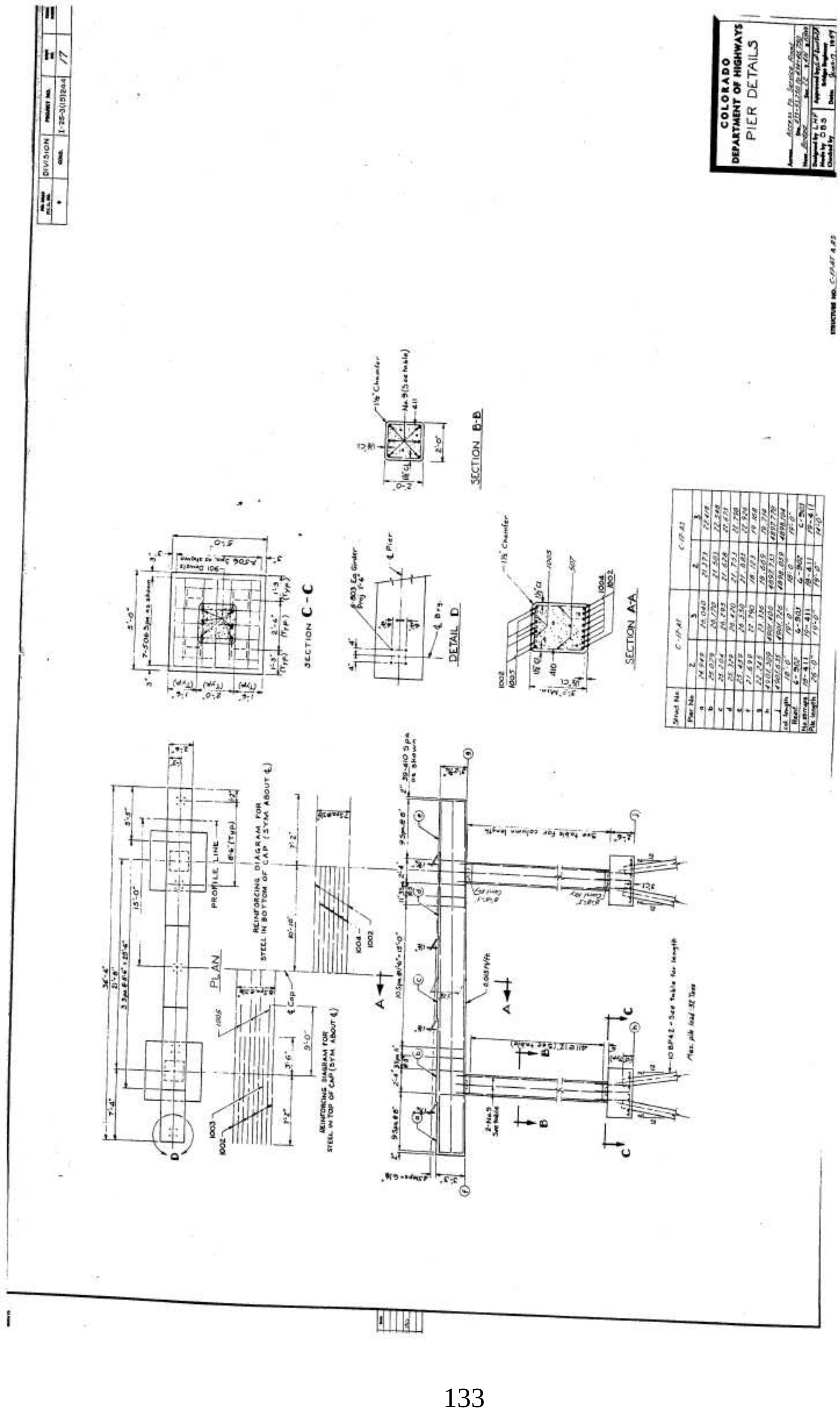
COLORADO
DEPARTMENT OF HIGHWAYS
PIER DETAILS
DIVISION
PLAN
PROFILE LINE
REINFORCING DIAGRAM FOR STEEL IN BOTTOM OF CAP (SYM ABOUT ℄)
REINFORCING DIAGRAM FOR STEEL IN TOP OF CAP (SYM ABOUT ℄)
SECTION C-C
DETAIL D
SECTION A-A
SECTION B-B

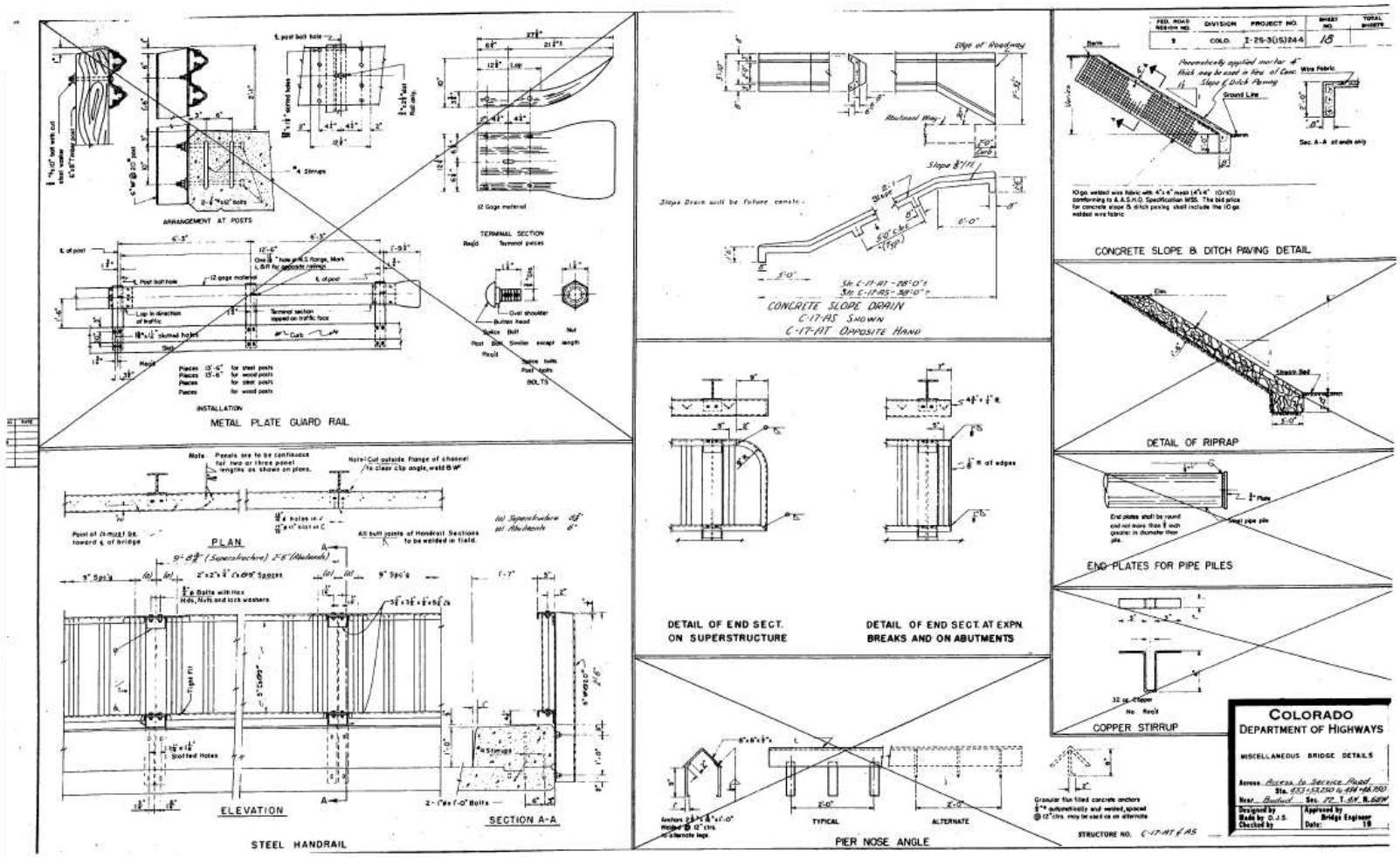
ARRANGEMENT AT POSTS
TERMINAL SECTION
INSTALLATION
METAL PLATE GUARD RAIL
PLAN
ELEVATION
SECTION A-A
STEEL HANDRAIL
CONCRETE SLOPE DRAIN
C-17-AS SHOWN
C-17-AT OPPOSITE HAND
DETAIL OF END SECT. ON SUPERSTRUCTURE
DETAIL OF END SECT. AT EXPN. BREAKS AND ON ABUTMENTS
TYPICAL
ALTERNATE
PIER NOSE ANGLE
CONCRETE SLOPE & DITCH PAVING DETAIL
DETAIL OF RIPRAP
END PLATES FOR PIPE PILES
COPPER STIRRUP
COLORADO
DEPARTMENT OF HIGHWAYS
MISCELLANEOUS BRIDGE DETAILS
STRUCTURE NO. C-17-AT & AS

APPENDIX B.

INSTRUMENTATION PLAN FOR C-17-AT

Overview

Bridge C-17-AT will be partially closed to allow CSU research group to instrument the bridge. The bridge to be closed is on I-25. The instrumentation will take approximately 12-16 hours. 2 flaggers will be needed from CDOT. Proper PPE will be worn by all present. 4 to 6 members of the CSU research team will be on site. Jessica Martinez and possibly David Weld of CDOT will be on site as well.

Steps to Instrumentation

1. **I necessary close East lane of bridge – Instrumentation will be on the east side of the bridge – Might not be necessary**
2. **Locate inspection truck near joint between span 2 and span 3 under the north lane of bridge.**
   a. Install 3 linear potentiometers on joint. This is the east side and north end of the bridge.
      i. C17AT_LP_1 is installed at mid-thickness on the concrete deck about 3.75" from the top of the deck. The exact distance from the center of the linear potentiometer and the top of the deck is recorded. This sensor will be installed on the east side of the deck joint.
      ii. C17AT _LP_2 is installed on the concrete girder about 3" from the bottom of the deck/top of the girder. The exact distance from the center of the linear potentiometer to the top of the deck is recorded. This sensor will be installed on the east side of the deck joint.
      iii. C17AT_LP_3 is installed on the concrete girder about 3" above the bottom of the girder. The exact distance from the center of the linear potentiometer to the top of the deck is recorded. Approximately 21" from the top of the girder. This sensor will be installed on the east side of the deck joint.

   b. Install 4 thermocouples on girder near the joint
      i. C17AT_TH_1 is installed on the concrete deck at about 2" from the top of the deck. The exact distance from the center of the thermocouple and the top of the deck is recorded. This distance should be about 2 inch. This sensor will be installed on the north side of the deck joint (the northward girder).
      ii. C17AT _TH_2 is installed on the concrete girder about 2" from the top of the girder. The exact distance from the center of the thermocouple and the top of the girder is recorded. This distance should be about 2 inch. This sensor will be installed on the north side of the joint (the northward girder).
      iii. C17AT _TH_3 is installed on the north side of the joint. It will be located in the center of the vertical face of the girder. The exact distance from the center of the thermocouple

and the top of the deck is recorded. This distance should be approximately 19-20.5 inches.

iv. C17AT _TH_4 is installed on the north side of the joint. It will be located at about 2" from the bottom of the girder. The exact distance from the center of the thermocouple and the top of the deck is recorded. This distance should approximately 22 inches from the top of the girder/2 inches from the bottom of the girder.

c. Install 8 strain gages on girder near the joint

i. C17AT _SG_1 is installed on the concrete deck as close to the top of the deck as possible. The distance from the center of the strain gage and the top of the deck is recorded. This distance should be about 1 inch. This sensor will be installed on the south side of the deck joint (the southward girder).

ii. C17AT _SG_2 is installed on the concrete deck as close to the top of the deck as possible. The distance from the center of the strain gage and the top of the deck is recorded. This distance should be about 1 inch. This sensor will be installed on the north side of the deck joint (the northward girder).

iii. C17AT _SG_3 is installed on the north side of the joint on the concrete deck as close to the bottom of the deck as possible. The distance from the center of the strain gage and the top of the deck is recorded. This distance should be about 6.5 inches from the top of the deck (about 1in from the bottom of the deck). This sensor will be installed on the north side of the deck joint (the northward girder).

iv. C17AT _SG_4 is installed on the north side of the joint. It will be located as close to the top of the girder as possible. The distance from the center of the strain gage and the top of the deck is recorded. This distance should be about 8.5 inches (about 1 in below the top of the girder/bottom of the deck). This sensor will be installed on the north side of the deck joint (the northward girder).

v. C17AT _SG_5 is installed on the north side of the joint. It will be located at mid depth of the girder (about 12" from the bottom of the girder). The exact location from the bottom of the girder will be measured and recorded. This sensor will be installed on the north side of the deck joint (the northward girder).

vi. C17AT _SG_6 is installed on the south side of the joint. It will be located at the base of the girder. The exact distance from the center of the strain gage and the top of the girder is recorded. This distance should be about 23 inches/1 inch above the bottom of the girder. This sensor will be installed on the south side of the deck joint (the southward girder).

vii. C17AT _SG_7 is installed on the north side of the joint. It will be located at the base of the girder. The exact distance from the center of the strain gage and the top of the girder is recorded. This distance should be about 23 inches/1 inch above the bottom of the girder. This sensor will be installed on the north side of the deck joint (the northward girder).

3. **Locate instrumentation Truck near mid-span of northernmost span under the East lane of the bridge.**
    a. Install 1 strain gage on web of girder near bottom of web at mid-span. C17AT _SG_8 will be installed as close to the bottom of the girder at mid-span as possible.

4. **Zero strain gages and record linear potentiometer measurements for Control Load Testing??**
5. **Control Load Testing – To be done in the evening – Date & Time: TBA**
    a. Close easternmost (right) lane of bridge entirely – Drive truck over during gaps between northbound traffic
    b. During gaps in traffic drive CDOT specified truck to drive over bridge on closed lane 3x at 5 mph
    c. During gaps in traffic drive CDOT specified truck to drive over bridge on closed lane 3x at 30 mph
    d. During gaps in traffic drive have CDOT specified truck sit with front axil over midspan for 5 minutes
    e. During gaps in traffic drive have CDOT specified truck sit with back axil over midspan for 5 minutes
    f. Clean Up
    g. Open bridge entirely

Detour Information

During the controlled load testing of the bridge, the east lane will need to be closed

Figure. B-1 Top of C-17-AT

Figure. B-2 Side View of C-17-AT

Figure B-3. Under Side of West Joint C-17-AT

Figure B-4. Second Side View of C-17-AT

APPENDIX C.

LCCA MATLAB CODE

LCC analysis and simulation - Test 1

```
%General Parameters - Joints only

Cc=20; % Cost of cleaning a joint per linear foot
Cr=350; % Cost of replacing a joint per linear foot
Crm=205; % Cost of removing a joint per linear foot
Cs=0.75; % Cost of sealing cracks per linear foot
Pc= 0.0000001; % Probability that a joint will be cleaned every 6
 months
tc=0.5; % frequency a joint should be cleaned in years.
DL=30;  % remaining design life of bridge years
d=DL/tc; % number of times a joint would be cleaned if done every 6
 months

N=4; % Number of joints on bridge including abutment joints
Nb=2; % Number of abutment joints
Nj=N-Nb; % Number of bridge joints
w=24; % width of bridge, ie length of joint
n=N*w; % number of linear feet of joint to be replaced or cleaned
nabt=Nb*w; % number of linear feet of joint at abutments
njt=n-nabt; % number of linear feet of joints not at abutment
trp=0.5; %maximum time in years for joint replacement to be considered
 prompt.
trpmax=3.5; % maximum time in years it can take to replace a joint.
plnsavgmin=3; % min average joint life in plains
plnsavgmax=6; % max average joint life in plains
mntsavgmin=7; % min average joint life in plains
mntsavgmax=10; % max average joirepnt life in plains
f=4; % the compressive strength of the concrete abutment in ksi
sf=0.85; %safety factor for compressive strength of abutment
rf=0.75; %reduction factor to account for some compressive stress
 being absorbed by soil behind abutment
%Additional Parameters - joints, abutments, and pier caps

Cabtr=1800; % cost of repairing damaged abutment
Cpcr=2000; % cost of repairing damaged pier cap
P10clg=0.05; %probability of cracking due to clogging stiffness 10kip/
in Assumed.
P20clg=0.10; %probability of cracking due to clogging stiffness 20kip/
in Assumed.
P30clg=0.15; %probability of cracking due to clogging stiffness 30kip/
in Assumed.
% All probabilities are per 6 months of the joint remainging damaged.
T=12*trp; % is the time in months that a joint has remained damaged.
xx=1000; % number of simulations run for corrosion analysis
tcs=6;% assume crack sealing is required every 6 years as the average
 of the typcial CDOT range of 5-7 years
%%Mountain Range (3-6 years)

%Simulate Joint Failures
rng(0,'twister');
```

```
a=plnsavgmin;
b=plnsavgmax;
rm=(b-a).*rand(1000,1)+a;
rm_range=[min(rm) max(rm)];
state = [mean(rm) std(rm) var(rm)];

% Calculate the number of failurs at each year interval
three=sum(rm(:,1)<=3.5);
four=sum(rm(:,1)<=4.5)-three;
five=sum(rm(:,1)<=5.5)-four-three;
six=sum(rm(:,1)>=5.5);

%Calculate the probability of failure in each year
P3=three/1000
P4=four/1000
P5=five/1000
P6=six/1000


%Calculate the LCC for replacing the joint in the mountains for
 replacement
%times of 3,4,5,and 6 years.

t3=3; %years
t4=4; %years
t5=5; %years
t6=6; %years


Pm=[P3,P4,P5,P6]; %probability that a joint will have a respective
 average joint life
tm=[t3,t4,t5,t6]; % average joint life for mountain bridges
tpr=[0,0.5,1,1.5,2,2.5,3,3.5]; % time until replacement after failure

%%Plains Range (7-10 years)
rng(0,'twister');
ap=mntsavgmin;
bp=mntsavgmax;
rp=(bp-ap).*rand(1000,1)+ap;
rp_range=[min(rp) max(rp)];
state = [mean(rp) std(rp) var(rp)];
% Calculate the number of failurs at each year interval
seven=sum(rp(:,1)<=7.5);
eight=sum(rp(:,1)<=8.5)-seven;
nine=sum(rp(:,1)<=9.5)-eight-seven;
ten=sum(rp(:,1)>=9.5);
%Calculate the probability of failure in each year
P7=seven/1000
P8=eight/1000
P9=nine/1000
P10=ten/1000

%Calculate the LCC for replacing the joint in the plains for
 replacement
```

```
%times of 7,8,9,and 10 years.

t7=7; %years
t8=8; %years
t9=9; %years
t10=10; %years


Pp=[P7,P8,P9,P10]; %probability that a joint will have a respective
 average joint life
tp=[t7,t8,t9,t10]; % average joint life for mountain bridges
tpr=[0,0.5,1,1.5,2,2.5,3,3.5]; % time until replacement after failure
```

```
P3 =

    0.1760


P4 =

    0.3360


P5 =

    0.3520


P6 =

    0.1360


P7 =

    0.1760


P8 =

    0.3360


P9 =

    0.3520


P10 =

    0.1360
```

LCCA of joints impacts on pier caps and abutments

```
% If joint is clogged but not leaking - failed joint impact abutment
% If joint is fully clogged - LCCA based on Temperature induced
 expansion
% Forces

% For Steel Girder Bridges
rng(0,'twister');
Tmin=0;
Tmax=100;
Trang=(Tmax-Tmin).*rand(1000,1)+Tmin;
z=1;
for i=1:1000;
    Trang(i); % temp increase on bridge, normal distribution between
 0-100
    F(i)=0.306*Trang(i); % relationship between temperature and stress
 induced by end girders on the abutment.

    if F(i)>f/sf; %account for safety factor
        Fc(z)=F(i);
        T(z)=Trang(i);
        prevz=z;
        z=prevz+1;
    else Fs(i)=F(i);
        z=z;
    end
end
Tc=z; % number of times temp caused force greater than 4ksi
Ttot=1000; % total number of temps analyzed
Pts=rf*(Tc/Ttot); % probability T will cause crushing of the abutment;
%plot temp vs. force greater than 4 ksi
z;

%If joint is clogged, find the LCCA for the bridge if abutment is
 crushing
%due to temp load.


%For Joints leaking onto Pier Caps, probabilty of corrosion
Tf=[3,4,5,6,7,8,9,10]; % Time it takes joint to fail
Tr=[0,0.5,1,1.5,2,2.5,3,3.5]; % Time it takes to replace joint after
 failure
Conc=[0,0.02084,0.04167,0.06251,0.08334,0.10418,0.12501,0.14585];
% % wt. conc. of chloride on surface

for i=1:xx
r(i)=0;
prevr=r(i);
Tf1(i)=0; %selecty time it takes joint to fail
prevTf=Tf1(i); %set failure time equal to previous
```

```
Tri(1)=0;%select time it takes to replace joint
prevTr=Tri(1);%set failure time equal to previous
    while r(1)<0.383 %sum times until concentration (n) equals
 critical corrosion conc.
    rng('shuffle');
    Tfi(1)=Tf(randi(8))+prevTf;
    prevTf=Tfi(1);
    rng('shuffle');
    p=randi(8);
    Tri(1)=Tr(p)+prevTr;
    prevTr=Tri(1);
    Tt(1)=Tfi(1)+Tri(1);
    r(1)=prevr+Conc(p);
    prevr=r(1);
    end
    prevTt=Tt(1);
    Tt(1)=prevTt+6; %6 years is the time from threshold to signficant
 cracking due to corrosion
end
ten=sum(Tt(1,:)<=10); % sum number of times critical conc. is reach
 within ten years and so forth.
twenty=sum(Tt(1,:)<=20)-ten;
thirty=sum(Tt(1,:)<=30)-ten-twenty;
forty=sum(Tt(1,:)<=40)-ten-twenty-thirty;
fifty=sum(Tt(1,:)<=50)-ten-twenty-thirty-forty;
sixty=sum(Tt(1,:)<=60)-ten-twenty-thirty-forty-fifty;
seventy=sum(Tt(1,:)<=70)-ten-twenty-thirty-forty-fifty-sixty;
eighty=sum(Tt(1,:)<=80)-ten-twenty-thirty-forty-fifty-sixty-seventy;
ninety=sum(Tt(1,:)<=90)-ten-twenty-thirty-forty-fifty-sixty-seventy-
eighty;
hundred=sum(Tt(1,:)>90);
b=(ten+twenty+thirty+forty+fifty+sixty+seventy+eighty+ninety+hundred);
% calculate probabilities
P=[0,ten/xx,twenty/xx,thirty/xx,forty/xx,fifty/xx,sixty/xx,seventy/
xx,eighty/xx,ninety/xx,hundred/xx]
x=[0,10,20,30,40,50,60,70,80,90,100];
% plot probability vs time in years
figure(8);
plot(x,P,'-b')
title('Corrosion Probability vs. Years')
xlabel('Time (years)')
ylabel('Probability')

% calculate cumulative sums
ten1=sum(Tt(1,:)<=10);
twenty1=sum(Tt(1,:)<=20);
thirty1=sum(Tt(1,:)<=30);
forty1=sum(Tt(1,:)<=40);
fifty1=sum(Tt(1,:)<=50);
sixty1=sum(Tt(1,:)<=60);
seventy1=sum(Tt(1,:)<=70);
eighty1=sum(Tt(1,:)<=80);
ninety1=sum(Tt(1,:)<=90);
hundred1=sum(Tt(1,:)<=100);
```

```
%calculate cumulative probabilities
P1=[0,ten1/xx,twenty1/xx,thirty1/xx,forty1/xx,fifty1/xx,sixty1/
xx,seventy1/xx,eighty1/xx,ninety1/xx,hundred1/xx]
% plot cumulative probability vs time in years
figure(9);
plot(x,P1,'-g')
title('Cumulative Corrosion Probability vs. Years')
xlabel('Time (years)')
ylabel('Probability')


%Calculate the LCC for corrosion inclusion based on the probabilities
 from
%Life-365 calculated above. Select the correct probabilty based on the
%remaing design life, DL, of the bridge in question.
y=(DL/10)+1; %Note Design life, DL, should be rounded to the nearest
 10. if the remaining design life is less than 6 years corrosion is
 not a concern.
% for mountain bridges:


%%Total LCC Combined for Bridges if Joints are Replaced - Scenario 4

% For Steel Girder Bridges


%For bridges in mountains
tt=0; %total years of joint life and replacement
prevtt=tt;

LCCM=Pc*Cc*d*n; % LCC for mountain bridges Scenario 1 Alternative 1
prevLCCM=LCCM;
LCCMR=Pc*Cc*d*nabt+Crm*njt+Cs*njt*(DL/tcs); % LCC for mountain bridges
 Scenario 1 Alternative 2
prevLCCMR=LCCMR;

LCCMpcr=Pc*Cc*d*n; % LCC for mountain bridges Scenario 2 Alternative 1
prevLCCMpcr=LCCMpcr;

LCCMabtS=Pc*Cc*d*n; % LCC for mountain bridges Scenario 3 Alternative
 1
prevLCCMabtS=LCCMabtS;
LCCMRabtS=Pc*Cc*d*nabt+Crm*njt+Cs*njt*(DL/tcs); % LCC for mountain
 bridges Scenario 3 Alternative 2
prevLCCMRabtS=LCCMRabtS;

LCCMtotS=Pc*Cc*d*n; % LCC for mountain bridges Scenario 4 Alternative
 1
prevLCCMtotS=LCCMtotS;
LCCMRtotS=Pc*Cc*d*nabt+Crm*njt+Cs*njt*(DL/tcs); % LCC for mountain
 bridges Scenario 4 Alternative 2
prevLCCMRtotS=LCCMRtotS;
while tt<DL; %continue loop until the end of the remaining design life
 of the bridge
```

```
    rng('shuffle');
    q=randi(4);
    %scenario 1
    LCCM=prevLCCM+Pm(q)*Cr*n;
    prevLCCM=LCCM;
    LCCMR=prevLCCMR+Pm(q)*Cr*nabt;
    prevLCCMR=LCCMR;
    %scenario 2
    LCCMpcr=prevLCCMpcr+Pm(q)*(Cr*n+Pl(y)*Cpcr*Nj);
    prevLCCMpcr=LCCMpcr;
    %scenario 3
    LCCMabtS=prevLCCMabtS+Pm(q)*(Cr*n+Pts*Cabtr*nabt);
    prevLCCMabtS=LCCMabtS;
    LCCMRabtS=prevLCCMRabtS+Pm(q)*(Cr*nabt+Pts*Cabtr*nabt);
    prevLCCMRabtS=LCCMRabtS;
    %scenario 4
    LCCMtotS=prevLCCMtotS+Pm(q)*(Cr*n+Pl(y)*Cpcr*Nj+Pts*Cabtr*nabt);
    prevLCCMtotS=LCCMtotS;
    LCCMRtotS=prevLCCMRtotS+Pm(q)*(Cr*nabt+Pts*Cabtr*nabt);
    prevLCCMRtotS=LCCMRtotS;

    rng('shuffle');
    r=randi(8);
    tt=prevtt+tm(q)+tpr(r);
    prevtt=tt;

end
%scenario 1
LCCM
LCCMR
LCCMRall=Crm*n+Cs*n*(DL/tcs)

%scenario 2
LCCMpcr
% LCC for mountain bridges Scenario 2 Alternative 2  is the same as
 Scenario 1 Alternative 2
LCCMRpcr=LCCMR
LCCMRpcrall=LCCMRall

%scenario 3
LCCMabtS
LCCMRabtS
tt
LCCMRabtallS=LCCMRall

%scenario 4
LCCMtotS
LCCMRtotS
LCCMRtotSall=LCCMRall
tt


%for bridges in plains
tt=0; %total years of joint life and replacement
```

```
prevtt=tt;
LCCP=Pc*Cc*d*n; % LCC for plains bridges Scenario 1 Alternative 1
prevLCCP=LCCP;
LCCPR=Pc*Cc*d*nabt+Crm*njt+Cs*njt*(DL/tcs); % LCC for plains bridges
 Scenario 1 Alternative 2
prevLCCPR=LCCPR;

LCCPpcr=Pc*Cc*d*n; % LCC for plains bridges Scenario 2 Alternative 1
prevLCCPpcr=LCCPpcr;

LCCPabtS=Pc*Cc*d*n; % LCC for plains bridges Scenario 3 Alternative 1
prevLCCPabtS=LCCPabtS;
LCCPRabtS=Pc*Cc*d*nabt+Crm*njt+Cs*njt*(DL/tcs); % LCC for plains
 bridges Scenario 3 Alternative 2
prevLCCPRabtS=LCCPRabtS;

LCCPtotS=Pc*Cc*d*n; % LCC for plains bridges Scenario 4 Alternative 1
prevLCCPtotS=LCCPtotS;
LCCPRtotS=Pc*Cc*d*nabt+Crm*njt+Cs*njt*(DL/tcs); % LCC for plains
 bridges Scenario 4 Alternative 2
prevLCCPRtotS=LCCPRtotS;
while tt<DL; %continue loop until the end of the remaining design life
 of the bridge
    rng('shuffle');
    q=randi(4);
    %scenario 1
    LCCP=prevLCCP+Pp(q)*Cr*n;
    prevLCCP=LCCP;
    LCCPR=prevLCCPR+Pp(q)*Cr*nabt;
    prevLCCPR=LCCPR;
    %scenario 2
    LCCPpcr=prevLCCPpcr+Pp(q)*(Cr*n+Pl(y)*Cpcr*Nj);
    prevLCCPpcr=LCCPpcr;
    %scenario 3
    LCCPabtS=prevLCCPabtS+Pp(q)*(Cr*n+Pts*Cabtr*nabt);
    prevLCCPabtS=LCCPabtS;
    LCCPRabtS=prevLCCPRabtS+Pp(q)*(Cr*nabt+Pts*Cabtr*nabt);
    prevLCCPRabtS=LCCPRabtS;
    %scenario 4
    LCCPtotS=prevLCCPtotS+Pp(q)*(Cr*n+Pl(y)*Cpcr*Nj+Pts*Cabtr*nabt);
    prevLCCPtotS=LCCPtotS;
    LCCPRtotS=prevLCCPRtotS+Pp(q)*(Cr*nabt+Pts*Cabtr*nabt);
    prevLCCPRtotS=LCCPRtotS;

    rng('shuffle');
    r=randi(8);
    tt=prevtt+tp(q)+tpr(r);
    prevtt=tt;

end
%scenario 1
LCCP
LCCPR
LCCPRall=Crm*n+Cs*n*(DL/tcs)
```

```
%scenario 2
LCCPpcr
% LCC for plains bridges Scenario 2 Alternative 2  is the same as
 Scenario 1 Alternative 2
LCCPRpcr=LCCPR
LCCPRpcrall=LCCPRall

%scenario 3
LCCPabtS
LCCPRabtS
LCCPRabtallS=LCCPRall

%scenario 4
LCCPtotS
LCCPRtotS
LCCPRtotSall=LCCPRall
tt


%Plot LCCs

A1M=[LCCM,LCCMpcr,LCCMabtS,LCCMtotS];
X1=[1,2,3,4];
A2M=[LCCMR,LCCMRall,LCCMRpcr,LCCMRpcrall,LCCMRabtS,LCCMRabtallS,LCCMRtotS,LCCMRtot
X2=[1,2,3,4,5,5,6,7,8];
A1P=[LCCP,LCCPpcr,LCCPabtS,LCCPtotS];
A2P=[LCCPR,LCCPRall,LCCPRpcr,LCCPRpcrall,LCCPRabtS,LCCPRabtallS,LCCPRtotS,LCCPRtot

S1=[LCCM,LCCP,LCCMR,LCCMRall,LCCPR,LCCPRall];
S2=[LCCMpcr,LCCPpcr,LCCMRpcr,LCCMRpcrall,LCCPRpcr,LCCPRpcrall];
S3=[LCCMabtS,LCCPabtS,LCCMRabtS,LCCMRabtallS,LCCPRabtS,LCCPRabtallS];
S4=[LCCMtotS,LCCPtotS,LCCMRtotS,LCCMRtotSall,LCCPRtotS,LCCPRtotSall];
X3=[1,2,3,4,5,6];


figure(10); hold on
plot(X3,S1,'-o');
title('LCC for Scenario 1')
xlabel('Alternative')
ylabel('LCC ($)')

figure(11); hold on
plot(X3,S2,'-o');
title('LCC for Scenario 2')
xlabel('Alternative')
ylabel('LCC ($)')

figure(12); hold on
plot(X3,S3,'-o');
title('LCC for Scenario 3')
xlabel('Alternative')
ylabel('LCC ($)')
```

```
figure(13); hold on
plot(X3,S4,'-o');
title('LCC for Scenario 4')
xlabel('Alternative')
ylabel('LCC ($)')

figure(14); hold on
plot(X3,S1,'-o',X3,S2,'--+',X3,S3,'-.p',X3,S4,':x');
y1='Scenario 1';
y2='Scenario 2';
y3='Scenario 3';
y4='Scenario 4';
legend (y1,y2,y3,y4);
title('LCC for all Scenarios')
xlabel('Alternative')
ylabel('LCC ($)')

figure(15); hold on
plot(X1,A1M,'-o',X1,A1P,'--+');
y1='Alternative 1-Mountains';
y2='Alternative 1-Plains';
legend (y1,y2);
title('LCC for Alternative 1')
xlabel('Scenario')
ylabel('LCC ($)')

figure(16); hold on
plot(X2,A2P,'-o',X2,A2M,'--+');
y1='Alternative 2-Mountains';
y2='Alternative 2-Plains';
legend (y2,y1);
title('LCC for Alternative 2')
xlabel('Scenario')
ylabel('LCC ($)')

figure(17); hold on
plot(X1,A1P,'-o',X2,A2P,'--+',X1,A1M,':p',X2,A2M,'-.x');
y1='Alternative 1-Replace Pln';
y2='Alternative 2-Retrofit Pln';
y3='Alternative 1-Replace Mnt';
y4='Alternative 2-Retrofit Mnt';
legend (y1,y2,y3,y4);
title('LCC for Bridges')
xlabel('Scenario')
ylabel('LCC ($)')
```